Application of Sliding Isolation Bearings with Upward Lifting Mechanism for Seismic Performance Enhancement of Multi-Story Structures

Muhannad Yacoub FAKHOURI

2012

Application of Sliding Isolation Bearings with Upward Lifting Mechanism for Seismic Performance Enhancement of Multi-Story Structures

A dissertation submitted in partial fulfillment
of the requirements for the degree of
Doctor of Philosophy in Engineering

Graduate School of Engineering
Kyoto University, Japan
2012

by

Muhannad Yacoub FAKHOURI

Examination Committee: Professor Akira Igarashi (Supervisor)
Professor Takeshi Koike (Chairman)
Professor Izuru Takewaki

"Not to us, O LORD, not to us but to your name be the glory, because of your love and faithfulness."
Psalm 115:1

"He has made everything beautiful in its time…"
Ecclesiastes 3:11

To my beloved family,

With your unconditional love, prayers and unlimited support
you made this possible!

Abstract

A new and distinctive type of friction-based seismic isolation bearing, namely the uplifting slide bearing (UPSS), is introduced in this research. The UPSS Bearing is a simple sliding device consists of one horizontal and two inclined plane sliding surfaces at both ends set in series. These three surfaces are based on PTFE and highly polished stainless steel (SUS) interface. During normal or low intensity earthquakes, the isolator behaves as a pure friction isolator with sliding only in the horizontal direction. However, during a severe earthquake, sliding will be activated in the inclined surface producing displacements in both horizontal and vertical directions.

The main purpose to develop such a device was to fulfill the need for a seismic isolation device that is simple, and effective in reducing the horizontal displacement with a low cost. The UPSS bearing possesses unique features depend essentially on the geometrical configuration and the sliding mechanism that make it superior to other types of bearings. Some of the special features that make UPSS an attractive bearing and a good choice for the designers: geometrical configuration creativity, efficiency in controlling the displacement thus avoiding pounding of adjacent structures, architecturally flexible and aesthetic solution and a feasible solution for seismic retrofitting of existing buildings with soft stories.

The dissertation can be classified into four core themes: dynamic response control of multi-story structures by the UPSS, UPSS bearing for seismic retrofitting of frame structures with soft first stories, verification of the actual behavior of the UPSS through both the component test and the shake table test and performance-based design of seismically isolated frame structures by the UPSS bearing based on building code in Japan.

The assessment and simulation results indicate that the UPSS bearing is more effective in preserving multi-story buildings from damage than the conventional rubber bearing and the pure friction slider in term of peak horizontal displacement. It has also been shown that the seismic interface that consists of UPSS bearings can be considered

as one of the prominent cost effective solutions that can overcome the dilemma between the need for soft story and its vulnerability to collapse. Moreover, the proposed system also offers a feasible solution that is simple and practical to be implemented for seismic retrofitting of existing building with soft stories.

Acknowledgement

This dissertation is a contribution of my Ph.D. study as a member of the Structural Dynamics Laboratory in the Graduate School of Engineering of Kyoto University.

I would like to express my heartfelt gratitude to the Ministry of Education, Culture, Sports, Science and Technology, Japan (MEXT) for granting me the financial support "Monbugakakusho Scholarship" during my stay in Japan.

I am immensely indebted to the guidance of Professor Akira Igarashi, who was not only a great supervisor but also a genuine teacher and a kind mentor, during my doctoral research endeavor. His constructive advice and beneficial suggestions mainly helped me to establish the overall direction of my research and to develop the systematic thinking behind it.

My sincere appreciation is also extended to the dissertation committee Professor Takeshi Koike and Professor Izuru Takewaki for their valuable advice and contribution in reviewing my Ph.D. dissertation.

I gratefully acknowledge the contribution of Dr. Hiroshige Uno of Oiles Corporation for providing me the component test data used in this study. Also, I would like to express my gratitude towards Dr. Yukio Adachi of Hanshin Expressway Corporation, Mr. Tomoaki Sato, Mr. Yoshihisa Kato, and Mr. Yasuyuki Ishii and Miss Shiraishi Haruko for their valuable advice, support and suggestions on this research.

My sincere appreciation to all of the members in the Structural Dynamics Laboratory for their warm friendship, for sharing their time together with me, and for helping me unconditionally during my stay in Japan.

Many thanks to all of my good friends in in Japan, especially all the members of the Kyoto Assembly Church, for their kind encouragement and prayer support that made my life in Japan more enjoyable and more meaningful.

Last but not least, I would like to dedicate this dissertation to my beloved family. With

their unconditional love, great understanding, inspiration, unlimited encouragement and support during the tough times in my life, they have made it possible for me to complete this study.

Muhannad Yacoub Fakhouri
Dec. 12th 2011, Kyoto, Japan

Table of Contents

Chapter 7: Performance-based design of seismically isolated frame structures by the UPSS Bearing based on building code in Japan

Chapter 8: Conclusion and Future Work

List of Figures

List of Tables

Chapter 1

Introduction and Overview

The first chapter of this dissertation intends to introduce the background and motivation of this study. The scope of study and dissertation Outline are provided at the end of this chapter.

1.1 Background

Over the past decades seismic isolation has gained popularity and momentum especially after the seismically isolated structures have been performed well and demonstrated the reduction in seismic response when subjected to real and strong earthquake excitations. For example, the seismic isolation technique has been confirmed once again through the observed records of the test buildings that stood near the epicenter of the 2011 Earthquake off the Pacific coast of Tohoku (Shimizu Corporation 2011a). The magnitude of the 2011 Tohoku-Pacific Earthquake was reported as being 9.0, the highest magnitude ever recorded in Japan. The scale of this event ranks fourth in the world. The observed ground motions had a definite feature of a long duration because of the large scale of the fault plane, compared to those of some previous destructive earthquakes (Shimizu Corporation 2011b), as shown in the Fig 1.1. Two of these seismic isolated buildings that stand in Shimizu Corporation institute are shown in Figs 1.2 and 1.3. It is obvious that the observed accelerations on the floors were reduced to about half compared to those on the ground. In another test seismic isolated building, jointly built by Shimizu Corporation and Tohoku University within the Sendai campus in Miyagi prefecture in Tohoku University, the observed accelerations on the roof were reduced to about one third compared to those in the

adjacent conventional seismically designed building; see Fig 1.4, (Shimizu Corporation 2011b).

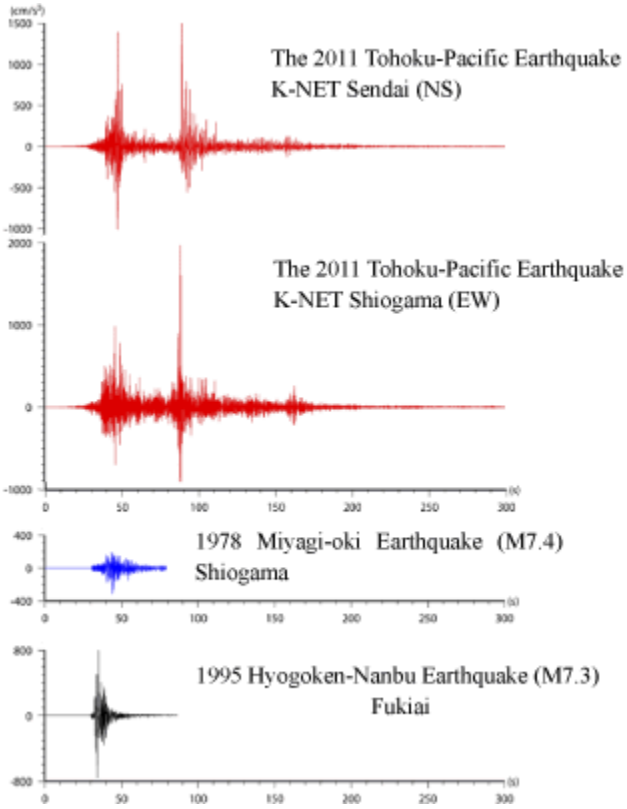

Figure 1.1 A Comparison of the observed records at the K-NET Sendai (NS) and the K-NET Shiogama (EW) of the 2011 Tohoku-Pacific Earthquake with those from previous destructive earthquakes (Shimizu Corporation 2011b)

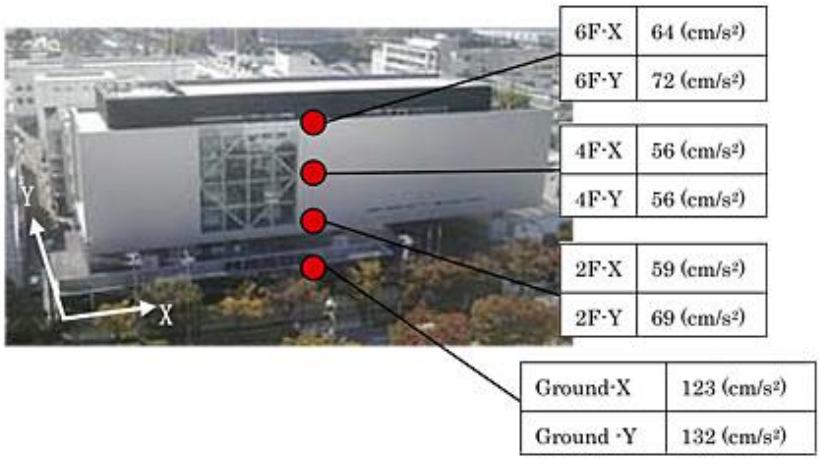

Figure 1.2 Main Building of Institute of Technology (Column-top seismic isolation) (Shimizu Corporation 2011a)

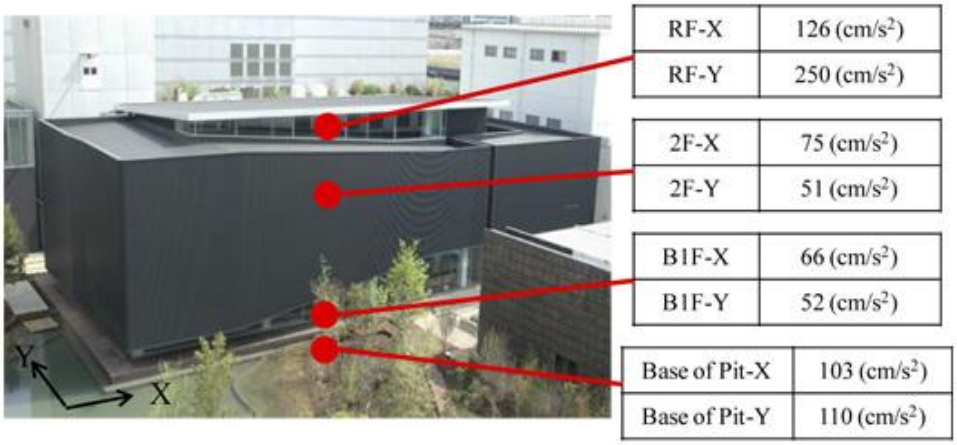

Figure 1.3 Wind Tunnel Testing Laboratory (Partially-floating seismic isolation) (Shimizu Corporation 2011a)

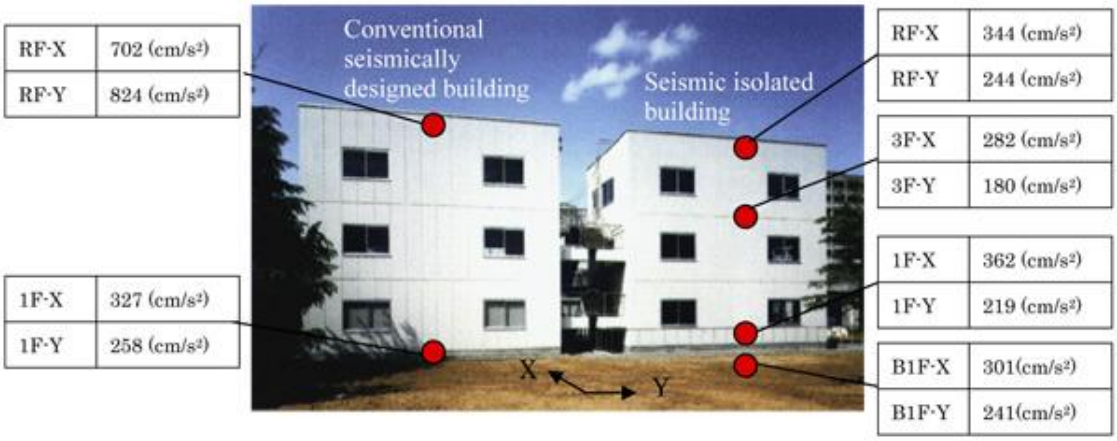

Figure 1.4 Test Buildings in Tohoku University (Left: Conventional seismically designed building; Right: Seismic isolated building) (Shimizu Corporation 2011a)

Seismic isolation has also been proven to be an efficient approach to mitigate the damage of high-rise buildings. For examples, the isolated Sendai MT Building and Apple Towers Sendai building remained undamaged during the Great East Japan Earthquake; see Fig 1.5. According to data on structural displacement relative to the ground, the aforementioned two buildings recorded a maximum horizontal displacement of 14cm and 23cm (Web Japan 2011), respectively; see Fig. 1.6. Recently, a series of shaking table tests on full scale base isolated four-story RC structures serving as hospital were conducted at E-defense. The results verified the satisfactory performance of base isolated structures for both near-fault and long-period ground motion (Sato et al 2011).

A feasibility study should be carried out in the initial planning phase of the building to insure the suitability and cost effectiveness of seismic isolation. The need for seismic isolation depends on the seismicity of the area where the building is to be constructed and on the seismic design requirement. Therefore, the seismic isolation is best suited for moderate and high seismic area, and where the seismic design doesn't add to the costs significantly (Kelly et al 2010). Other important factors in making the decision are the soil profile and the location of structure from fault. Furthermore, the structure period, weight and structural elements configuration play additional role in the process of selection.

(a)  (b) 

Figure 1.5 (a) Apple Towers Sendai building (b) Sendai MT Building

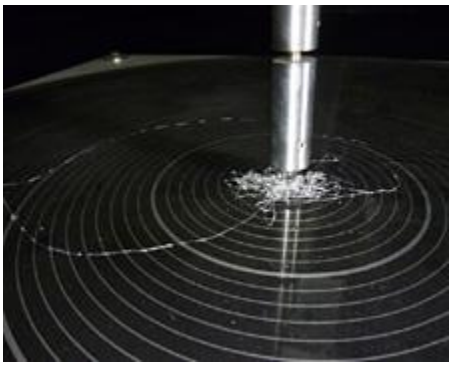

Figure 1.6 Measurement equipment shows that the Sendai MT Building experienced as much as 23cm of horizontal displacement (Photo: Mori Trust Co., Ltd.)

An example of a feasibility and design study is the one performed for the Museum of New Zealand, Te Papa Tongaraw. The study has demonstrated that a seismic isolation can be installed for almost the same first cost as a conventional, fixed base structure. It has been found that to obtain approximately similar levels of structural damage the conventional structure requires larger columns and beams and also a larger number of shear walls compared to the isolated structure (Kelly et al 2010). Another example is the feasibility study for a nuclear power plant which showed that installing seismic isolation results in cost saving of the order of 2% of the initial cost (Sigal and Tsirk 1983).

The most suitable buildings are those with a critical civil defense role which requires to be operating immediately after severe earthquakes, like hospitals, bridges and emergency centers. In addition, historical or monumental structures of high culture value and structures with valuable contents or operations are also considered as good candidates for seismic isolation. Moreover, Seismic isolation provides an efficient solution in retrofitting existing building with low ductility.

1.2 Motivation and Scope of Study

The effort of developing new isolators is now blossoming, with seismic isolation becoming increasingly recognized as a viable design alternative in the major seismic region in the word. The growing need for seismic isolation in construction projects is due to its excellent performance that was verified in many past and recent strong earthquakes as discussed in the aforementioned section.

As a part of this effort of developing new isolators, this research introduces a unique type of friction-based bearings namely, the uplifting Slide Bearing (UPSS). The UPSS bearing is a simple sliding device consists of one horizontal and two inclined plane sliding surfaces at both ends set in series. These three surfaces are based on PTFE and highly polished stainless steel (SUS) interface.

The UPSS has distinctive features that are not found in any other isolators. The uniqueness of this device depends essentially on the geometrical configuration and the sliding mechanism that make it superior to other types of bearings. The simplicity and the cost effectiveness are some of the competitive factors of the UPSS bearing. Besides, the UPSS bearing possess a high capability in controlling the displacement response

even for the near-fault and long-period ground motion cases. The uniqueness and advantages of the UPSS bearing over other type of bearings are discussed thoroughly in section 2.4.

The main scope of this research is to extend the application of UPSS bearing that was first introduced to upgrade the seismic performance of multi-span continuous girder bridges to include multi-story structures. Other objective is to present a design procedure that can help the structural designer in the process of designing the seismic isolation interface for the multi-story structure by the UPSS bearings. Further extent is to investigate the efficiency of introducing a seismic interface consists of UPSS bearings to retrofit existing buildings with inadequate soft stories as well as new structures to be constructed with soft first story intended for architectural or functional purposes.

1.3 Dissertation Outline

This dissertation consists of eight chapters. The following presents an overview of the contents of this dissertation and allows a selective reading.

The second chapter of this dissertation intends to introduce the Uplifting Sliding Bearing (UPSS) and establish the underlying principles of operation and the mechanism of sliding. The concept of displacement reduction in analogy of a dynamic sliding block on an inclined plane is also presented. In addition, a detailed review of the friction based isolators is discussed. Moreover, the emphasis on the advantages and uniqueness of UPSS over other bearings is presented.

The third chapter intends to examine the UPSS concept based on the perception of friction pendulum system (FPS) due its maturity and well recognition as a very efficient tool for controlling the seismic response of a structure during an earthquake. The main objectives are to investigate the efficiency of implementing a plane surface in sliding isolators in the analogy of the clearance length in the UPSS and to study its influence on the seismic response of multi-story base-isolated structure.

Chapter four aims to investigate the efficiency of using the multiple-slider bearing based on the concept of UPSS to isolate multi-story shear type structures. The principles of operation and force displacement relationship for the isolator are introduced. The seismic behavior of the base isolated building by the UPSS bearing

subjected to seismic excitation is investigated, comparing with conventional rubber bearing and pure friction slider isolating systems. Moreover, extensive parametric investigations are performed in order to achieve an optimum performance of the isolator with respect to three main properties which define the device: clearance length, the inclination angle and the friction coefficient. The results show the effectiveness of the UPSS in minimizing the damage from earthquakes. The UPSS proves to have a high potential in minimizing the effect of the ground displacement pulses through its operation mechanism and its unique feature that permits the use of different set of friction coefficients on each sliding surface. In addition, a principle to define the optimum value of the friction coefficient is developed.

Chapter five of this dissertation intends to verify the actual behavior of the UPSS through both the component test and the shake table test. Two analytical models are presented in this chapter to simulate the behavior of the UPSS namely; the simplified model and spring model. The verification analysis to the shaking table experiment results was done. As a result, it was confirmed that the analytical result and the outcome of an experiment showed a good agreement.

In chapter six, UPSS bearing is proposed to retrofit existing buildings with inadequate soft stories as well as new structures to be constructed with soft first story intended for architectural or functional purposes. The seismic interface is an assembly of bearings set in parallel on the top of the first story columns; the UPSS bearings and rubber bearings. A numerical example of five-story reinforced concrete shear frame with a soft first story is considered and analyzed to demonstrate the efficiency of the proposed isolation system in reducing the ductility demand and damage in the structure while maintaining the superstructure above the bearings to behave nearly in the elastic range with controlled bearing displacement. Comparative study with the conventional system as well as various isolation systems such as rubber bearing interface and resilient sliding isolation is carried out. Moreover, an optimum design procedure for the UPSS bearing is proposed through the trade-off between the maximum bearing displacement and the first story ductility demand ratio. The results of extensive numerical analysis verify the effectiveness of the multiple-slider bearing in minimizing the damage from earthquake and preserving the soft first story from excessively large ductility demand.

In chapter seven, a design procedure is proposed for seismically isolated frame structures by the UPSS bearings. This design procedure is based on the basic concepts

of performance-based seismic and structural code introduced by the Japanese Building Research Institute (BRI). The reliability of the simplified design procedure evaluated using equivalent linearization system is assessed and validated through nonlinear time history analysis. In addition, modified deign procedure is proposed to take into account the effect of vertical damping.

This dissertation is finished in the chapter eight with the conclusion of the present work and perspectives towards future tasks.

References

Sato E, Furukawa S, Kakehi A, Nakashima M. Full-scale shaking table test for examination of safety and functionality of base-isolated medical facilities. *Earthquake Engineering & Structural Dynamics* 2011; 40(13): 1435–1453.

Sigal G, Tsirk A. Seismic Isolation Studies for Liquid Metal Fast Breeder Reactor (LMFBR) Plants, *report of the Nuclear Projects Division*, Burns and Roe, Oradell, NJ, 1983.

Kelly T, Skinner R, and Robinson B. Seismic Isolation for Designers and Structural Engineers. *National Information Center of Earthquake engineering* (NICEE); 2010.

Shimizu Corporation. Report on the Tohoku Area Pacific Offshore Earthquake, Effects of seismic isolation 2011b; Retrieved from http://www.shimz.co.jp/english/theme/earthquake/effect.html.

Shimizu Corporation. Report on the Tohoku Area Pacific Offshore Earthquake, General Perspectives 2011a; Retrieved from http://www.shimz.co.jp/english/theme/earthquake/outline.html

Web Japan. Trends in Japan, Sci-tech, Japanese Earthquake Resistance and Seismic Isolation Technologies July, 2011. http://web-japan.org/trends/11_sci-tech/sci110728.html

Chapter 2

The Uplifting Slide Bearing (UPSS)

The second chapter of this dissertation intends to introduce the Uplifting Sliding Bearing (UPSS) and establish the underlying principles of operation and the mechanism of sliding. The concept of displacement reduction in analogy of a dynamic sliding block on an inclined plane is also presented. In addition, a detailed review of the friction based isolators is discussed. Moreover, the emphasis on the advantages and uniqueness of UPSS over other bearings is presented.

2.1 Seismic Isolation

Seismic isolation has been proven to be an efficient approach to earthquake resistant-design of structures based on the concept of reducing the seismic demand rather than increasing the seismic resistance capacity of the structure, and is one of the preferable alternatives in seismic retrofitting of historic structures without impairing their architectural characteristics.

The effectiveness of seismic isolation structures has been demonstrated and verified during real and strong earthquakes. As a result, the number of projects on seismic isolation buildings has been remarkably increased. Seismic isolation has been actively adopted and recognized as a viable technique in construction of bridges, buildings and other structures. Since then, researchers and engineers in this field have been working to develop seismic isolation devices as a part of their efforts to offer earthquake resistant structures and many developed systems have successfully been put forward into practice. Extensive reviews on different types of isolation devices and their applications to structures have been provided by many researches (Su et al. 1989, Buckle and Mayes 1990, Skinner and Robinson 1993, Jangid and Data 1995,

Qamaruddin 1998, Kunde and Jangid 2003).

Seismic isolation can be seen as good alternative for the conventional method as it simply detach the structure from its support by mean of an isolation system to provide a discontinuity between two bodies in contact so that the motion of either body, in the direction of the discontinuity cannot be fully transmitted, thus reduce the plastic deformation in the structure and concentrate them in the isolators. These systems shall contain three basic functions: flexibility to lengthen the period and produce the isolation effect, energy dissipation capability to reduce displacements to practical design level and means of providing rigidity under service loads such as wind and vertical loads.

The objective of isolation in a building structure and bridge structure is different. In buildings, isolation is installed to reduce the inertia force transmitted into the structure above in order to reduce the demand on the structural elements. In bridges, isolation is typically installed on the top of the piers with the main purpose of protecting the pier by reducing the inertia loads transmitted from superstructure. Bridge isolation does not have the objective of reducing floor accelerations which is common for most building structures. For this reason, there is no imposed upper limit on damping provided by isolation system (Kelly 2010). Many isolation systems for bridges are designed to maximum energy dissipation rather than providing a significant period shift.

Seismic base isolation is not a very new idea. The first evidence of architects using the principle of base isolation for earthquake protection was discovered in Pasargadae, a city in ancient Persia, now Iran: it goes back to 6th century BC, see Fig 2.1. Recent research has shown that the foundations are insulated from the effects of seismic activity to safeguard it from an earthquake (Islam et al. 2011).

In 1891, Kawai, a Japanese person, proposed a base-isolated structure with timber logs placed in several layers in the longitudinal and transverse direction (Iemura et al 2005) as shown in Fig 2.2. In 1906, Jacob Bechtold of Germany applied for a U.S. patent in which he proposed to place building on rigid plate, supported on spherical bodies of hard material (Buckle and Mayes, 1990).

Figure 2.1 The oldest base isolated structure of the world, Mausoleum of Cyrus

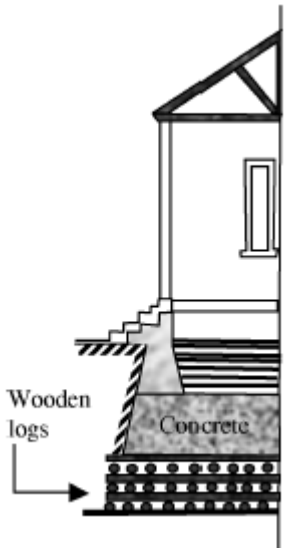

Figure 2.2 Base isolation by wooden logs (Iemura et al 2005)

In 1969, the construction of an elementary school in Skopje, Macedonia, was completed, making it the first structure in the world to have base isolation constructed of rubber. However, these rubber blocks are unreinforced and bulge sideways under the weight of this concrete structure. In an earthquake, the building will likely "bounce and rock backwards and forwards" because the vertical and horizontal stiffness are the same (Kelly 1997).

2.2 Sliding Isolators: literature review

Base isolation seismic control devices vary in size, shape, element composition, degree of seismic resistance and many other properties. Based on the mechanical characteristics, seismic isolators can be classified as elastomeric or sliding bearings. Sliding bearings are the main concern in this research.

A considerable amount of theoretical analysis as well as experimental works has been done on isolated structures by pure friction isolators (PF) systems subjected to harmonic and earthquake excitations (Westermo and Udwadia 1983, Mostaghel and Tanbakuchi 1983, Younis and Tadjbakhsh 1984, Yang et al 1990, LU and Yang 1997, Vafai et al 2001).

The earliest and simplest purely isolation sliding system has been proposed in 1909 by a medical doctor in England who suggested separating the structure from the foundation by layer of talc (Naeim and Kelly 1999) as shown in Fig 2.3.

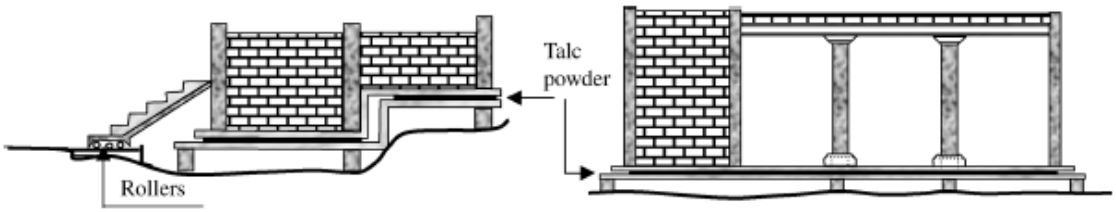

Figure 2.3 Calantarients's base isolation system (Iemura et al 2005)

This basic concept has been used and developed for low rise housing in China (Li 1984). The system consisted of laying a special screened sand layer between terrazzo plates on the base floor level. Nowadays, a typical example for flat slider bearing is the pot-type bearings have a layer of PTFE bonded to the base of the pot sliding on a stainless steel surface as in Fig 2.4. The pot portion of the bearing consists of a steel piston, inside a steel cylinder, bearing on a confined rubber layer. The pot allows rotations of typically up to at least 0.20 radians (Kelly et al 2010). Another example is the linear guide CLB isolator developed by THK Company that accommodates a heavy sustained load with extremely low frictional force, because the balls in the LM guide rotate on raceways cut into the LM rail while circulating through the block as shown in Fig 2.5. Since the LM block is equipped with an LM rail and balls, the bearings can

also accept a pulling load.

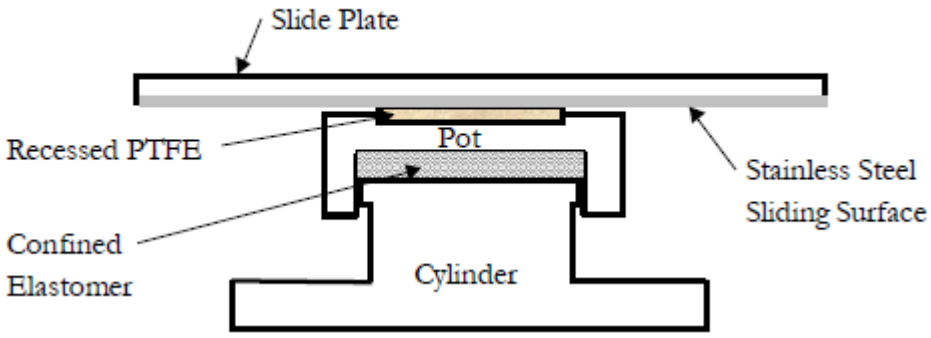

Figure 2.4 Section through Pot Bearing (Kelly 2001)

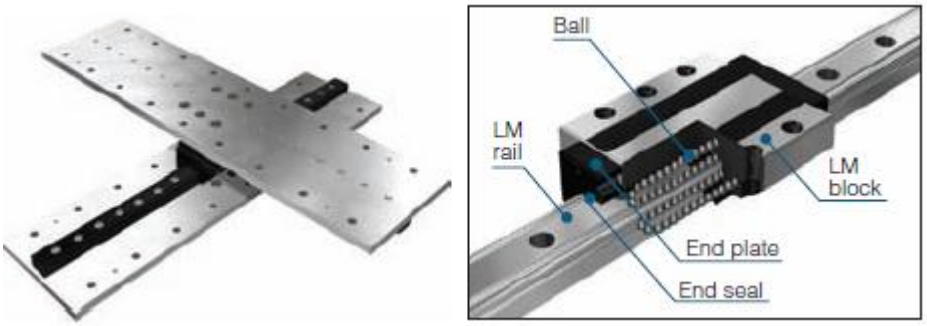

Figure 2.5 Linear re-circulating guide CLB (THK base isolation catalog)

Generally speaking, sliding isolators alone are impractical due to lack of restoring capability. The practical effectiveness of sliding isolators can be enhanced by adding restoring force mechanism to reduce the residual displacements in a level that can be incorporated in structural design requirements.

A rolling friction isolator device has been proposed for protecting the structures from earthquakes. This device consists of two sets of mutually orthogonal free rolling rods under the basement of the structure (Lin and Hone 1993). The attraction of this device comes from the small coefficient of rolling friction, thus structure can be isolated excellently from the support excitation. However, this system suffers from the

residual displacement due to the lack of any restoring force. Therefore, other alternative have been suggested using an elliptical shape instead of the circular one (Janjid and Londhe 1998). Due to the eccentricity of the elliptical rolling rods a restoring force is developed which brings back the structure to its originally position.

A unique type of sliding isolators, which was design for the base isolation of nuclear power plants, was developed under the auspices of Electricite de France (EDF) (Gueraud 1985). An EDF isolator system consists of a laminated, steel reinforced, neoprene pad topped by a lead-bronze plate that is in frictional contact with steel plate anchored to the base raft of the structure as shown in Fig 2.6. The neoprene bearing and the friction plates are essentially in series. During low intensity earthquake, EDF behaves like rubber bearing. However, when the frictional resistance is exceeded, a sliding will occur between the lead-bronze interface.

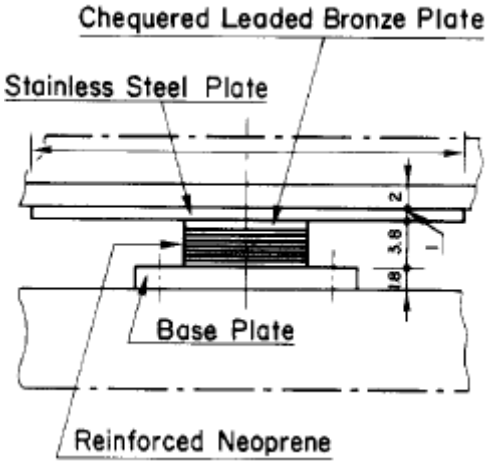

Figure 2.6 EDF isolator system

Various sliding isolators including a restoring force mechanism capability have been proposed and studied. The R-FBI (Mostaghel and Khodaverdian 1987) is composed of a set of concentric ring layers of Teflon coated plates that are in friction contact with each other with a central rubber core and/or peripheral rubber cores. This system makes use of the parallel action of resiliency of rubber and the interfacial friction force as shown in Fig 2.7.

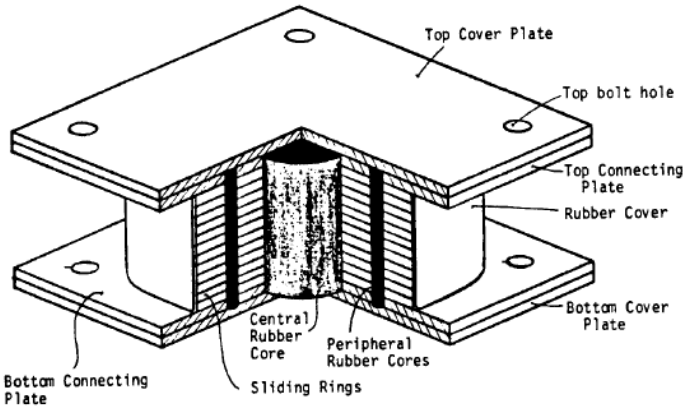

Figure 2.7 The R-FBI system (Mostaghel and Khodaverdian 1987)

Later on, a new sliding device which combines the desirable features of the EDF and the R-FBI was proposed (Su et al 1991) which is referred to as the sliding resilient-friction (SR-F). In this design, a friction plate replaces the upper surface of the R-FBI. Therefore, whenever there is no sliding in the upper plate, the SR-F system behaves like the R-FBI system.

Another innovative sliding isolation system called TASS (TAISEI Shake Suppression) system has been developed (Kawamura et al 1988). It consists of PTFE-elastomeric sliding bearings and neoprene springs as shown in Fig 2.8. PTFE-bearings support the vertical load and reduce horizontal seismic forces by sliding during severe earthquake motions. Horizontal springs provide weak lateral stiffness and restrain displacement.

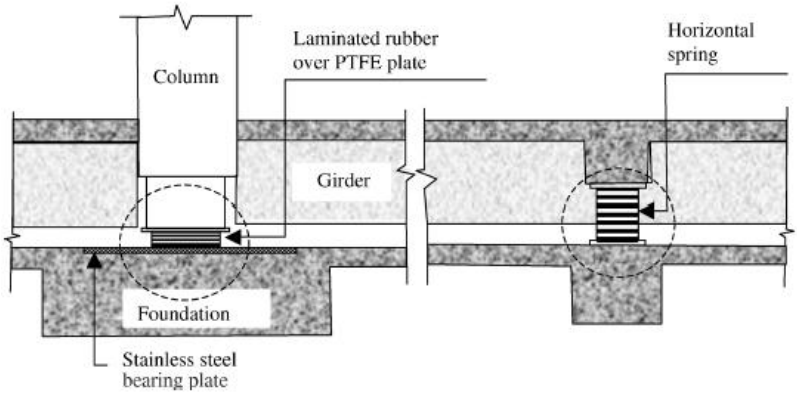

Figure 2.8 TAISEI shake suppression system (Kawamura et al 1988)

An effective mechanism to provide recentering force by gravity has been utilized in the

friction pendulum system (FPS) (Zayas and Low 1990). A spherical sliding interface was introduced to provide restoring stiffness, while the friction between the sliding interfaces helps in dissipating energy as shown in Fig 2.9.

Figure 2.9 Components of the Friction Pendulum System (Eröz M and DesRoches 2008)

The restoring force is provided by the component of the self-weight tangent to sliding surface. However, since the restoring force varies linearly to the sliding displacement, the effectiveness of FPS may reduce particularly in case of high-intensity earthquakes or a low coefficient of friction. To overcome this problem, the variable frequency pendulum isolator VFPI was proposed (Paresh and Sinha 2000), in which the geometry of the concave surface is designed such that the oscillation frequency decreasing with sliding displacement and the restoring force has an upper bound so that the force transmitted to the structure is limited.

Earthquakes with long predominant periods often produce significant displacement responses in the isolators of base-isolated structures. To counter this, an isolator called the multiple friction pendulum system (MFPS) or multi-stage friction pendulum bearing with two spherical concave surfaces and an articulated slider was proposed (Tsai et al 2006), see Fig. 2.10. A follow up research was carried out by Fenz and Constantinou on friction pendulum bearings with two spherical surfaces (DCFP) and distinct friction coefficients on each sliding interface, leading to sliding behavior that exhibits multi-stage hysteretic response (Fenz and Constantinou 2006), see Fig 2.11.

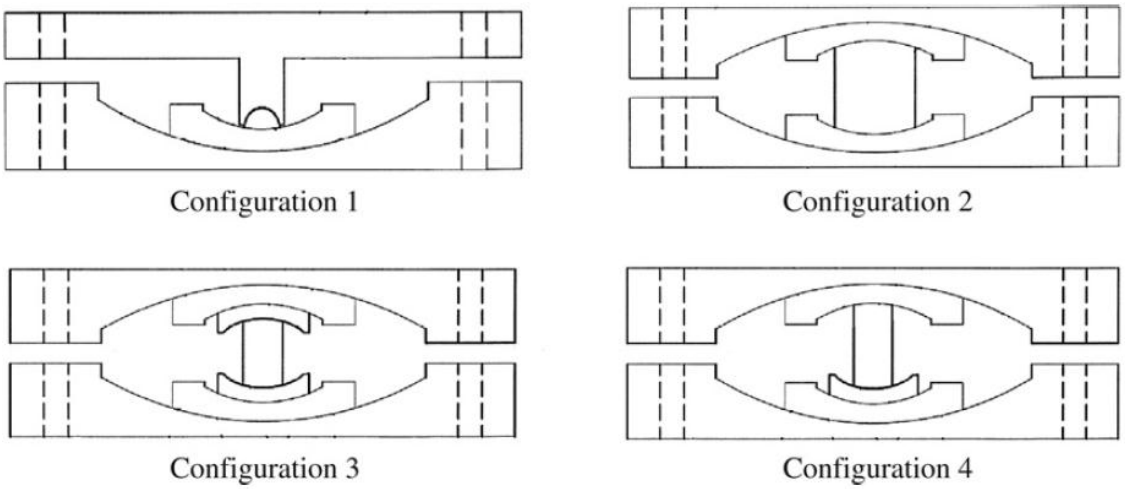

Figure 2.10 Four types of MFPS isolators (Tsai et al 2008)

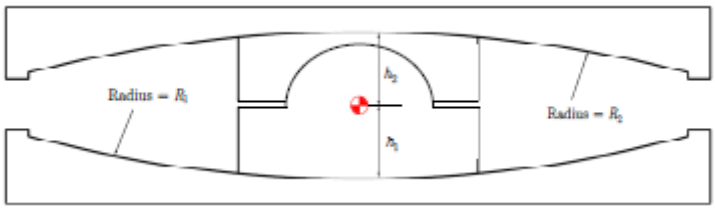

Figure 2.11 Section through DCFP bearing

Recently, RoGlider has been developed for the seismic isolation of both light and heavy vertical loads and can be readily designed to accommodate extreme displacements (Robinson 2006), see Fig 2.12.

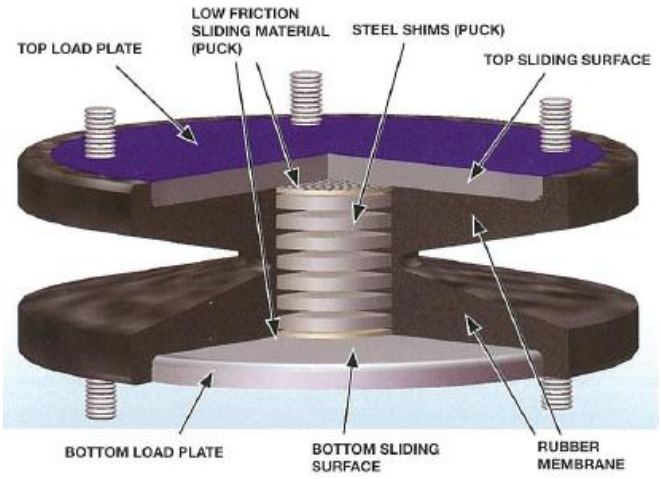

Figure 2.12 Section through RoGlider bearing

The RoGlider is a sliding bearing which includes an elastic restoring force provided by two rubber membranes. This double acting RoGlider consists of two stainless steel plates with a PTFE ended puck sitting between the plates. Two rubber membranes are attached to the puck with each being joined to the top or bottom plates. When the top and bottom plates slide sideways with respect to each other diagonally opposite parts of the membrane undergo tension or compression.

2.3 Uplifting Slide Bearing (UPSS): background, component and mechanism

The 1995 Hyogo-ken Nanbu earthquake caused extensive damage to the transportation infrastructure in and around Kobe, Japan. Of considerable surprise and engineering significance, was the damage of many bridges. Owing to this experience, the demand for seismic isolation system becomes a vital issue. Since then, major construction companies in Japan have been working to develop seismic isolation devices.

Recently, the Uplifting Slide Bearing is a simple sliding device consists of one horizontal and two inclined plane sliding surfaces at both ends set in series (Igarashi et al 2008, Igarashi 2009), as shown in Fig 2.13. These three surfaces are based on PTFE and highly polished stainless steel (SUS) interface.

Figure 2.13 Uplifting Slide Bearing (UPSS)

During normal or low intensity earthquakes, the isolator behaves as a pure friction isolator with sliding only in the horizontal direction. However, during a severe earthquake, sliding will be activated in the inclined surface producing displacements

in both horizontal and vertical directions as shown in Fig 2.14.

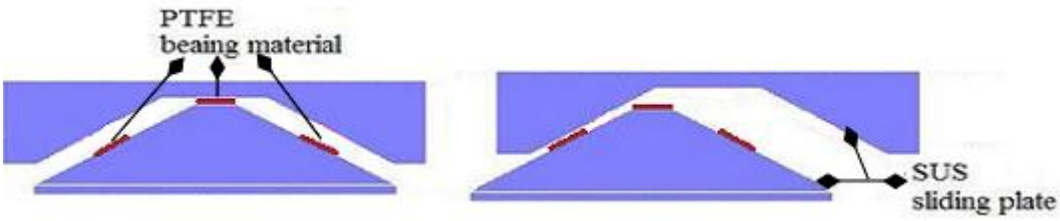

Figure 2.14 Schematic diagram of the UPSS

The concept of this type of bearing was proposed to upgrade the seismic performance of multi-span continuous girder bridges by installing the UPSS on the top of middle piers while the rubber bearings are installed only at the two abutments ends as shown in Fig 2.15.

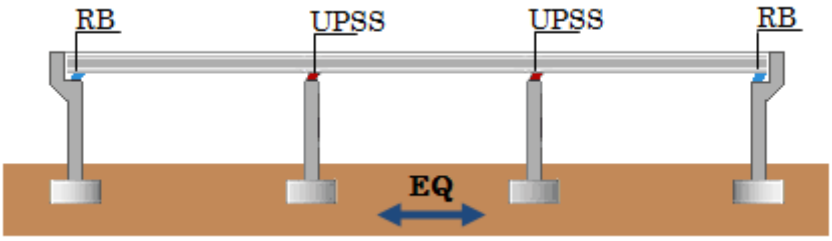

Figure 2.15 Application of bridge isolated with UPSS

The main purpose to develop such a device was to fulfill the need for a seismic isolation device that is simple, and effective in reducing the horizontal displacement with a low cost in order to be implemented in multi-span continuous bridges. It was set forward in competence with the laminated rubber bearings which tend to respond with a large horizontal displacement values during earthquake excitations, which in turn leads to a larger expansion joint and an increase in the maintenance cost. In this research, the concept and principle of operation of the UPSS is adopted and extended to isolate multi-story structures.

The principle of utilizing an inclined plane to achieve a seismic isolation has been found in the taper dry-friction damper wedgeblocks (Dudchenko 2001) as shown in Fig 2.16. Another type of isolators that utilizes a slope surface is the sloped rolling-type bearing. A concept of steel cylinder rolling on a V-shape surface has been proposed (Tsai et al 2007). The basic unit of the rolling type bearing consists of three

components: an upper plate, a sold roller, and a lower plate, as shown in Fig. 2.17.

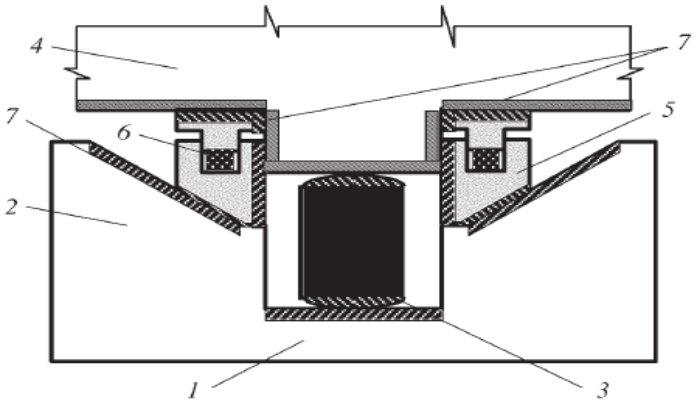

Figure 2.16 Seismic isolation by the taper dry-friction damper (1) Lower support block (2) Can (3)Seismic isolation post with spherical ends (4) Upper support block (5)Wedgeblock damper (6) Elastic element (7) fittings.

(a)

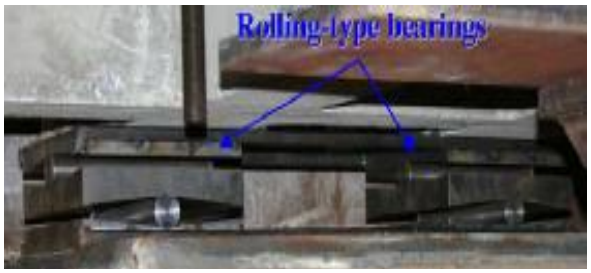

(b)

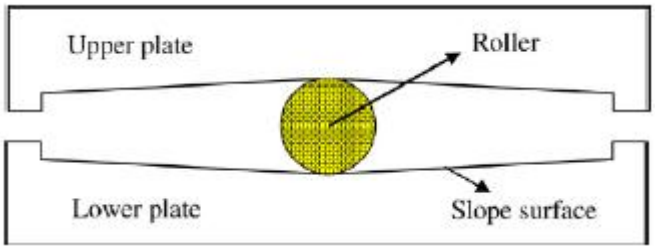

Figure 2.17 (a) The rolling type bearings assembly (b) Schematic of the rolling type

2.4 Uniqueness and advantages of the UPSS bearing

The UPSS bearing possesses unique features depend essentially on the geometrical configuration and the sliding mechanism that make it superior to other types of bearings. These advantages can be summarized as follows:

1. No inherit natural period and therefore, are insensitive to the variation of the frequency content of ground excitation (Mostaghel and Khodaverdian 1987). In other words, they don't resonate to any type of excitation unless extremely strong restoring force overwhelming the friction is applied (Kawamura et al 1988).

2. The acceleration at the base of the structure is limited to the coefficient of friction. Thus, by keeping this coefficient of friction at the sliding interface low, the acceleration is significantly transmitted to the structure reduced.

3. Their outstanding performance in cold temperature testing has proven their efficacy in cold weather regions (Watson 2007).

4. Durability and stability characteristics. Tests of full size sliding bearings show that these isolators retain their full strength and stability throughout their displacement range with high strength factor of safety and with no degradation of hysteretic loop under repeated cyclic loading (Earthquake Protection Systems 2003).

5. The system provides a natural source of damping through friction since the horizontal friction force at the sliding surface offers resistance to motion and dissipates energy. The hysteresis of PTFE-stainless steel interface is a rectangle that provides optimum equivalent viscous damping of $2/\pi = 63.7\%$.

6. Sliding bearings using Teflon as a sliding surface can take much higher compressive stresses than elastomeric bearing (60 MPa or more versus 15 MP or so for elastomeric) and are especially suitable at the ends of shear walls (Kelly et al 2010).

7. The main characteristic of friction-based isolator is the high initial lateral stiffness which is attractive feature to reduce the stiffness of large deformations of isolated buildings and to resist frequent lateral load caused by

wind. For example, most of base isolated high-rise buildings in Japan contain friction-type base isolated systems (Takewaki 2008). In recent years, use of friction-based isolators increases in Japan, and devices having various properties have been made available (Pan et al 2005).

Special features that make UPSS an attractive bearing and a good choice for the designers:

1. Geometrical configuration creativity: the geometry of this device was chosen to help in controlling the horizontal displacement by preventing the motion to be fully activated in the horizontal direction, and allowing part of the earthquake transmitted energy to be transferred into a gravitational potential energy through the diagonal sliding.

2. Avoiding pounding effect by efficiently controlling the displacement: The need for controlling displacement to a minimum level is a vital issue especially in big and crowded cities. Building are often built closely to each other because of the limited availability and high cost of the land, possibly causing pounding of adjacent buildings due to the insufficient or inadequate separation and can be a serious hazard in seismically active area (Agarwal et al 2007, Polycarpou and Komodromos 2010), see Fig 2.18. The verification of UPSS efficiency to control displacement is numerically presented in the following chapters.

Figure 2.18 Adjacent buildings in a crowded city

3. UPSS is a cost effective solution for seismic isolation. Sliding bearings have found more and more applications in recent years over rubber

bearing for economic reasons. UPSS is basically made from three surfaces of stainless steel and PTFE interface. Therefore, the ease of manufacturing adds significant reduction to its cost.

4. The hysteretic behavior of the UPSS provides more freedom in the process of design which requires the determination of three parameters: clearance length (L) i.e. the specified distance prior to the diagonal sliding, the inclination angle (θ) and the friction coefficient (μ) for the three surfaces in contact.

5. The configuration of the device as discussed later has the potential of using different frictional bearing in each plane surface which has been found to add more reduction to the horizontal displacement response.

6. It is worth pointing out that the isolator provides an architecturally flexible and aesthetic solution in terms of integration into the structural system for cases in which space consideration is an important factor, rendering the conventional rubber bearing under walls problematic.

7. The proposed system also offers a feasible solution for seismic retrofitting of existing buildings with soft stories in area where clearance between adjacent buildings is limited. A whole chapter is designated in this thesis to discuss the retrofitting by UPSS.

8. The UPSS is vertically stiff, minimizing the vertical deflections of columns that occur during bearing installation in retrofit application avoiding damage to architectural finishes in upper stories.

9. On the contrary of the friction pendulum system (FPS) which utilizes a spherical sliding surface to develop a restoring force, the slope angle of the inclined surfaces in the UPSS bearing is much larger than the range of the tangential angles of the sliding surfaces of FPS, so that the vertical component of the structural motion is explicitly intended and a constant restoring force is generated due to the parallel component of gravity load along the sliding surfaces.

10. During large displacement response, the horizontal force in the UPSS is kept constant with the increase in displacement. On the other hand, the

curved surface in FPS may result an increase in the horizontal force with larger displacement since the force is directly proportioned to the displacement.

2.5 Maximum displacement reduction principle

The dynamic behavior of the UPSS and its supported can be represented by a simplified free body diagram shown in Figure 2.19. The mechanism of the inclined surface in reducing the peak horizontal displacement in comparison with conventional isolation bearings is described in this section, utilizing the analogy of a dynamic sliding block on an inclined plane. The motion of a mass on a frictional inclined plane is the interplay of different force types and the characterizing features of the incline surface.

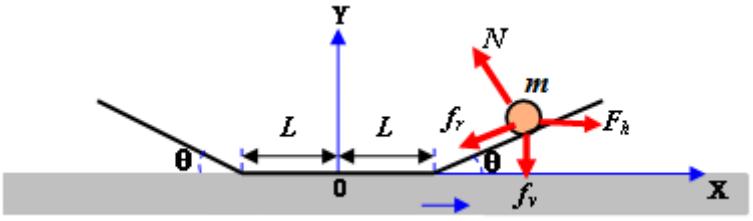

Figure 2.19 Mechanical model of the UPSS bearing

If a block mass (m) placed on an inclined plane, which is accelerated towards left with a horizontal acceleration at the top of first story (a_h), as shown in Fig 2.20.

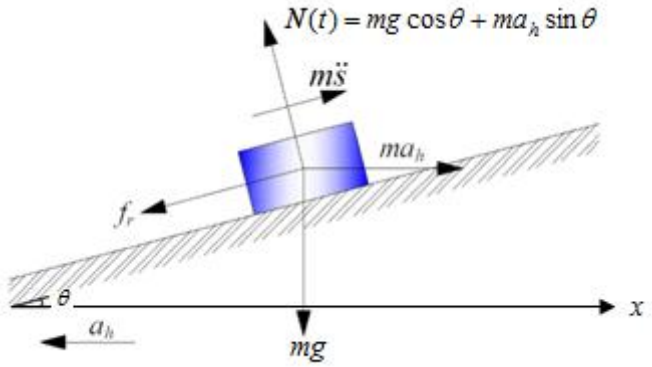

Figure 2.20 Free-body diagrams of an accelerated mass object on an inclined

The angle of incline is (θ) and friction coefficient is (μ) at the contact surface. Assuming the block mass stays in contact with the inclined surface, the normal force (N) is expressed by $N(t) = mg\cos\theta + ma_h \sin\theta$. Therefore, when the mass is sliding upward, the net horizontal reaction force to the block mass, or the reaction force acting on the column top yields to:

$$F_x = m\left[a_h\left(\mu\sin\theta\cos\theta - \sin^2\theta\right) - g\left(\sin\theta\cos\theta + \mu\cos^2\theta\right)\right] \tag{2.1}$$

Based on the energy conservation law, the maximum horizontal displacement (x_{max}) can be written as:

$$x_{\max} = \frac{1}{2}v_\circ^{\,2} \times \frac{\cos\theta}{\left[g\sin\theta - a_h\cos\theta + \mu g\cos\theta + \mu a_h\sin\theta\right]} \tag{2.2}$$

where v_o is the initial velocity, if the horizontal acceleration (a_h) is assumed to be constant within the duration of sliding considered. Combining Eq. (1) and Eq. (2), x_{max} can be expressed as:

$$x_{\max} = \frac{1}{2}mv_\circ^{\,2} \times \frac{\cos^2\theta}{-F_x + ma_h\left[2\mu\sin\theta\cos\theta - 1\right]} \tag{2.3}$$

In the same manner, the maximum horizontal displacement for the conventional rubber bearing (x_{rmax}) assuming the simplest case where the conventional isolation bearing's resisting horizontal forces (F_x) are kept constant can be represented:

$$x_{r\max} = \frac{1}{2}mv_\circ^{\,2} \times \frac{1}{-F_x - ma_h} \tag{2.4}$$

The above formulation can also be seen as a flat plane when setting θ equal to zero in Eq. (3). This is useful observation for assessing the reduction effectiveness of the inclination surface. Comparing Eqs. (3) and (4) reveals that x_{max} is always less than the $x_{r,max}$ i.e.

$$\frac{x_{\max}}{x_{r\max}} = \left[\cos^2\theta \times \frac{-F_x - ma_h}{-F_x - ma_h\alpha}\right] < 1.0 \tag{2.5}$$

where $\alpha = [1 - 2\mu \sin\theta \cos\theta]$ is a constant less than unity for any combinations of θ and μ. Eq. (5) implies the effectiveness of inclined surface in reducing the peak horizontal displacement compared to conventional isolation bearings for the same level of horizontal reaction force on the first story top column. The fraction of reduction depending mainly on both factors simultaneously: $\cos^2\theta$ and α.

2.6 Rigid body response of UPSS under horizontal excitation

A general formulation for the equation of motion can be written depending on the direction and section of sliding. These have a great significance because the direction determines if the most "deleterious" pulses of the excitation tend to move the block mass upward or downward (Gazetas et al 2009). For the flat plane section, two phases can be identified sliding and non-sliding phases. In the non-sliding phase, the shear force at the interface is smaller than the resistance friction force and the structure can be treated as a fixed base system. Once the lateral shear force exceeds the friction force the structure will start to slide. The horizontal friction force at the sliding interface offers resistance to relative motion and help in dissipating the energy of structural response. The relative acceleration response can be written for both cases as:

$$\ddot{x}(t) = \begin{cases} 0 & \Rightarrow \textit{stick phase} \\ -\mu g \,\mathrm{sgn}(\dot{x}(t)) - a_h(t) & \Rightarrow \textit{sliding phase} \end{cases} \tag{2.6}$$

where sgn( ) is the signum function. The maximum absolute acceleration is $|\ddot{x}_a| = \mu g$. For the inclined plane section, the normal force can be written for the right side and left slope as follows:

$$N(t) = m\left(g\cos\theta \pm a_h(t)\sin\theta\right) \tag{2.7}$$

Since the critical acceleration of the mass directly depends on the direction of excitation, upward and downward motions are dealt separately. It is clear that the horizontal acceleration a_h must be either,

$$\begin{cases} a_h \le -\dfrac{\mu\cos\theta - \sin\theta}{\cos\theta + \mu\sin\theta} \rightarrow downward \\ a_h \ge \dfrac{\mu\cos\theta + \sin\theta}{\cos\theta - \mu\sin\theta} \rightarrow upward \end{cases} \tag{2.8}$$

for the transition from the stick phase to the sliding phase. This implies that higher inertia force is required to trigger the upward sliding than that in the downward direction. This is another insight on the effectiveness of the proposed geometry in reducing the peak displacement. An extensive series of shaking table tests of the multiple-slider bearing were performed by Igarashi et al. [Igarashi et al 2009, Igarashi et al.2010], and the effect of the maximum displacement has been experimentally confirmed.

A proper design of the isolator is accomplished by understanding the sensitivity of selecting the device parameters and their effects in de-amplification of the input motion. The multiple-slider bearing is defined by three main factors: The clearance (L) i.e. the horizontal distance prior the sliding along the inclined surface, the inclination angle (θ) and the friction coefficient (μ).

References

Agarwal VK, Niedzwecki JM, van de Lindt JW. Earthquake induced pounding in friction varying base isolated buildings. *Engineering Structures* 2007; 29 (11): 2825–2832.

Buckle I, Mayes R. Seismic isolation: history, application and performance a world overview. *Earthquake Spectra* 1990; 6(2): 161-202.

Dudchenko SV. Damping of a seismically isolated building by dry-friction wedgeblocks. *Journal of Mathematical Sciences* 2001; 103(3): 169–173

Earthquake Protection Systems. *Technical Characteristics of Friction Pendulum Bearings*. Vallejo: California; 2003.

Eröz M, DesRoches R. Bridge seismic response as a function of the friction pendulum system (FPS) modeling assumptions. *Engineering Structures* 2008; 30**:** 3204–3212.

Fenz DM, Constantinou MC. Behaviour of the double concave Friction Pendulum bearing. *Earthquake Engineering and Structural Dynamics* 2006; 35(11):1403-1422.

Gazetas G, Garini E, Anastasopoulos I, Georgarakos T. Effects of near-fault ground shaking on sliding systems. *ASCE Journal of Geotechnics and Geoenvironmental Engineering* 2009; 135(12): 1906–1921.

Gueraud R, N.-Leroux JP, Livolant M, Michalopoulos AP. Seismic isolation using sliding-elastomer bearing pads, *Nuclear Engineering and Design* 1985; 84: 363-377.

Iemura H, Jain SK, E. Pradono MH. Seismic Base Isolation and Vibration Control, *Chapter 29 of the Vibration and Shock Handbook*, Editor-in-Chief, C.W. de Silva, CRC Press, Taylor & Francis Group, LLC, 2005.

Igarashi A, Adachi Y, Kato Y, Uno H, Sato T. et al. Development of Uplifting Slide Bearing (1)-(3) (11 papers). Proceedings of 64th JSCE Annual Meeting 2009; 785-794, 798-808 (in Japanese).

Igarashi A, Sato T, Shinohara M, Katou Y, Uno H, Adachi Y, Takahashi T. Uplifting Slide Bearing (1) – Characterization of Dynamic Properties. *34th IABSE Symposium on Large Structures and Infrastructures for Environmentally Constrained and Urbanised Areas*, Venice, Italy 2010; 1-8.

Igarashi A, Sato T, Shinohara M, Katou Y, Uno H, Adachi Y. Uplifting Slide Bearing (2) – Verification of Seismic Response by Tests. *34th IABSE Symposium on Large Structures and Infrastructures for Environmentally Constrained and Urbanised Areas*, Venice, Italy 2010; 47-54.

Igarashi A, Sato T, Shinohara M, Katou Y, Uno H, Adachi Y. Uplifting Slide Bearing (3) – Development of the Analytical Model. *34th IABSE Symposium on Large Structures and Infrastructures for Environmentally Constrained and Urbanised Areas*, Venice, Italy 2010; 55-62.

Igarashi A, Sato T, Shinohara M, Katou Y, Uno H, Adachi Y. Uplifting Slide Bearing (4) – Application for a 3-Span Steel Girder. *34th IABSE Symposium on Large Structures and Infrastructures for Environmentally Constrained and Urbanised Areas*, Venice, Italy 2010; 24-30.

Islam ABMS, Jameel M, Jumaat MZ. Seismic isolation in buildings to be a practical reality: Behavior of structure and installation technique. *Journal of Engineering* Technology Research 2011; 3(4):97-117.

Jangid R, Data TK. Seismic behavior of base isolated buildings-A state-of-the art-review. *Journal of Structures and Buildings* 1995; 110: 186–203.

Jangid RS, Londhe YB. Effectiveness of rolling rods for base isolation, *Journal of Structural Engineering*, ASCE 1998; 124, 469-472.

Kawamura S, Kitazawa K, Hisano M, Nagashima I. Study of a sliding-type base isolation system - system composition and element properties. *Proceedings of 9th WCEE*, Tokyo-Kyoto 1988; 5: 735-740.

Kelly, James M. *Earthquake-Resistant Design With Rubber*, London, Spinger-Verlag Limited 1997.

Kelly TE. Base Isolation of Structures. Design Guidelines, Holmes Consulting Group Ltd. 2001.

Kelly T, Skinner R, and Robinson B. Seismic Isolation for Designers and Structural Engineers. *National Information Center of Earthquake engineering* (NICEE); 2010.

Kunde MC, Jangid RS. Seismic behavior of isolated bridges: A state-of-the-art review. Electronic *Journal of Structural Engineering* 2003; 3: 140-170.

Li L. Base isolation measure for aseismic building in China. *Proc. of the 8th World Conference on Earthquake Engineering* 1984, San Francisco, CA.

Lin TW, Hone CC. Base isolation by free rolling rods under basement, *Earthquake Engineering and Structural Dynamics* 1993; 22: 261-273.

LU L, Yang Y. Dynamic Response of Equipment in Structures with Sliding Support. *Earthquake Engineering and Structural Dynamics* 1997; 26: 61-77.

Mostaghel N, Tanbakuchi J. Response of Sliding Structures to Earthquake Support Motion. *Earthquake Engineering and Structural Dynamics* 1983; 11: 729-748.

Mostaghel, N, Khodaverdian, M. Dynamics of Resilient-Friction Base Isolator (R-FBI). *Earthquake Engineering and Structural Dynamics* 1987; 15: 379-390.

Naeim F, Kelly J. *Design of Seismic Isolated Structures*. John Wiley: England; 1999.

Polycarpou PC, Komodromos P. Earthquake-induced poundings of a seismically isolated building with adjacent structures. *Engineering Structures* 2010; 32: 1937-1951.

Paresh M, Ravi Sinha. VFPI: an isolation device for aseismic design. *Earthquake engineering and structural dynamics* 2000; 29: 603-627.

Pan P, Zamfirescu D, Nakashima M, Nakayasu N, Kashiwa H. (2005). Base-isolation design practice: in Japan: Introduction to the post-Kobe approach, *Journal of Earthquake Engineering* 2005; 9(1): 147:171.

Qamaruddin M. A-state-of-the-art-review of Seismic Isolation Scheme for Masonry Buildings. ISET *Journal of Earthquake Technology* 1998; Paper No. 376, 35(4): 77-93.

Robinson WH, Gannon CR, Meyer J. The RoGliderTM – A sliding bearing with an elastic restoring force. *Bulletin of the New Zealand Society of Earthquake Engineering* 2006; 39(1), 81–84.

Skinner R, Robinson W. *An Introduction to Seismic Isolation*. England: John Wiley;

1993.

Su L, Ahmadi G, Tadjbakhsh IG. A comparative study of performance of various base isolation systems, Part. I: shear beam structures. *Earthquake Engineering and Structural Dynamics* 1989; 18: 11-32.

Su L, Ahmadi G, Tadjbakhsh IG. Performance of sliding resilient friction base isolation system. *Journal of Structural Engineering* 1991; 117: 165-181.

Takewaki I. Robustness of base-isolated high-rise buildings under code-specified ground motions. *The Structural Design of Tall and Special Buildings* 2008; 17: 257–271.

Tsai CS, Chen WS, Chiang TC, Chen BJ. Component and shaking table tests for full scale multiple friction pendulum system. *Earthquake Engineering and Structural Dynamics* 2006; 35(13):1653–75.

Tsai CS, Lu PC, Chen WS, Chiang TC, Yang TC, Lin YC. Finite element formulations and shaking table tests of direction-optimized friction pendulum system. *Engineering Structures* 2008; 30(9),2321-2329

Tsai M-H, Wu S-Y, Chang K-C, Lee GC. Shaking table tests of a scaled bridge model with rolling-type seismic isolation bearings. *Engineering Structures* 2007; 29(5):694–702.

Watson RJ. Sliding Isolation Bearings in Cold Weather Climates. In: Khaled M. Mahmoud, editor. *Innovations in Bridge Engineering Technology*. London: Taylor and Francis Group 2007; 103-110.

Westermo B, Udwadia F. Periodic response of a sliding oscillator system to harmonic excitation. *Earthquake Engineering and Structural Dynamics* 1983; 11:135-146.

Vafai A, Hamid M, Ahmadi G. Numerical Modeling of MDOF structures with sliding supports using rigid-plastic link. *Earthquake Engineering and Structural Dynamics* 2001; 30: 27-42.

Yang YB, Lee TY, Tsai IC. Response of multi-degree-of-freedom structures with sliding supports. *Earthquake Engineering and Structural Dynamics* 1990; 19: 739-752.

Younis CJ, Tadjbakhsh IJ. Response of sliding rigid structure to base excitation. *Journal of Engineering Mechanics* 1984; 110: 417-432.

Zayas V, Low S. A Simple Pendulum Technique for Achieving Seismic Isolation. *Earthquake Spectra* 1990; 6(2), *Earthquake Engineering Research Institute*, Oakland, California.

Chapter 3

An investigation on the efficiency of implementing a plane surface in FPS based on the concept of UPSS

The third chapter of this dissertation intends to examine the UPSS concept based on the perception of friction pendulum system (FPS) due its maturity and well recognition as a very efficient tool for controlling the seismic response of a structure during an earthquake. The main objectives are to investigate the efficiency of implementing a plane surface in sliding isolators in the analogy of the clearance length in the UPSS and to study its influence on the seismic response of multi-story base-isolated structure.

3.1 Introduction

The sliding surface of UPSS consists of one horizontal and two inclined plane sliding surfaces on both ends as shown in Fig 2.13. The general mechanism can be seen similar to the concept of FPS, if we consider the radius of curvature is infinite at both side or a restoring mechanism such as laminated rubber bearing is provided. However, the main difference is the presence clearance distance due to the central horizontal surface.

This study intends to focus on the effect of the horizontal plane sliding part on the response of isolated multistory building under harmonic motion. Analogy to the UPSS isolator, a modified FPS with plane surface is used in this study. The main objectives

of this study can be stated as: (i) identify the mechanism and operation of FPS with plane sliding surface, hereafter MFPS; (ii) investigate the efficiency of implementing a plane surface in sliding isolators (iii) examine the behavior of multistory building isolated by MFPS; (iv) comparative study between MPFS with other sliding isolator namely, pure friction isolator PF and FPS.

3.2 *Friction Pendulum System with horizontal sliding surface (MFPS)*

Modifying FPS in analogy with the UPSS is shown in Fig 3.1. Where W is the total weight of superstructure, R is the radius of curvature of the sliding surface, L is the length of the plane sliding surface, μ is the friction coefficient, and N is the normal weight. The presence of a horizontal sliding part in this arrangement has an advantage in delaying the uplift mechanism of the FPS which may contribute in reducing the restoring force in the FPS which varies linearly with the sliding displacement. Besides, this bearing does not restrain the superstructure's thermal expansion and contraction.

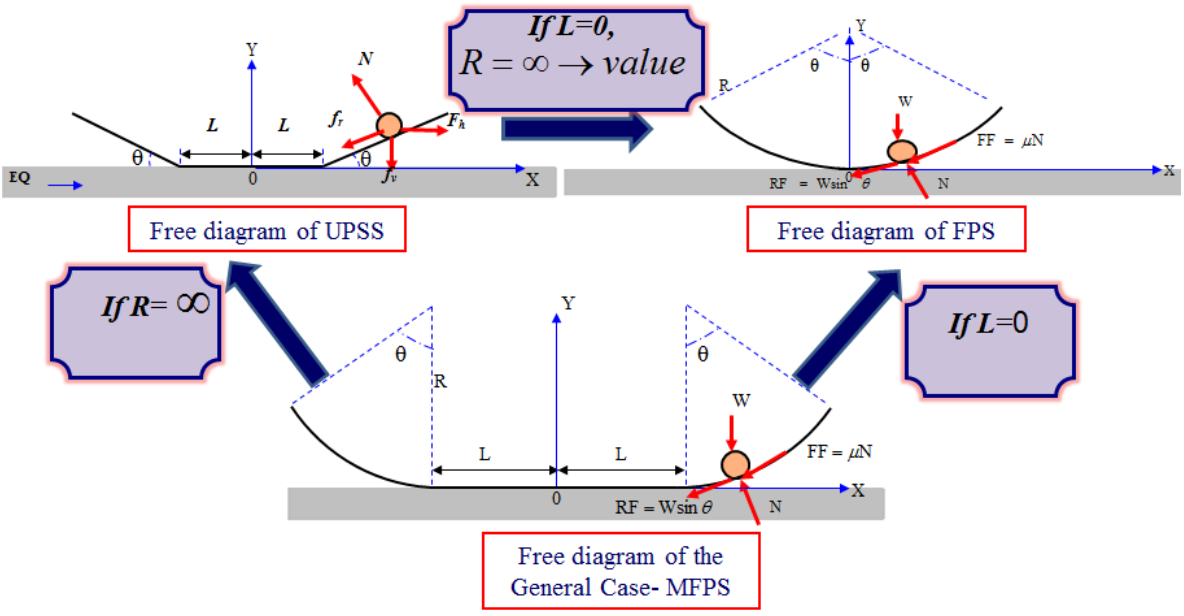

Figure 3.1 Relationship of the three sliding bearings: UPSS, FPS and MFPS

The MFPS bearing can be seen as a dual combination of PF and FPS. Therefore, this device performs as a PF at low or medium excitation in which maximum restoring force would be limited to frictional yielding limit as long isolator displacement does not exceed the clearance value (L) value. Therefore, the hysteresis loop of MPFS can be plotted as shown in Fig 3.2. It can be stated that FPS hysteresis loop is a special case of MFPS when L equal zero. In the same manner, UPSS hysteresis loop is also a special case of MFPS when radius of curvature is infinity. In the next section, the response of multi-story shear-type building isolated by MFPS subjected to harmonic excitation is simulated. The response of isolated structures with PF and FPS are also compared with performance. Only unidirectional harmonic excitation is considered in this example.

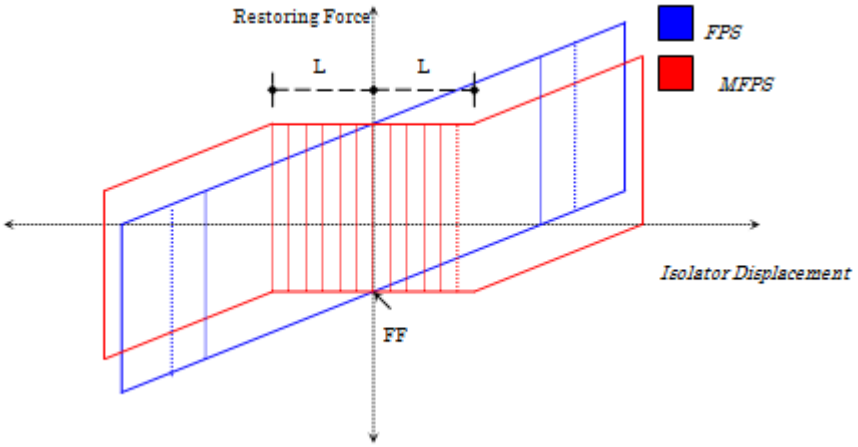

Figure 3.2 Force-displacement relationship of the MFPS and UPSS bearing

3.3 Modeling of isolated shear-type building by MFPS

For the purpose of illustration three-story shear type building will be studied as shown in Fig. 3.3. The properties of the model are adopted from reference (Fan et al 1990a). It is assumed that $m_{1\text{-}3}/m_b$=1.0 and the stiffness for all stories are set equal. The fundamental period of the fixed base building T_1 is 0.3 s and the damping ratio for the fundamental mode ζ_1 is 0.02, and the natural frequencies and modal damping are as follows: $\omega_2 = 2.802\,\omega_1$, $\omega_3 = 4.049\,\omega_1$,and ζ_1 =2.802 , ζ_1=4.049 .

The proposed MFPS isolator requires the specification of three parameters to be modeled, namely friction coefficient μ, length of flat sliding part L and the isolation period T_b. The MFPS isolator properties for the building have been chosen to give a period of isolation T_b is 4.0 s. The friction coefficient of the MFPS is assumed to be independent of the relative velocity of sliding i.e. Coulomb friction. This assumption does not affect the peak responses of the structure and lead only to slight changes in the spectra curves (Fan et al 1990a). The frictional coefficient μ is taken 0.1 and the length L is taken 10cm.

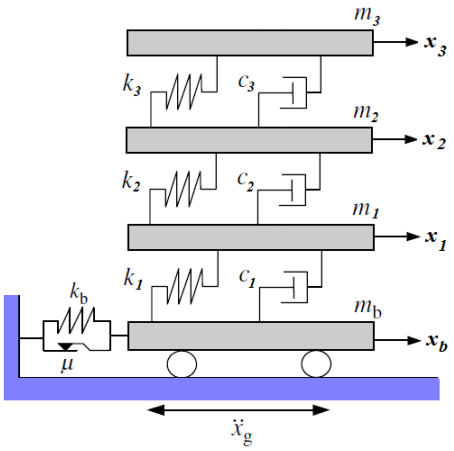

Figure 3.3 Three-story shear-building isolated by MFPS

The mathematical formulation of the response has been developed based on various assumptions which are commonly used in the field of analyzing isolated structures and do not introduce large errors on response calculations (Paresh and Sinha 2000):

I. The overturning or tilting effect of the structure during sliding has been neglected.

II. All floors in the structural model are assumed rigid.

III. The superstructure is assumed to behave elastically linear which is compatible with the main purpose of base isolation.

IV. Only unidirectional harmonic excitation is considered.

V. The post yielding stiffness of the isolator K_b is assumed linear and can be approximately calculated by Eq. (3.1).

$$K_b = \frac{W}{R} \tag{3.1}$$

Where W is the total weight of superstructure, R is the radius of curvature of the sliding surface. The isolation period T_b of MFPS is only related to the radius R at both ends which can be expressed in Eq. (3.2).

$$T_b = 2\pi\sqrt{\frac{R}{g}} \tag{3.3}$$

where g is the gravitational acceleration.

3.4 Mathematical formulation

The isolated structures by sliding devices subjected to ground excitation are subjected to repeatedly transition phases between stick and slip phases, which introduce discontinuity and high nonlinearity. One of the most efficient methods which have been proposed for solving the discontinuities occurring in analysis of sliding structure is the frictional spring method (Yang et al 1990). Later this method has been reformulated the method into a state-space form for the analysis of equipment mounted on a sliding structure (Lu and Yang 1997). By this method, a fictitious spring, K_f, is introduced between the base mat and the ground, as in Fig. 3.4, to represent the mechanism of friction. The fictitious spring constant K_f is taken as zero for the sliding phase and as a very large number for the non-sliding phase. This can be assumed true knowing that sliding frictional isolator incapable of reproducing truly rigid-plastic behavior as Teflon-steel interfaces undergo some very small elastic displacement before sliding (Constantinou et al 1990). This displacement consists primarily of small elastics shear deformation of Teflon.

The equation of motion as a result can be written as follows:

$$[M]\{\ddot{x}(t)\}+[C]\{\dot{x}(t)\}+[K]\{x(t)\}+\{r_1\}f_n(t)=-[M]\{r_2\}\ddot{x}_g(t) \tag{3.4}$$

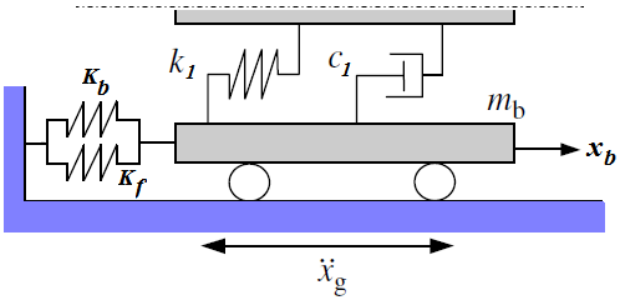

Figure 3.4 Model of shear building isolated by MFPS

Where the mass matrix [*M*] is

$$[M]=\begin{bmatrix} m_1 & 0 & 0 & 0 \\ 0 & m_2 & 0 & 0 \\ 0 & 0 & m_3 & 0 \\ 0 & 0 & 0 & m_b \end{bmatrix} \tag{3.5}$$

in which m_1 to m_3 is the mass of each floor and m_b is the foundation mass, and damping matrix [*C*] is

$$[C]=\begin{bmatrix} c_1 & -c_1 & 0 & 0 \\ -c_1 & c_1+c_2 & -c_2 & 0 \\ 0 & -c_3 & c_2+c_3 & -c_3 \\ 0 & 0 & -c_3 & c_3 \end{bmatrix} \tag{3.6}$$

in which c_1 to c_3 is the viscous damping of each floor. The matrix [*C*] has been constructed based on either the modal damping or Rayleigh type. Stiffness matrix [*K*] is

$$[K]=\begin{bmatrix} k_1 & -k_1 & 0 & 0 \\ -k_1 & k_1+k_2 & -k_2 & 0 \\ 0 & -k_2 & k_2+k_3 & -k_3 \\ 0 & 0 & -k_3 & k_3+k_b \end{bmatrix} \tag{3.7}$$

in which k_1 to k_3 is the stiffness of each floor and k_b is the stiffness of isolator as defined previously.

Relative displacement $\{x(t)\}$, velocity $\{\dot{x}(t)\}$ and $\{\ddot{x}(t)\}^T$ acceleration vectors of the isolated structure are defined respectively as follows:

$$\{x(t)\}^T = \{x_1 \quad x_2 \quad x_3 \quad x_b\}^T \tag{3.8}$$

$$\{\dot{x}(t)\}^T = \{\dot{x}_1 \quad \dot{x}_2 \quad \dot{x}_3 \quad \dot{x}_b\}^T \tag{3.9}$$

$$\{\ddot{x}(t)\}^T = [\ddot{x}_1 \quad \ddot{x}_2 \quad \ddot{x}_3 \quad \ddot{x}_b]^T \tag{3.10}$$

f_n is the non-linear isolator force. The structure will remain in non-sliding phase as long as the frictional force f_r mobilized at the interface of isolator attains the limiting frictional force i.e. $|f_r|$ < frictional force limit and once exceeded the structure starts to slide. f_r can be represented as:

$$fr = \begin{cases} K_f x_b; & for\ non-sliding\ phase \\ \mu W \operatorname{sgn}(\dot{x}_b); & for\ sliding\ phase \end{cases} \tag{3.11}$$

Force distribution loading vectors r_1 and r_2 are defined respectively as:

$$r_1 = \{0 \quad 0 \quad 0 \quad 1\}^T \tag{3.12}$$

$$r_2 = \{1 \quad 1 \quad 1 \quad 1\}^T \tag{3.13}$$

A sinusoidal ground motion excitation used in this study is given as:

$$\ddot{x}_g = a \sin(2\pi t / T_g) \tag{3.14}$$

where a is the excitation intensity taken as 0.80g, T_g is the period of harmonic excitation taken as 0.8 s.

Due to the high nonlinearity hysteretic behavior of the isolator classical modal superposition cannot be used to solve the second order deferential equation of motion. Therefore, Numerical technique in a small incremental step by step form has been used to solve the problem. Newmark β-method technique has been used (Newmark 1959), assuming average acceleration method i.e. β=1/4, γ=1/2, making the use of the

advantage of this technique of being unconditionally stable. The development of the time stepping method is based upon the following two equations:

$$[\dot{x}_{i+1}] = [\dot{x}_i] + (1-\gamma)\Delta t\ [\ddot{x}_i] + (\gamma\Delta t)[\ddot{x}_{i+1}] \tag{3.15}$$

$$[x_{i+1}] = [x_i] + (\Delta t)[\dot{x}_i] + (0.5-\beta)(\Delta t)^2[\ddot{x}_i] + \left(\beta(\Delta t)^2\right)[\ddot{x}_{i+1}] \tag{3.16}$$

Programming and simulation for the isolated three-story shear type building has been done by the assistance of MATLAB software.

For the purpose of comparison of responses, PF and FPS are considered. In which the isolators' properties where taken as: μ is 0.1 for both bearings and isolation period for FPS T_b is 4.0.

3.5 Simulation Results

In the proceeding discussion, the analysis results of the three isolated shear-type building by MFPS are presented. For the isolated structures, the response quantities of interest are isolator displacement x_b and top absolute floor acceleration $\ddot{x}_a$, due to the fact that acceleration is directly proportioned to the force exerted on the structure and displacement of isolator is one of the most important parameter in the process of design.

Fig 3.5a shows the top absolute acceleration response of the isolated building by MFPS compared with the fixed based structure. The time history shows clearly the efficiency of MPFS in reducing the acceleration response more than two times the fixed base i.e. from 1.34g to 0.62g. The peaks seen in Fig 3.5 are generated by the slip-stick action due to the sudden changes in friction force value in the transition phase which exerts shock impulses on the support.

Fig 3.5b shows that the sliding device is very efficient in preserving the structure from the energy content of earthquake excitation and a very small portion of strain energy has been transmitted to the superstructure. The same true for base shear transmitted to the superstructure which has been reduced about 5 times the peak response of fixed based structure, Fig 3.5c.

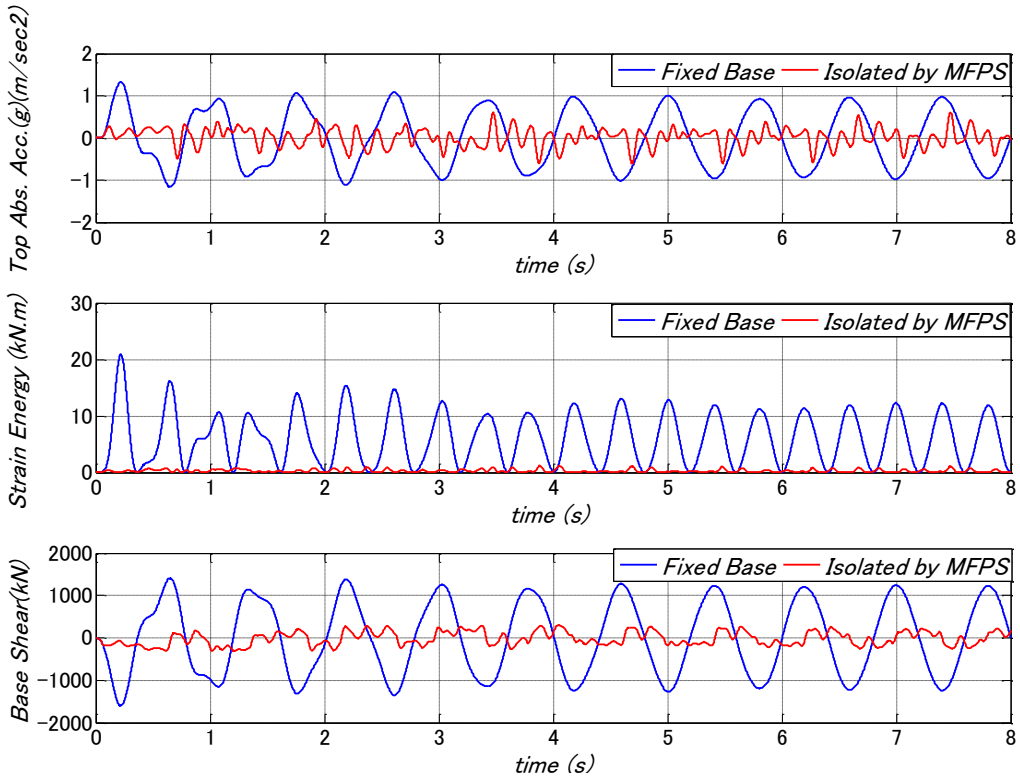

Figure 3.5 Comparison of fixed base and isolated building by MFPS

In Fig. 3.6b the isolated superstructure behaves as a rigid body in contrast with its behavior in the case of fixed base superstructure Fig 3.6a.

The displacement response history of each floor in Fig 3.6b returns to original position without any residual displacement at the end of the excitation. Fig 3.6c indicates the mechanical characteristics of the non-linear device of MPFS. The enclosed area in the diagram represents the portion of the energy dissipated by friction mechanism at the sliding interface. The hysteretic loop shows a softening in the restoring force in comparison with the FPS ideal hysteretic loop due to implementing the horizontal plane surface *L*.

The comparison of response performance of three different sliding isolators namely, PF, FPS and MFPS for the same building configuration mentioned above has been conducted. Fig 3.7 demonstrates that PF bearing exhibits the largest displacement of the isolators and results in a high residual displacement at the end of the excitation

action.

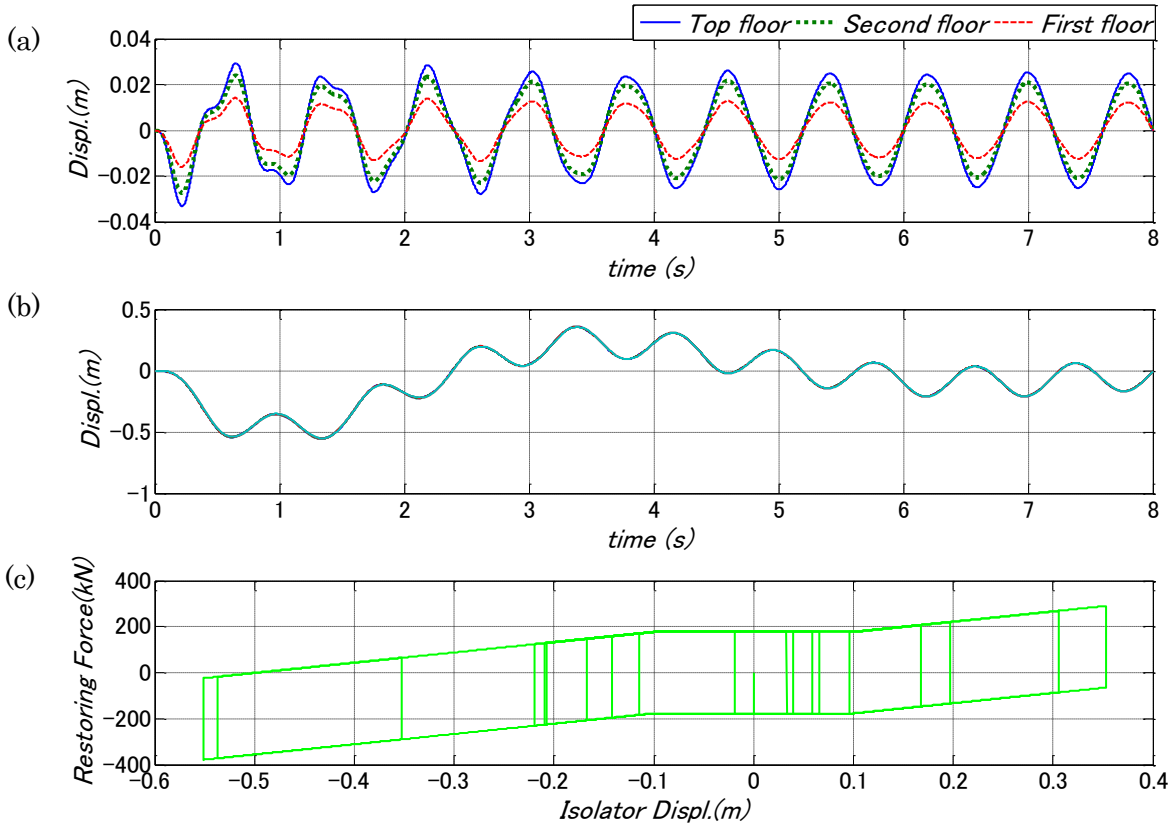

Figure 3.6 (a) Displacement response for fixed base building (b) Displacement response for isolated building by MFPS (c) Hysteresis loop of MFPS

The reduction in base shear is in the expense of increasing the horizontal displacement. The peak top absolute acceleration of PF leads also to a higher response of 0.77g than the other isolators. Due to the aforementioned observations, the FPS and MPFS gives a better performance than PF.

MPFS and FPS have similarity behavior except that the presence of the plane surface *L* has modified the hysteresis loop of MFPS in which the effect can be seen clearly in Fig 3.7c which contains a combined behavior of both PF and FPS. This leads to a reduction in the base shear and strain energy Fig 3.8 make the performance of MFPS the most efficient isolator in our case study. For example, the peak base shear for PF, FPS, and MFPS respectively is 340, 370, 315 kN, and the maximum strain energy exerted as 2.1, 1.4, 1.2 kN.m.

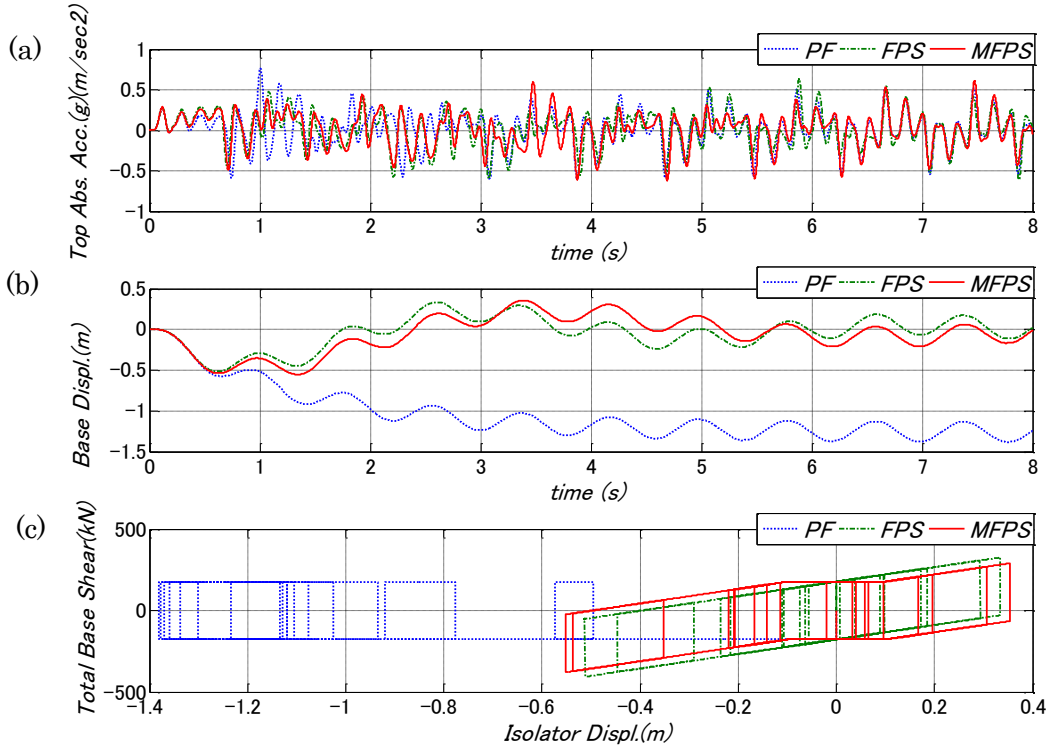

Figure 3.7 (a) Top absolute acceleration response (b) Displacement response (c) Hysteresis loop for isolated building with three different isolators PF, FPS, and MFPS

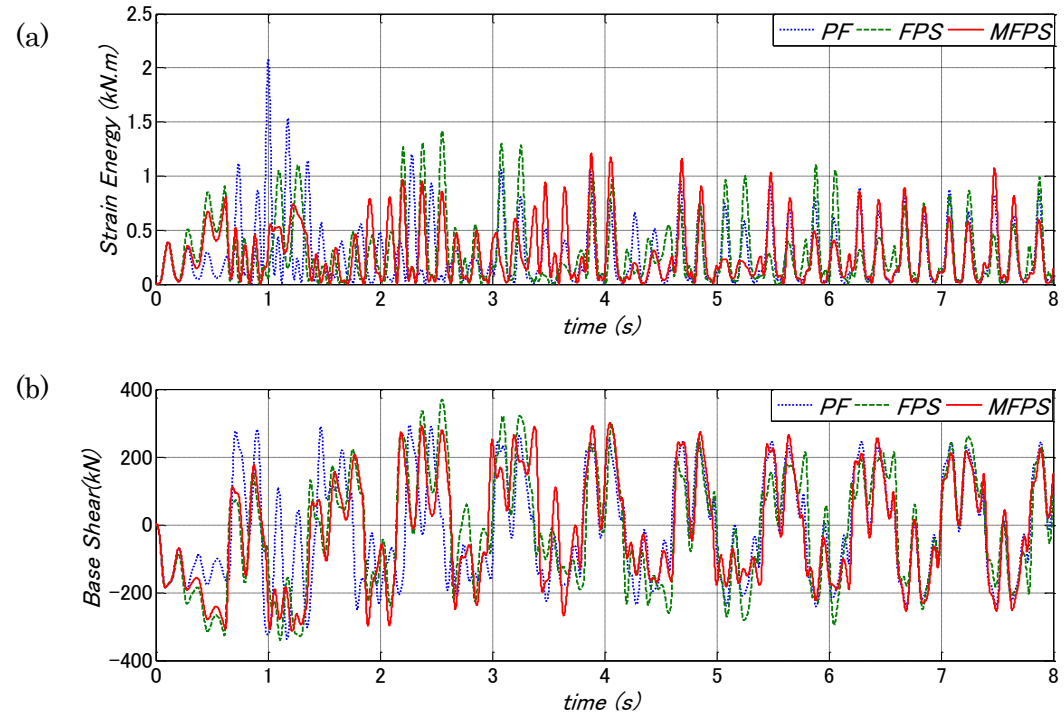

Figure 3.8 (a) Strain Energy (b) Base shear for isolated building with three different

Conclusions

Investigation the efficiency of implementing a plane surface in sliding isolators and its influence on the seismic response of multi-story base-isolated structure is carried out. FPS is modified in analogy with the UPSS to examine the plane surface effect on superstructure responses. For the purpose of illustration three-story shear type building isolated by MFPS is studied. Also, a comparative study with other sliding isolators such as PF and FPS is performed. From the trend of the numerical analysis the following results can be drawn:

1. MFPS shows effectiveness in reducing acceleration and base shear response compared to the fixed base superstructure. Besides, its efficiency in preserving the structure from the energy content of earthquake excitation.

2. The residual isolator displacement can be controlled to a minimum values using MFPS.

3. MPFS exhibits a dual behavior of PF and FPS. However, MFPS gives a better performance than PF. Also, MPFS can be superior to FPS if isolator's properties i.e. Length L, friction coefficient μ and radius of curvature R; are chosen carefully based on a series of sensitivity analysis.

4. Selecting the length of plane sliding surface should be decided through sensitivity analysis for an optimum and superior results.

References

Constantinou M., Mokha A., Reinhorn A.. Teflon Bearing in Base Isolation II: Modeling. *Journal of Structural Engineering* 1990; 116 (2): 455-473.

Fan FG, Ahmadi G, Tadjbakhsh IG. Multi-storey base-isolated buildings under a harmonic ground motion. Part I: A comparison of performances of various systems. *Nuclear Engineering and Design* 1990a; 123: 1-16.

Fan FG, Ahmadi G, Tadjbakhsh IG. Multi-storey base-isolated buildings under a harmonic ground motion. Part II: Sensitivity analysis. Nuclear Engineering and Design 1990b; 123:17-26.

Lu LY, Yang YB. Dynamic response of equipment in structures with sliding support, *Earthquake Engineering and Structural Dynamics* 1997; 26: 61-77.

Newmark NM. A method of computation for structural dynamics. *Journal of Engineering Mechanics ASCE* 1959; 85: 67-94.

Paresh M, Ravi Sinha. VFPI: an isolation device for aseismic design. Earthquake engineering and structural dynamics 2000; 29:603-627.

Yang YB, Lee TY, Tsai IC. Response of multi-degree-of-freedom structures with sliding supports. *Earthquake Engineering and Structural Dynamics* 1990; 19: 739-752.

Chapter 4

Dynamic response control of Multi-story structures by the UPSS: A parametric study

This chapter aims to investigate the efficiency of using the multiple-slider bearing based on the concept of UPSS to isolate multi-story shear type structures. The principles of operation and force displacement relationship for the isolator are introduced. The seismic behavior of the base isolated building by the UPSS bearing subjected to seismic excitation is investigated, comparing with conventional rubber bearing and pure friction slider isolating systems. Moreover, extensive parametric investigations are performed in order to achieve an optimum performance of the isolator with respect to three main properties which define the device: clearance length, the inclination angle and the friction coefficient. The results show the effectiveness of the UPSS in minimizing the damage from earthquakes. The UPSS proves to have a high potential in minimizing the effect of the ground displacement pulses through its operation mechanism and its unique feature that permits the use of different set of friction coefficients on each sliding surface. In addition, a principle to define the optimum value of the friction coefficient is developed.

4.1 Simplified Mathematical Model

In sliding devices, two phases can be assumed as sliding and non-sliding phases. In the non-sliding phase, the shear force at the interface is smaller than the resistance friction force and the structure can be treated as a fixed base system. Once the lateral

shear force exceeds the friction force, the structure will start to slide. The horizontal friction force at the sliding interface offers resistance to motion and help in dissipating the energy of structural response. The free body diagram for the UPSS in quasi-static equilibrium can be simplified as shown in Fig 4.1.

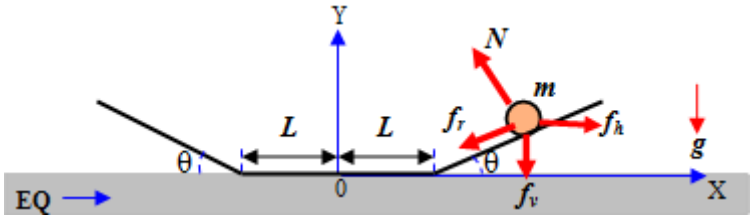

Figure 4.1 Mechanical model of the isolator with multiple plane sliding surfaces

While the horizontal displacement does not exceed L, the structure behaves in the same manner as of a structure isolated by pure friction isolators. Another advantage of the use of the clearance is that it may help in providing a force-soft mechanism that may delay uplift mechanism allowing reduction in restoring force.

The friction force (f_r) in the sliding phase can be expressed by:

$$f_r = \mu N \operatorname{sgn}(\dot{x}_b) \tag{4.1}$$

where μ is the friction coefficient; N is the normal force; $\dot{x}_b$ is the relative velocity of the bearing slider along the sliding surface, and sgn( ) is the signum function.

When the displacement exceeds L, the structure starts to slide on the inclined surface. The derivation for the horizontal force (f_h) and its relation with the vertical force (f_v) can be described as:

$$f_h = f_r \cos\theta \pm N \sin\theta \tag{4.2}$$

$$\frac{f_h}{f_v} = \frac{\pm\mu\cos\theta \pm \sin\theta}{\pm\mu\sin\theta \pm \cos\theta} \tag{4.3}$$

The sign of each term depends on the direction and the side of motion. The ratio between the horizontal and vertical reaction depends essentially on two important parameters which define the UPSS i.e. μ and θ. The quasi-static hysteretic behavior

can be idealized as shown in Fig 4.2.

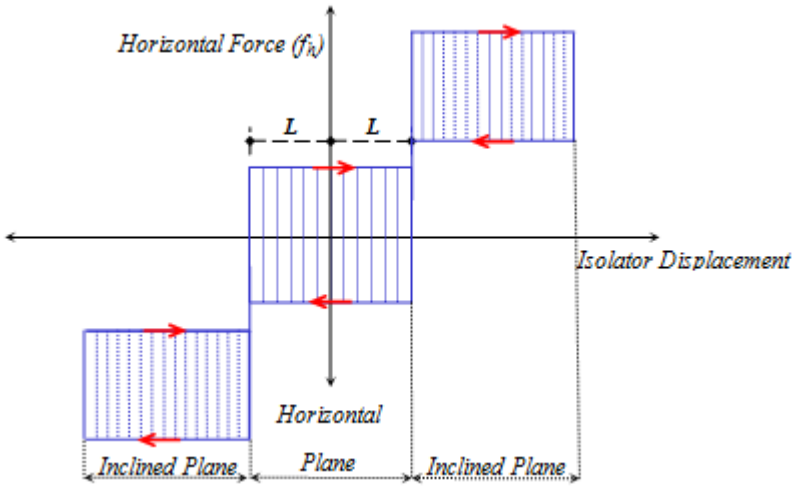

Figure 4.2 Idealized force-displacement relationship of UPSS bearing for a quasi-static cycle

There are differences in the force-displacement relationship for the case considering dynamic response of the structure and that for the quasi-static equilibrium, including the impact forces generated due to the transition from horizontal to the inclined surfaces, and vice versa (Igarashi et al 2010). However, for simplicity of the analysis, the force-displacement relationship shown in Fig.3 is regarded as a good approximation that covers the essential characteristics of the device, and is used in the response analysis of the system in this study.

4.2 Coefficient of Friction (μ)

One of the most important parameter that controls the dynamic characteristics of sliding isolators is the coefficient of friction. The most popular and well known sliding material is the polytetrafluoroethylene (PTFE) or its DuPont brand name 'Teflon'. It is greatly non-reactive, partly because of the strength of carbon-fluorine bond and it is also a high corrosion resistance material (E.I. du Pont de Nemours & Co. 1981). Due to its low friction of coefficient, with minimum values varies between 0.03 and 0.06 (Mokha et al 1990), it has been used for several years to accommodate the movement of deck due to thermal variation, creep and shrinkage movement. The friction force which is mobilized at the sliding interface depends on the normal force, bearing pressure, the

direction and value of sliding velocity and composition of the sliding interface (Constantinou 1994). Several models have been proposed to model the dynamic friction, including the one expressing the dependency of friction coefficient on the sliding velocity and the bearing pressure by the following expression (Constantinou et al 1990):

$$\mu = \mu_{\max} - (\mu_{\max} - \mu_{\min}) e^{-a|\dot{x}_b|} \tag{4.4}$$

where the parameters $\mu_{\min}$, $\mu_{\max}$ and a are functions of bearing pressure, surface roughness of stainless steel and composition of Teflon.

The simplest model is the Coulomb type which will be used in this study for simplicity in common with most of the researches which were carried out in recent years.

4.3 Numerical Example: Four-story shear-type building

The dynamic response of a flexible superstructure supported on the UPSS bearing system under earthquake motion is investigated and compared with the rubber bearing isolation system as well as pure friction sliders. The sliding devices are repeatedly subjected to transition phases between stick and slip modes, which introduces discontinuity and high nonlinearity. One of the most efficient methods which have been proposed for solving the discontinuities occurring in analysis of sliding structure is the fictitious spring approach (Yang et al 1990). By this method, a fictitious spring is introduced between the base mat and the ground to represent the mechanism of friction. The fictitious spring stiffness (k_f) is taken as zero for the sliding phase and as sufficiently large number for the non-sliding phase. This assumption is suitable with the mechanism of the sliding device, since Teflon-steel interfaces undergo some very small elastic displacement before sliding, partly due to small elastic shear deformation of the Teflon material (Constantinou et al 1990).

For the purpose of illustration, four-story shear-type building as shown in Fig. 4.3 will be studied.

The properties of the model are chosen to be identical to a model described in the reference (Yang et al 1990). It is assumed that story masses are equal so that m=350.2 kg and the mass of the foundation m_f =4m/3 and stiffness for all stories are set equal to k=573.6 103 N/m.

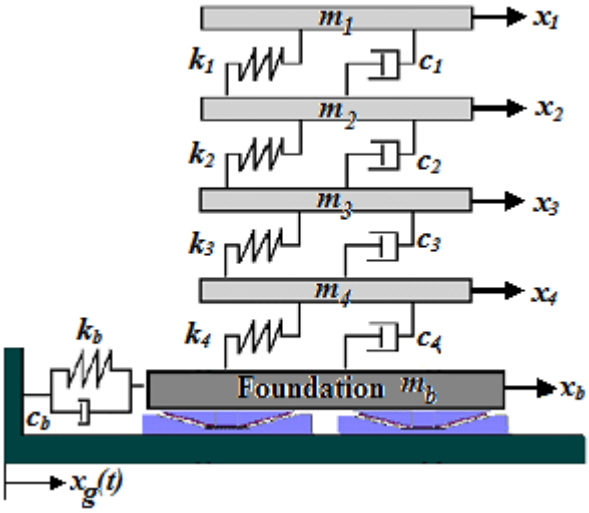

Figure 4.3 Four-story shear-building isolated by UPSS bearings

Rayleigh Damping is used to formulate the damping matrix. It has been assumed that the damping ratios ζ for the first two modes of vibration equal to 5%. The fundamental period of the fixed base building T_1 is 0.447 s. The UPSS bearing properties have been chosen with L=45 mm and θ=10°. The RB has chosen to give a period of isolation T_b of 3.0 s and the effective damping ratio ζ_b equal to 10%. The RB is a mean of providing a displacement restrain. Therefore, the total stiffness of RB is assigned as k_b=8320 N/m to achieve the desired isolation period. The dominant property of RB is the parallel action of linear stiffness and damping.

The restoring force (F_b) of RB has been modeled with a linear force-displacement relationship with viscous damping and can be expressed as follows:

$$F_b = k_b x_b + c_b \dot{x}_b \tag{4.5}$$

and

$$c_b = \zeta_b \times (2\omega_b m_t) \tag{4.6}$$

where c_b is the effective viscous damping coefficient of RB; m_t is the total mass of the superstructure including the foundation; ω_b is the angular isolation frequency i.e. $\sqrt{k_b / m_t}$.

The friction coefficient of the UPSS bearing for all the three sliding surfaces μ is

assumed to be 0.05. The superstructure is assumed to behave elastically linear which is compatible with the main purpose of base isolation and the overturning or tilting effect of the structure during sliding has been neglected.

The dynamic equation of motion for the shear type isolated building can be written as follows:

$$[M][\ddot{x}(t)]+[C][\dot{x}(t)]+[K][x(t)]=-[M][r_1]\{\ddot{x}_g(t)\}-[r_2]\{f_h(t)\} \tag{4.7}$$

Where *M*, *C*, *K* are, respectively, the $n\times n$ mass, damping, and stiffness matrices, and are defined as follows:

$$[\mathrm{M}]=\begin{bmatrix} m_1 & 0 & 0 & 0 & 0 \\ 0 & m_2 & 0 & 0 & 0 \\ 0 & 0 & m_3 & 0 & 0 \\ 0 & 0 & & m_4 & 0 \\ 0 & 0 & 0 & 0 & m_b \end{bmatrix} \tag{4.8}$$

$$[C]=\begin{bmatrix} c_1 & -c_1 & 0 & 0 & 0 \\ -c_1 & c_1+c_2 & -c_2 & 0 & 0 \\ 0 & -c_2 & c_2+c_3 & -c_3 & 0 \\ 0 & 0 & -c_3 & c_3+c_4 & -c_4 \\ 0 & 0 & 0 & -c_4 & c_4+c_b \end{bmatrix} \tag{4.9}$$

$$[K]=\begin{bmatrix} k_1 & -k_1 & 0 & 0 & 0 \\ -k_1 & k_1+k_2 & -k_2 & 0 & 0 \\ 0 & -k_2 & k_2+k_3 & -k_3 & 0 \\ 0 & 0 & -k_3 & k_3+k_4 & -k_4 \\ 0 & 0 & 0 & -k_4 & k_4+k_b \end{bmatrix} \tag{4.10}$$

$[x(t)]$, $[\dot{x}(t)]$ and $[\ddot{x}(t)]$ are $n\times 1$ relative displacement, velocity acceleration vectors respectively, $f_h(t)$ is $q\times 1$ the nonlinear isolator force and $\ddot{x}_g(t)$ is the ground acceleration.

$[r_1]$ and $[r_2]$ are the force distribution loading vectors expressed as:

$$r_1 = \begin{bmatrix} 1 \\ 1 \\ 1 \\ 1 \\ 1 \end{bmatrix}, \quad r_2 = \begin{bmatrix} 0 \\ 0 \\ 0 \\ 0 \\ 1 \end{bmatrix} \tag{4.11}$$

The numerical solution for the nonlinear dynamic equation is computed in this study based on the state-space formulation. The advantages of using this technique are the ability to provide a more systematic treatment with less computational efforts and the suitability in dealing with structures with multiple isolators undergoing independent motion conditions simultaneously (Wang et al 1998). The system of equations can be transferred into a set of first-order differential equation by introducing intermediate variables.

The equation of motion can be rewritten in the form:

$$\dot{z}(t) = Az(t) + B\ddot{x}_g + Df_h, \quad z(0) = z_0 \tag{4.12}$$

where

$$z(t) = \begin{bmatrix} \dot{x}(t) \\ x(t) \end{bmatrix} \text{ is the } 2n \times 1 \text{ state vector,} \tag{4.13}$$

$$A = \begin{bmatrix} -M^{-1}C & -M^{-1}K \\ I & 0 \end{bmatrix} \text{ is the } 2n \times 2n \text{ system matrix,} \tag{4.14}$$

$$B = \begin{bmatrix} -r_1 \\ 0 \end{bmatrix} \text{ is the } 2n \times 1 \text{ excitation distribution vector, and} \tag{4.15}$$

$$D = \begin{bmatrix} -M^{-1}r_2 \\ 0 \end{bmatrix} \text{ is the } 2n \times q \text{ location matrix specifying nonlinear UPSS force} \tag{4.16}$$

The general solution of the differential equation can be expressed in an incremental form as (Meirovitch 1990)

$$z(t_{i+1}) = e^{A\Delta t} z(t_i) + \left\{ \int_0^{\Delta t} e^{A\tau} d\tau \right\} \left(B\ddot{x}_g(t_i) + Df_h(t_i) \right) \tag{4.17}$$

where $e^{A\Delta t}$ is known as the transition matrix. Several methods can be used to determine the transition matrix. For small dimension matrix *A* and simple structure a closed form solution can be adopted. Other approaches such as Laplace transformation or by means of series can also be used.

Note that the solution for the current step $z(t_{i+1})$ is based on the previous step $z(t_i)$ and the ground excitation and the nonlinear force are assumed constant within each time increment Δt.

The general solution of Eq. 4.7 can be solved in a discrete-time system in the form:

$$z(i+1) = A^* z(i) + B^* \ddot{x}_g(i) + D^* f_h(i) \tag{4.18}$$

where

$$A^* = e^{A\Delta t} = \sum_{i=0}^{\infty} \frac{\Delta t^i}{i!} A^i \tag{4.19}$$

$$B^* = \left[\sum_{i=1}^{\infty} \frac{\Delta t^i}{i!} A^{i-1} \right] B \tag{4.20}$$

$$D^* = \left[\sum_{i=1}^{\infty} \frac{\Delta t^i}{i!} A^{i-1} \right] D \tag{4.21}$$

The procedure has been implemented in a MATLAB® (MathWorks 2007) code in order to analyze the four-story shear-type building isolated by multiple slider bearings.

4.4 Simulation Results

To verify the effectiveness of the isolator as a new promising alternative for seismic isolation sliding devices, reduction of two main response quantities, namely, the isolator displacement x_b and the top absolute floor acceleration, is the main concern. In order to clarify the advantage of the proposed device, the comparison with responses of the isolated building by RB and PF are also considered.

The structure is subjected to harmonic sinusoidal excitation with intensity taken as 0.50g high enough to insure sliding and uplift mechanism in the UPSS bearing and the period of excitation T_g taken as 0.6 s; a typical value sufficient smaller than T_b. Only unidirectional excitation is considered.

The simulation results shown in Fig. 4.4 demonstrate the efficiency of UPSS in comparison with the non-isolated building. The maximum absolute top floor acceleration has been reduced significantly from 1.81g to 0.77g, which means a reduction of about 60%, as shown in Fig. 4.4b. The small peaks seen in the acceleration time history are generated by the slip-stick action due to the sudden changes in the friction force value in the transition sliding phases which exerts shock impulses on the support. It is clearly indicated in Figs. 4.4c and 4.4d that UPSS bearing efficiently suppresses load transmitted into the superstructure, as well as the total base shear and strain energy.

From the comparison with RB and PF isolation systems shown in Fig. 4.5, the maximum top floor displacement for the UPSS bearing case has been found to be less than that for both RB and PF systems. This shows the effectiveness of this device in controlling the peak displacement values to acceptable limits, being one of the most important reasons to consider the bearing as a good alternative to solve the problem of large displacement of the RB and the residual displacement of the PF isolation system. The maximum displacement of the UPSS can be further reduced by a better selection of the three main parameters that define the device L, θ and μ as indicated by sensitivity analysis for these three parameters and their effect on the dynamic behavior described in the next section of this paper.

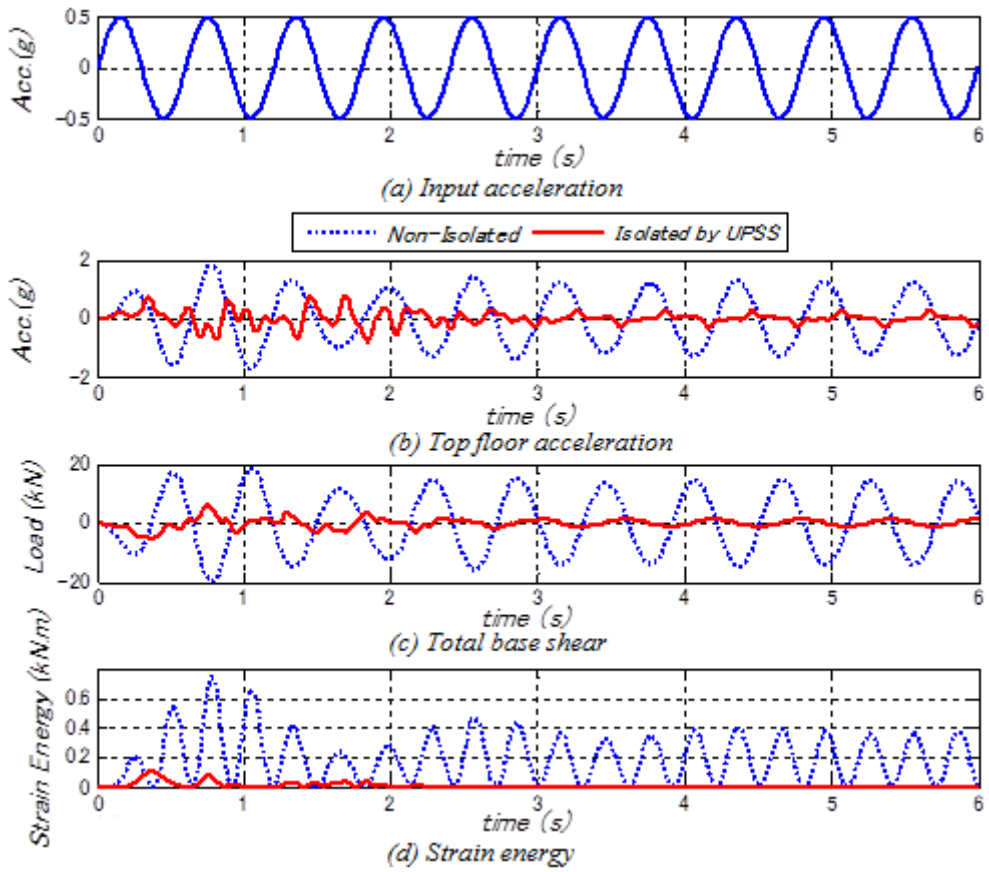

Figure 4.4 Comparison of non-isolated and isolated buildings

The dynamic characteristics of the UPSS bearing system under seismic excitation are illustrated by the response shown in Fig. 4.6. The enclosed area in the hysteretic force-displacement relationship Fig. 4.6a represents the portion of the energy dissipated by the friction mechanism. The hysteretic behavior indicates that after the displacement exceeds the clearance length, the uplift mechanism is activated to convert some of the kinetic energy to a potential one and to control the horizontal displacement, as can be noticed from the trace graph that depicts the relationship between the horizontal and vertical displacements in Fig. 4.6b.

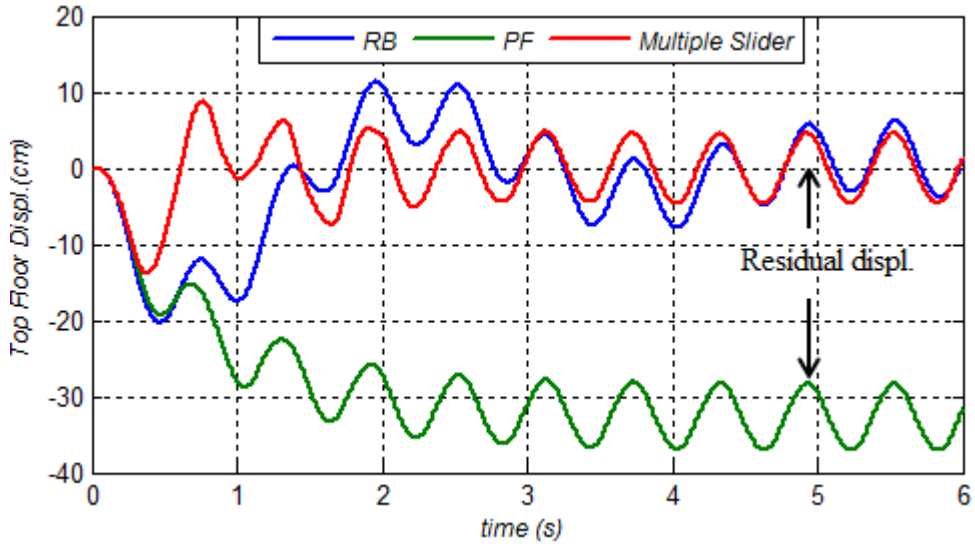

Figure 4.5 Comparison of top floor displacements with RB, PF and UPSS bearings

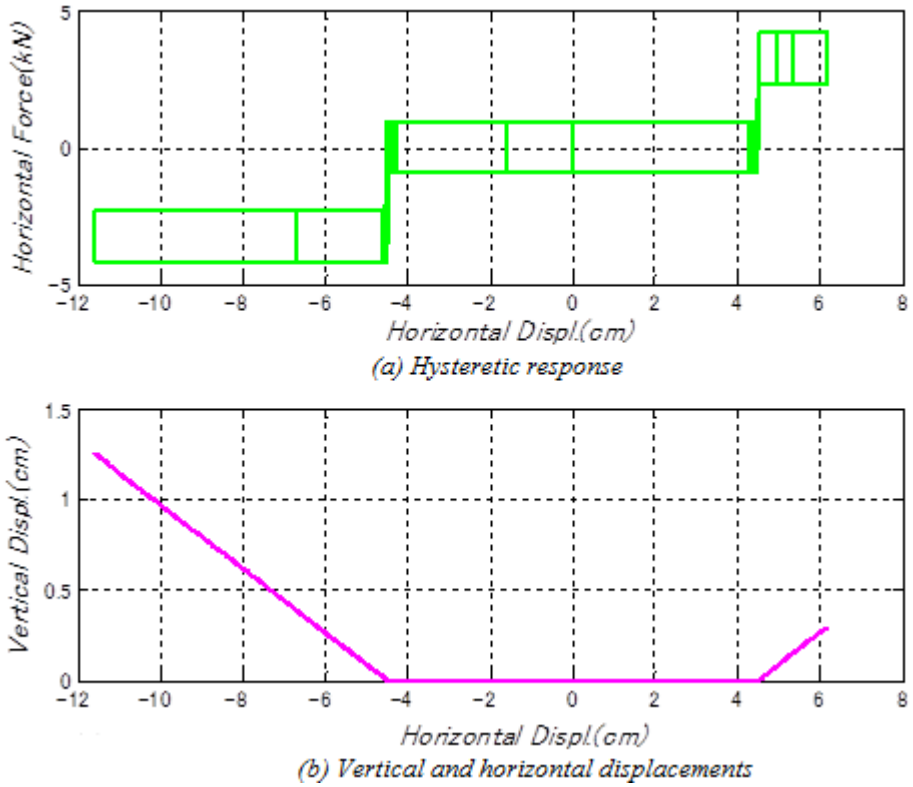

Figure 4.6 Hysteresis loop for the UPSS bearing

Design codes require that the isolation system should be able to provide restoring forces to bring the isolation device back to its original position prior to engagement. For example, the 1991 AASHTO Guide Specifications for Seismic Isolation Design (AASHTO 1991), require that the difference between the magnitude of the restoring force at design displacement and at 50% of the design displacement is larger than 2.5% of the tributary weight acting on the isolation bearings. For cases where this criterion is not met, the isolation system must be capable of accommodating displacements equal to the greater of three times the displacement calculated by the single mode analysis method, or 36ASi inches, where A and Si are the acceleration and site coefficients, respectively. The 1999 AASHTO Guide Specifications (AASHTO 1999) limit the post-elastic period to a maximum of 6 s. In the same manner, ASCE 7-05 (ASCE 2006) and Eurocode 8 (CEN 2004) states that an isolation unit should be capable of producing a value 2.5% multiplied by the seismic weight, greater than the lateral force at 50 percent of the total design displacement, in order to restore the isolator to its original intended position.

The unique fundamental dynamic behavior of the UPSS bearing is based on the geometry of the bearing that allows vertical movement through the sliding along the inclined surface. On the contrary of the friction pendulum system (FPS) which utilizes a spherical sliding surface to develop a restoring force, the slope angle of the inclined surfaces in the UPSS bearing is much larger than the range of the tangential angles of the sliding surfaces of FPS, so that the vertical component of the structural motion is explicitly intended and a constant restoring force is generated due to the component of self-weight tangent to sliding surfaces. Fig. 4.5 affirms the fact that the UPSS bearing inherit a self-centering mechanism in contrast with the pure slider (PF) which lacks the capability to return to the original position. However, to insure more safety conventional rubber bearing has been used in the numerical model as a mean of providing a displacement restrain, see Fig. 4.3.

4.5 Parametric Study

A properly designed base isolation is accomplished by understanding the sensitivity of the device parameter values and their influence on the structural response. In this section, the characteristics of the UPSS bearing with respect to the maximum horizontal displacement and base shear are examined with the variation of L, θ and μ.

The identical example model of the four-story shear-type building under the sinusoidal excitation is used for the analysis.

4.5.1 The Inclination Angle (θ) Effect

The isolator displacement is the main concern in the analysis described in this section. The relationship between the maximum base shear to total weight ratio and the variation in the inclination angle for μ=0.05 is shown in Fig. 4.7, which is obtained directly from Eq. 4.3 that depends on the inclination angle and the coefficient of friction. For practical purposes, the maximum angle was set equal to 45°.

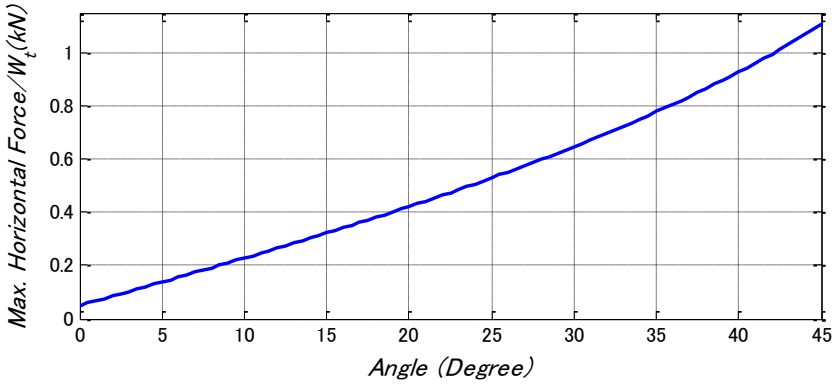

Figure 4.7 Maximum base shear to total weight ratio and the variation in the inclination angle for μ=0.05

The increase in the sliding angle will lead to an increase in the horizontal force as indicated in Fig. 4.7, resulting in an increase in the total base shear and the floor acceleration. The effect of variation of the inclination angle on the base floor horizontal displacement is shown in Fig. 4.8. The effect is also examined under various excitation intensities and periods of excitation. The isolated shear type building was subjected to excitation intensity up to 0.90g and period of excitation up to 1.00 s.

For low intensity input up to 0.4g, changing the angle does not significantly affect the maximum peak base displacement. However, for moderate to high intensity earthquakes exceeding 0.5g, the increase in the inclination angle is clearly effective in reducing the displacement demand.

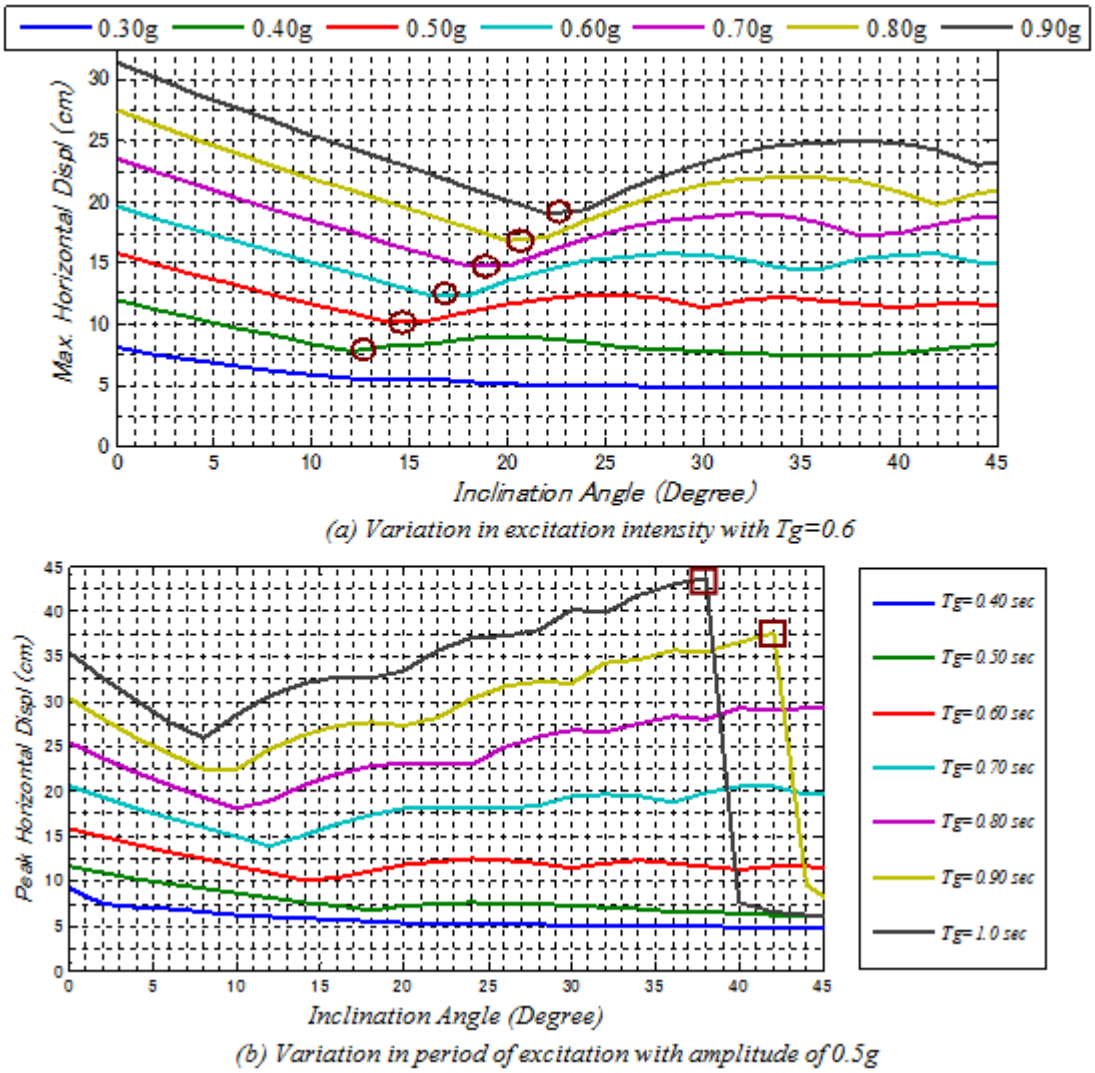

(a) Variation in excitation intensity with Tg=0.6

(b) Variation in period of excitation with amplitude of 0.5g

Figure 4.8 Maximum base horizontal displacement verses inclination angle

It is observed that there is an optimum angle for each case that gives the least minimum displacement, the higher the intensity the higher this optimum angle. A small circle is added to indicate these optimum values. The effect of the variation in the excitation frequency is shown in Fig. 4.8b. For periods of excitation 0.4 s and 0.5 s, a gradual reduction in the peak horizontal displacement occurs with the increase in the inclination angle. Nevertheless, for longer periods exceeding 0.6 s, the reduction occurs up to a certain limit then starts increasing. For the periods of 0.9 and 1.0 s, there exists a point where any further increase in the inclination angle would induce a sudden drop in the peak horizontal displacement and keep its value constant equal to the clearance length. This turning point, which is marked by a small square, can be seen as the

maximum angle for each period of excitation in which uplift mechanism cannot be developed further more. It is obvious that this angle is reached faster for long periods than shorter periods of excitation.

4.5.2 Clearance Length (L) Effect

To acquire a better understanding for L length on the structural response, the same four-story shear-building is used for the numerical calculation. *L* is been selected varies up to 20 cm. The captured response quantities of interest are the maximum top and base floor displacements and acceleration, as well as the maximum horizontal force, as shown in Fig. 4.9.

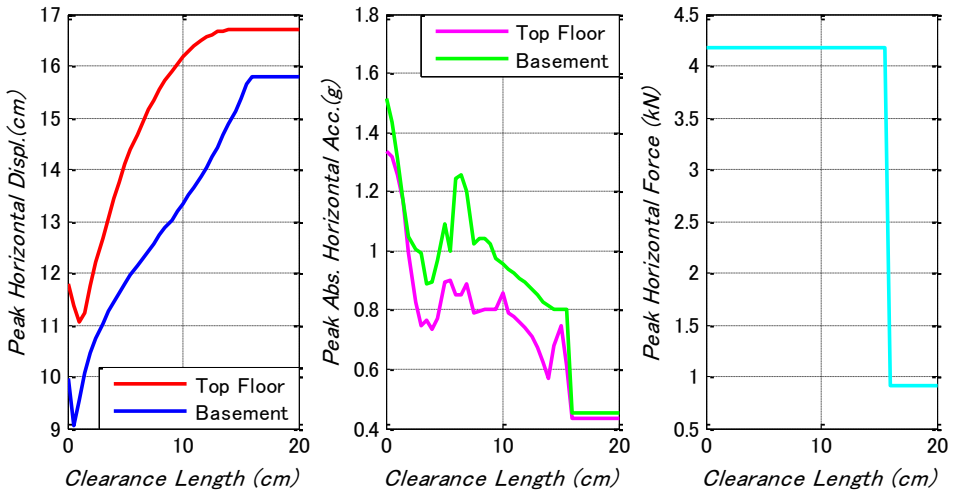

Figure 4.9 Clearance length vs. peak responses for the shear-type building

It is clearly shown by this graph that the longer the clearance length, the higher the peak displacement and the lower the absolute peak acceleration. The peak horizontal force is unchangeable with the change of clearance length since this mechanism of the UPSS bearing depends only on the inclination angle, the coefficient of friction and the total weight. The sudden drop in the restoring force indicates that the peak horizontal displacement is less than the clearance length which means the system truly behaves like a pure friction device without the uplift mechanism. It is obvious that using smaller clearance length may cause large reduction in the horizontal displacement but in the expense of higher top absolute acceleration. The designer should choose adequately

what the priority in the design is in term of cost and space limitations.

For a deeper understanding and clearer representation, Fig. 4.10 is established to relate simultaneously both the variation of clearance length and angle of inclination with two quantities of interest; the peak base displacement and top absolute peak acceleration. From Fig. 4.10, it is recommended to adopt a small angle of inclination when dealing with a small clearance length to avoid the high acceleration of top floor since such configuration may not allow the isolator to absorb the shock efficiently through the plane sliding part.

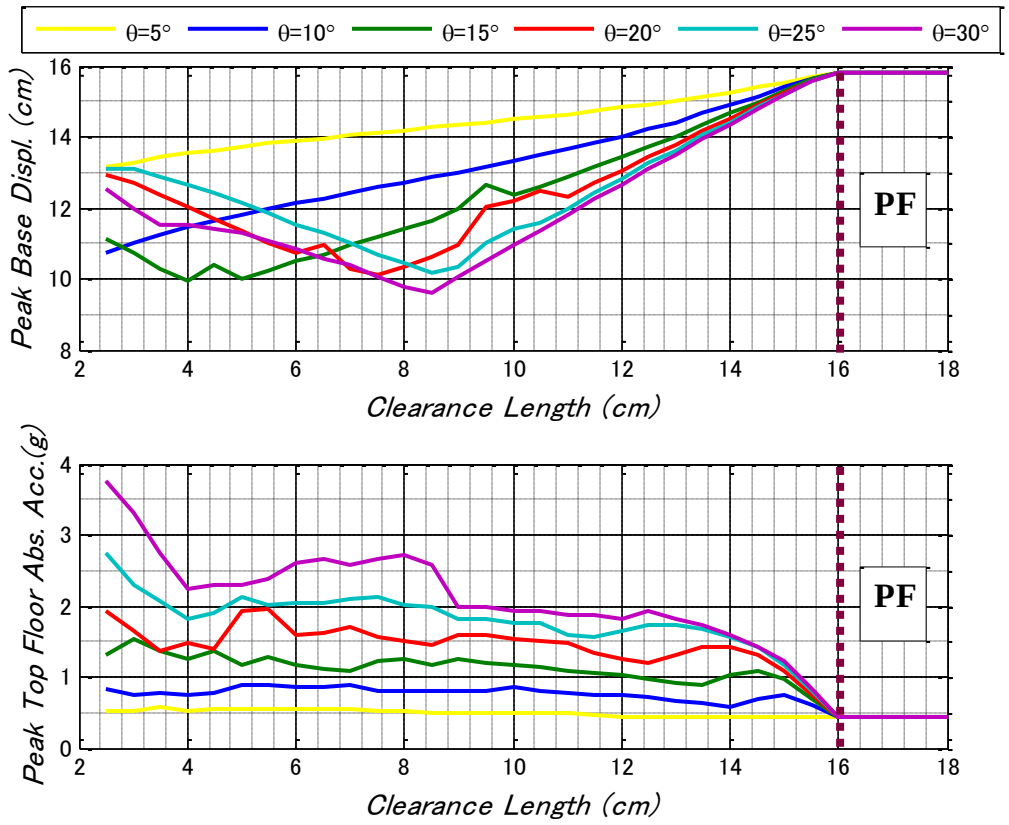

Figure 4.10 Clearance length vs. spectra responses under various inclination angles

4.5.3 Friction Coefficient Effect

In this section, the effect of the friction coefficient is investigated. As stated before, the UPSS bearing possesses a distinguishing feature that permits the use of variable friction coefficients. Therefore, the following discussion is divided into two cases: equal and non-equal friction coefficient cases. Several different friction coefficients ranging from 0.01 to 0.3 are considered in each case.

4.5.3.1 Equal Friction (μ)

Equal friction implies that the same sliding material is used for the three sliding surfaces in both the horizontal and inclined planes. To illustrate the effect of the friction coefficient values, the peak responses of the isolated superstructure and the isolator horizontal force versus the variation of friction coefficient values are shown in Fig. 4.11.

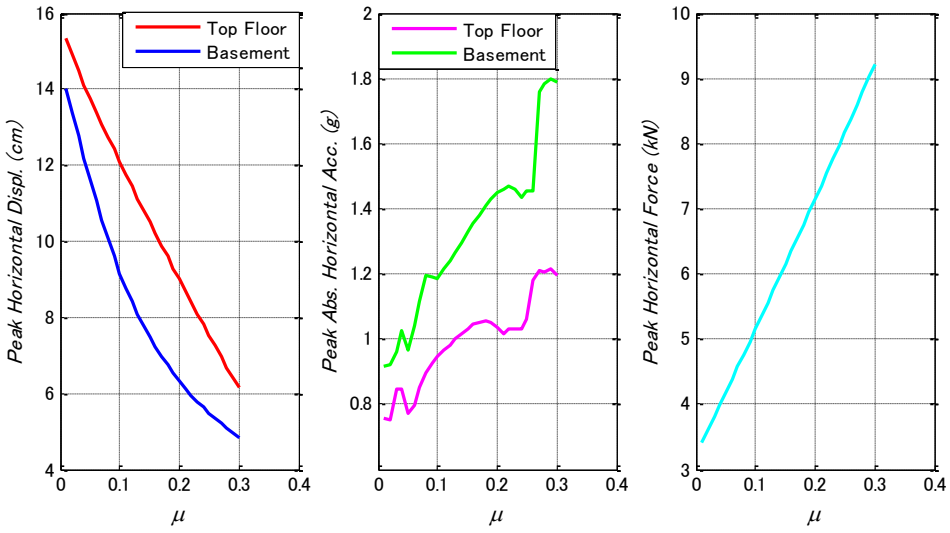

Figure 4.11 Friction coefficient vs. peak responses

It is observed that for smaller μ values, reduction in acceleration is more efficient accompanied with a higher peak displacement. In order to clearly show the difference in response behavior for different friction coefficient values, the hysteretic loops for two μ values of 0.01 and 0.10 are plotted in Fig. 4.12. It is obvious that the friction coefficient strongly controls the shape of the hysteretic curve; the lower the value, the narrower

band dissipation system with more softener mechanism is generated i.e. larger displacement and lower force.

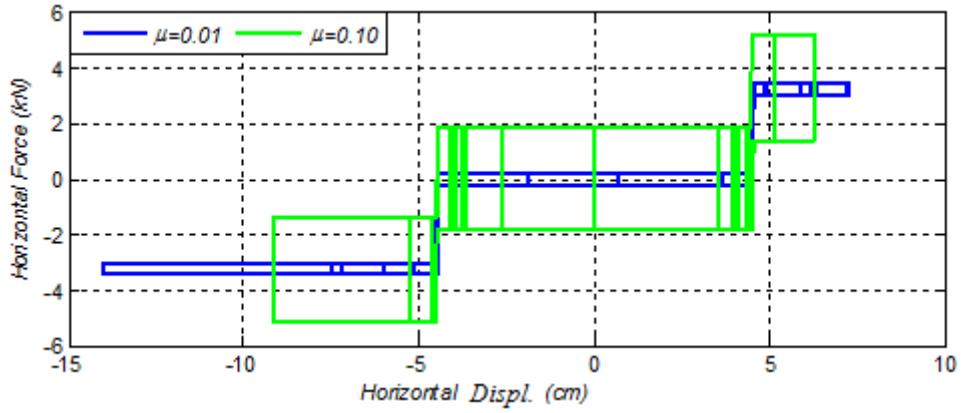

Figure 4.12 Hysteresis loop for UPSS for two different friction coefficient values

The influence of loading characteristics such as the intensity and period of excitation and its relationship with the friction coefficient on the peak base horizontal displacement and the peak top floor absolute acceleration is traced and plotted in Figs. 4.13 and 4.14.

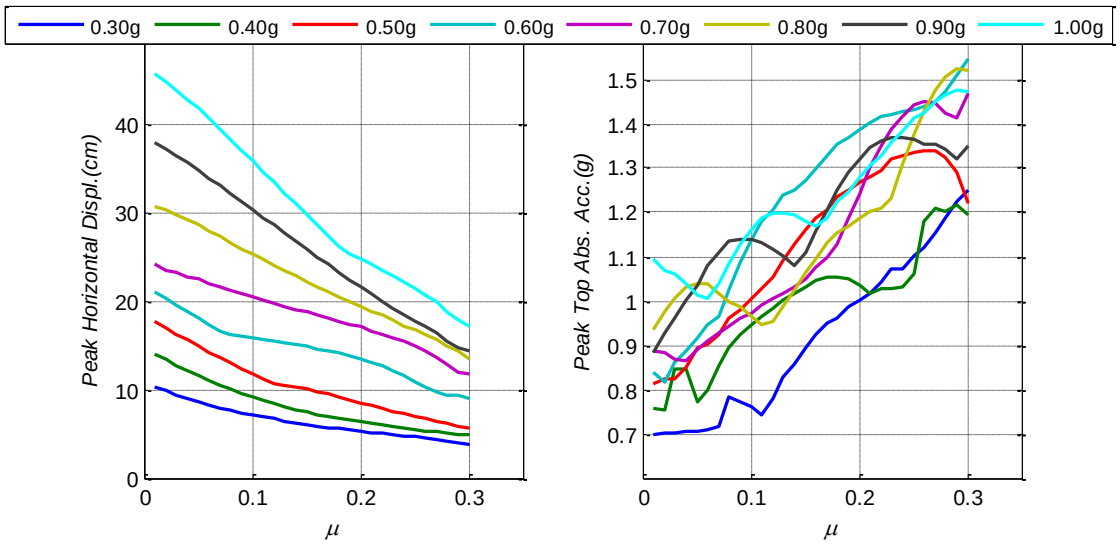

Figure 4.13 Relationship between peak response and friction coefficient with respect to T_g= 0.6 s

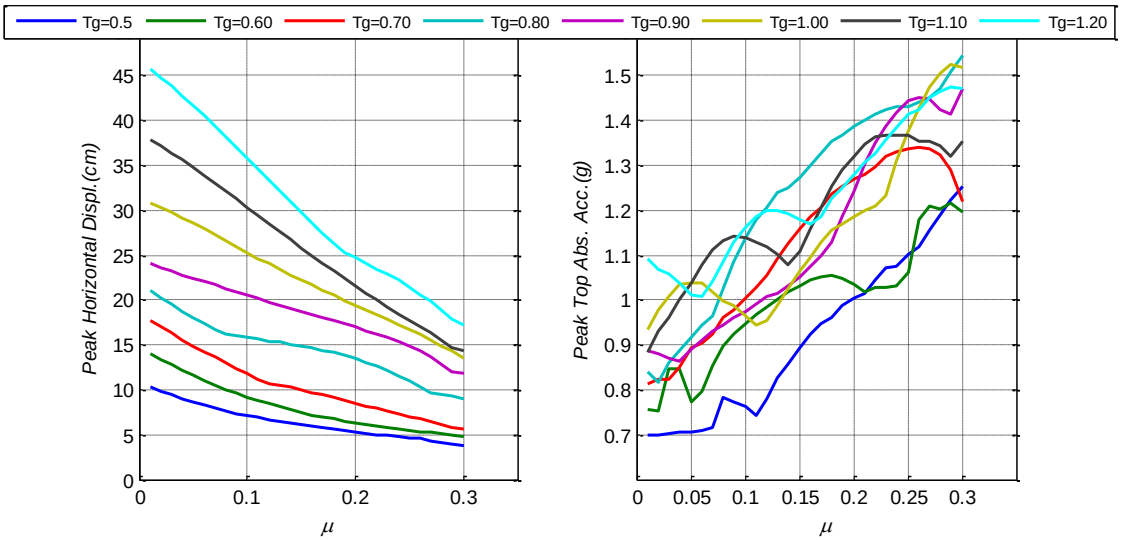

Figure 4.14 Relationship between peak response and friction coefficient at amplitude of 0.5g

Both diagrams clearly depict that the friction coefficients in all cases of excitation are approximately inversely proportional to the peak horizontal base displacement. On the other hand, the peak top absolute acceleration tends to increase with the increase of response with the increase of the friction coefficient. It is should be noted that for small friction coefficients, the top acceleration is not significantly affected by excitation intensity variation.

4.5.3.2 Non-Equal Friction (μ_1 & μ_2)

The geometry of UPSS bearing inherits a distinctive advantage that offers the ability to use different friction coefficients for each sliding surface, as seen in Figure 4.15. The use of such non-equal friction coefficients is expected to be helpful to control the isolator displacement.

Some researchers have investigated theoretically the effectiveness of varying the friction coefficient within the FPS by gradually varying the roughness of the spherical surface (Panchal and Jangid 2008). Such variation is selected with the criterion that the isolator displacement and building base shear decrease significantly without much alteration to superstructure acceleration. In this section, an investigation of using different sets of friction coefficient for each sliding surface is performed. The plane

sliding surface is assumed to have a friction coefficient (μ_1) and the two inclined surfaces are assumed to have the same friction coefficient (μ_2) for symmetry and practical purposes.

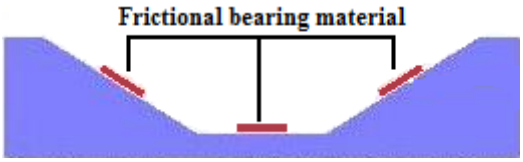

Figure 4.15 Locations of frictional bearing material in the UPSS bearing

Many researches showed that that isolated structures may be susceptible to near-fault ground motions such that the demand imposed by their displacement pulses can exceed the capacity of the isolators designed to current standards (Paresh and Sinha 2000, Hall et al 1995, Heaton et al 1995, Jangid and Kelly 2001). These ground-displacement pulses are associated directly with the fault-rupture process and can cause considerable damage to flexible structures. Such ground motions may have one or more displacement pulses ranging from 0.5m and higher with peak velocity of 1m/s or greater.

The presence of long-duration pulses has a large impact on isolated structures which requires a large displacement to be accommodated by the isolators, which may be excessively greater than a practically feasible value in engineering design. Some researchers suggested the use of a passive isolation system combined with a semi-active control device to enhance the safety of near fault structures (Yang and Agrawal 2008). The most common solution is the use of supplementary dampers to reduce such effect, on the expense of increasing the cost, the inter-story drift and floor superstructure acceleration (Paresh and Sinha 2000).

The UPSS has a high potential in controlling and minimizing the effect of the ground displacement pulses represented primarily through its operation mechanism. It will be shown that varying the friction coefficient also helps to maximize the efficiency of the bearing by reducing the displacement response especially in the cases of strong and near fault motions.

In order to study the dynamic behavior of the base-isolated shear type building with non-equal friction, 1995 Hanshin Kobe earthquake JMA record is used, see Fig. 4.16.

The Kobe earthquake record has peak ground acceleration of 0.83g, and duration of ground motion is considered to be 30 s. The same four-story shear type-building is used for this purpose, and the results are also compared with the equal friction coefficient bearing case.

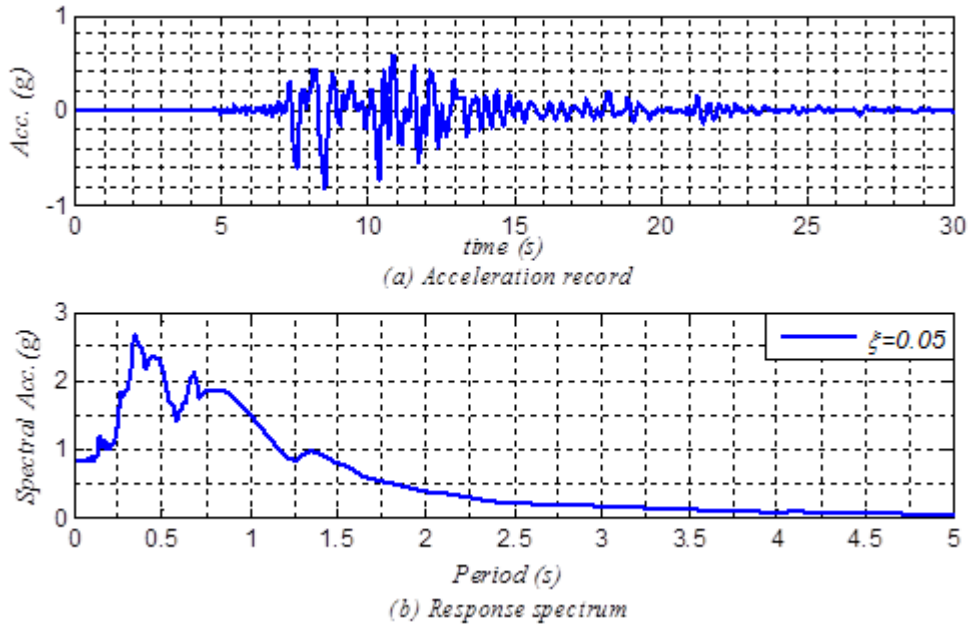

Figure 4.16 1995 Hanshin Kobe earthquake JMA record NS component

Three cases of equal and non-equal friction bearing material, shown in Fig. 4.17, are used first to determine whether the larger friction coefficient value should be placed at the plane surface or the inclined surface part to achieve a more reduction in horizontal displacement. The simulation results and the comparison between equal and non equal bearings are shown in Fig. 4.18.

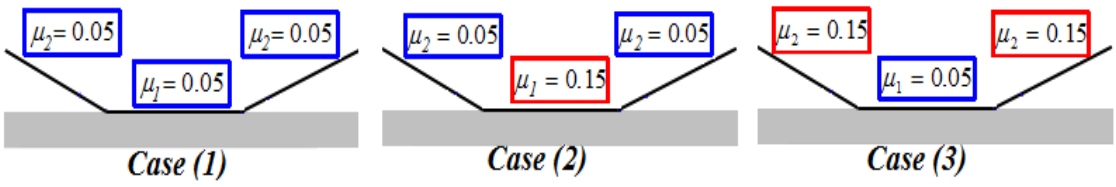

Figure 4.17 Free diagram of bearings: equal and non-equal friction coefficient at L=45 mm, θ=10 °

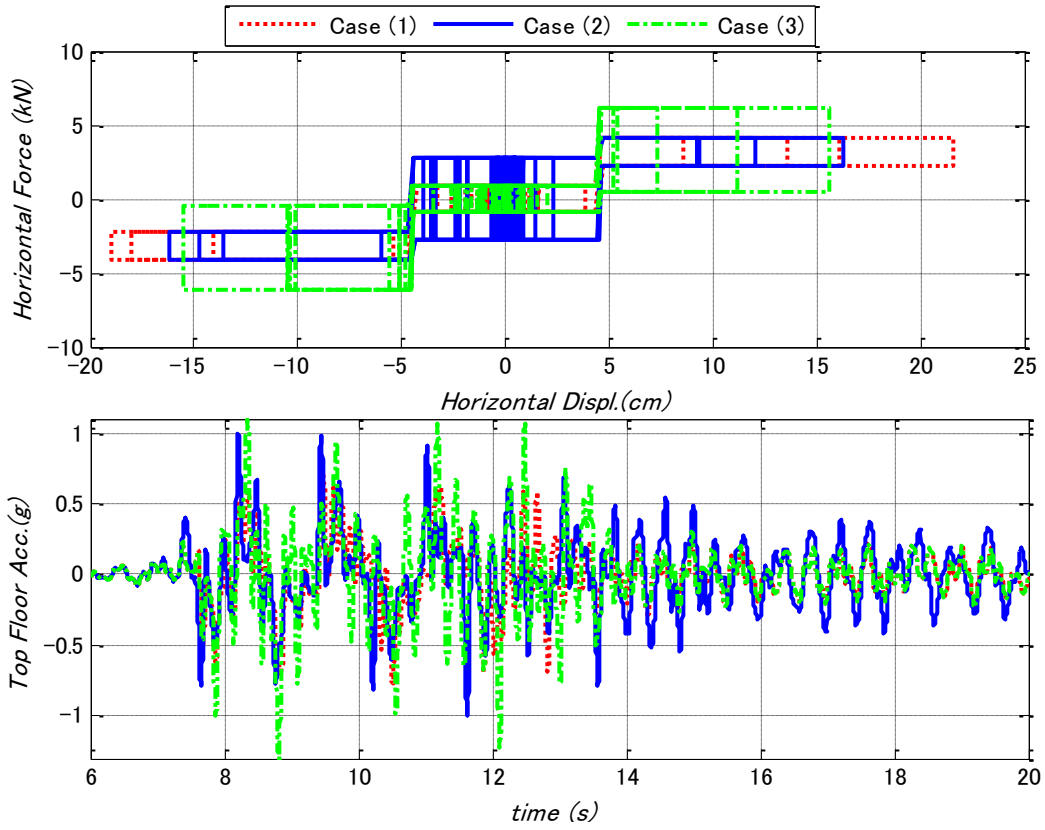

Figure 4.18 Comparison of responses for equal and non-equal UPSS bearing subjected to Kobe Earthquake

It can be concluded from Fig. 4.18 that for a better performance, the friction coefficient of plane surface should be taken larger than the friction coefficient of the inclined surface as in case (2). Contrary to case (3), case (2) can induce noticeable reduction in the maximum isolator displacement without any change in the maximum horizontal isolator force. However, this reduction may cause some increase in the top acceleration response due to the higher yielding frictional level in the plane surface which leads to a longer duration in the stick phase. The hysteresis behavior of the bearing indicates a significant reduction in the isolator peak horizontal displacement. The peak isolator displacement is efficiently reduced by 25% in case (2) using the non-equal friction coefficient.

Further investigation for the effect of varying the plane surface friction coefficient μ_1 on the maximum horizontal bearing displacement and horizontal force is carried out using several ground motion records. The earthquake ground motions considered are: (1) 1995

Hanshin Kobe record (PGA=0.82g); (2) 1980 Victoria, Mexico record (PGA=0.59g); (3) 1940 El-Centro record (PGA=0.32g); (4) 1999 Chichi-TCU-068 record (PGA=0.46g); (5) 1994 Northridge record (PGA=0.60g); (6) 1979 Imperial Valley, El-Centro Array #7 record (PGA=0.62g).

The above model is used with bearing properties of L=45 mm, θ=10° and μ_2=0.05. The simulation results are shown in Fig. 4.19.

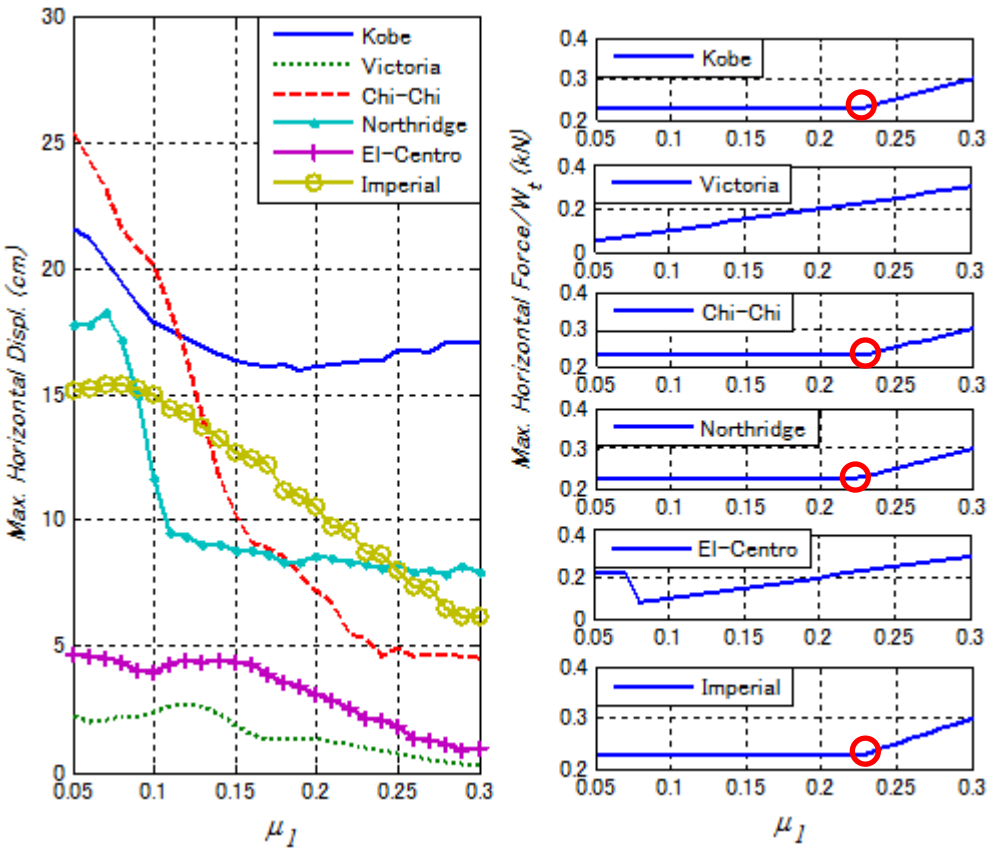

Figure 4.19 Relationship between μ_1 and maximum displacement and force under various earthquake ground motion records

The trend of horizontal displacement response curves reaffirms the above stated fact that a higher friction coefficient μ_1 leads to a higher reduction without any increase in the horizontal force up to a certain point where forces start increase. A small circle is added to these points. For some earthquakes such as Victoria and El-Centro records, although there is still a displacement reduction, it is observed that the force pattern is different than that of the rest earthquake record responses. The reason behind this

pattern in the case of Victoria record is due to earthquake wave characteristics that are not able to develop the uplift mechanism and all displacement responses are less than the clearance length for all combinations of μ_1.

Therefore, the linear increase of the horizontal force shown in Fig. 4.19 is due to the frictional force limit in the plane horizontal surface of the multiple-slider bearing proportioned to μ_1. As for El-Centro record, the forces kept constant until μ_1 reaches about 0.07 in which further increase in μ_1 prevents the development of uplift mechanism and the behavior continue similar to Victoria record.

It is clear that the point marked earlier can be considered as an optimum point in term of achieving a maximum displacement reduction without any change in the horizontal force. This point represents the value of μ_1 that produces a frictional yielding limit in the plane surface equal to that developed in the inclined surface. Based on Eq. (4.3), the optimum value μ_1^{opt} can be calculated as:

$$\mu_1^{opt} = \left[\frac{+\mu_2 \cos\theta + \sin\theta}{-\mu_2 \sin\theta + \cos\theta} \right] \tag{4.22}$$

Applying this formula to our example model the optimum μ_1^{opt} is equal 0.228 which matches with the same value in Fig. 4.19. Comparison of equal friction case (μ=0.05) and non-equal friction case (μ_1^{opt} =0.228, μ_2=0.05) under the various earthquake excitations is plotted in Fig. 4.20. This plot shows the high efficiency of using non-equal friction with an optimum value to achieve a large reduction up to 78% of the equal friction case as in Chichi earthquake.

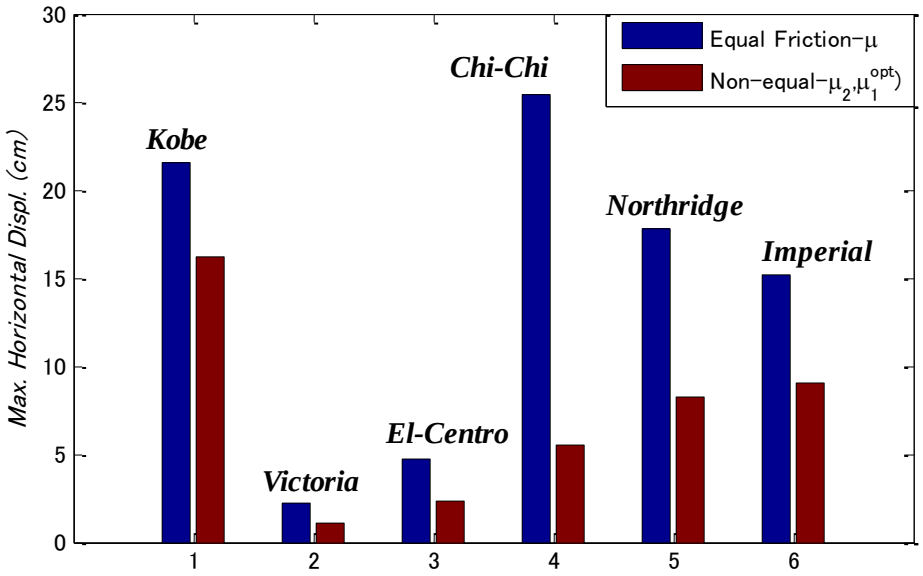

Figure 4.20 Comparison between equal and non-equal friction under various earthquakes

The remarkable performance in Chichi earthquake case compared with Kobe earthquake as shown in Fig. 4.21 is the result of the unique characteristics of each seismic wave.

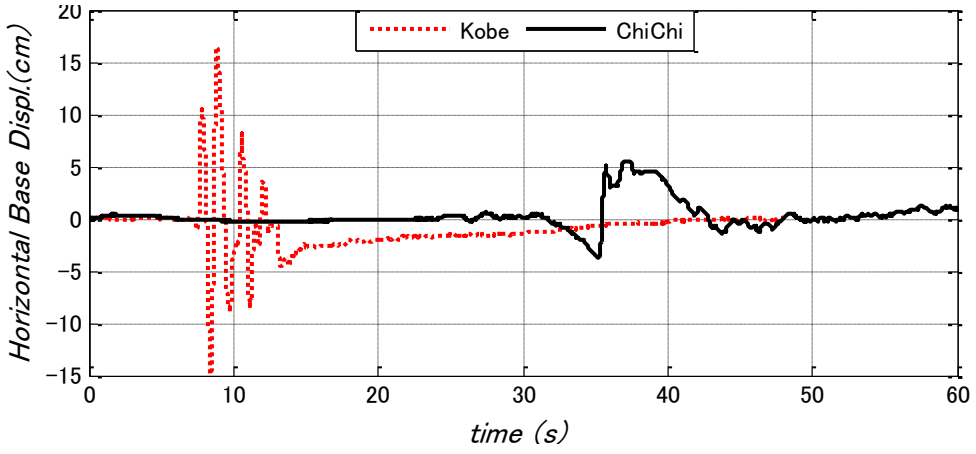

Figure 4.21 Displacement and acceleration time history (L=45[mm], θ=10° μ_1^{opt}=0.228, μ_2=0.05)

Fig. 4.22 also shows the Fourier and spectrum analysis comparison between these two records. The analysis of these two near fault ground waves indicates that Kobe record exhibits forward directivity effect while Chichi record exhibits fling-step effect. The forward directivity is characterized by a large pulse occurring at the beginning of the motion to be oriented in a direction perpendicular to the fault plane while the fling-step is the outcome of the tectonic permanent deformation oriented parallel to the fault (Gazetas et al 2009, Yan and Lee 2007, Kalkan and Kunnath 2008). The destructive potential of the permanent displacements of Chichi waves caused by the fling-step effect has been successfully absorbed and cut off through the response mechanism of the non-equal friction multiple-slider bearing causing such a significant displacement reduction more obvious than in Kobe earthquake case.

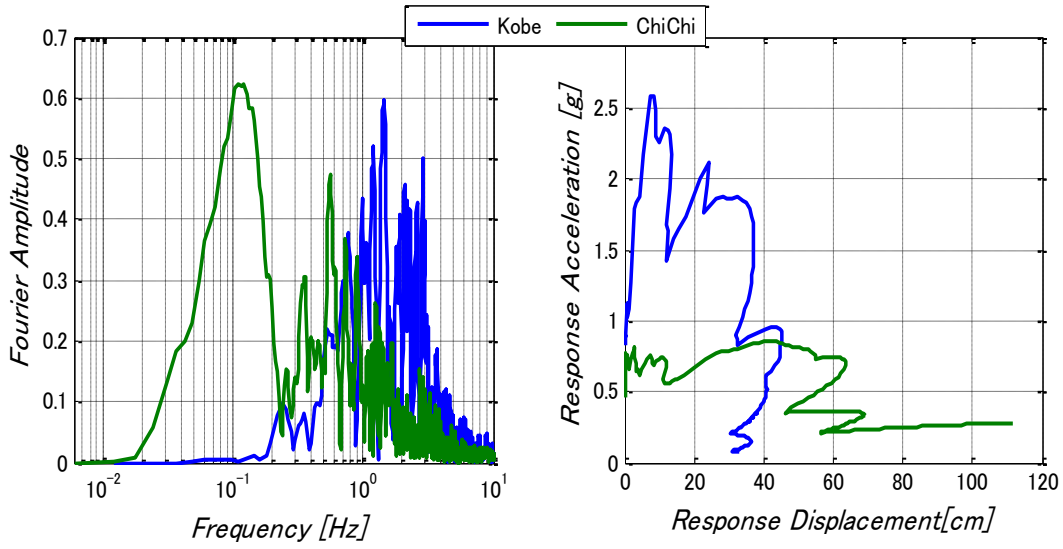

Figure 4.22 Fourier and spectrum analysis for Kobe and Chichi earthquakes

4.6 Conclusions

The UPSS bearing is introduced to enhance the seismic performance of multi-story structures and to reduce the horizontal displacement with a low cost. The UPSS bearing is composed of three sliding surfaces based on the PTFE and stainless steel interface; one horizontal and two inclined surfaces. A simplified mathematical model is used to

represent the mechanical behavior and the underlying principles of operation. The dynamic response of a flexible superstructure supported on the multiple-slider bearings system under earthquake motion is investigated and compared with rubber bearing and pure friction slider systems. Preliminary analysis on the influence of the variation of clearance length, the inclination angle and the friction coefficient on the response of multistory building and the unique feature of the multiple-slider bearing that permits the use of different friction coefficients is investigated. Based on the presented study, the following conclusions can be drawn:

1. Simulation results indicate that the newly proposed bearing is more effective in mitigating the risk of earthquake and preserving multi-story buildings from damage than the conventional rubber bearing and the pure friction slider in term of peak horizontal displacement.

2. Higher inclination angle is effective in reducing horizontal displacement especially in moderate to high excitation intensities but on the expense of higher forces. It was observed that there is an optimum angle that gives a minimum horizontal peak displacement and it depends on the excitation characteristics and structure properties.

3. The analysis indicates that the longer the clearance, the higher the peak displacement and the lower the absolute peak acceleration.

4. The peak horizontal displacement is approximately inversely proportional to the friction coefficient with all cases of excitation. It is also observed that for small friction coefficients, the top acceleration is not significantly altered with changing excitation intensity.

5. The geometry of the UPSS bearing inherits a distinctive advantage that offers the ability to use different friction coefficient for each sliding surface. This lead the bearing to possess a high potential in controlling and minimizing the peak horizontal displacement in addition to its primary reduction through the mechanism of uplift.

6. It has also been found that for a better performance of the proposed bearing, the friction coefficient of the horizontal plane surface should be taken larger than the friction coefficient of the inclined surface. Besides, there is an optimum

friction value that causes a high displacement reduction without any change in the horizontal force and the principle to define the optimal value is developed.

4.7 References

American Association of State Highway and Transportation Officials (AASHTO). *AASHTO guide specifications for seismic isolation design* 1991, Washington, D.C.

American Association of State Highway and Transportation Officials (AASHTO). *AASHTO guide specifications for seismic isolation design*; 1999, Washington, D.C.

American Society of Civil Engineers. ASCE 7-05. Minimum Design Loads for Buildings and Other Structures; 2006. *ASCE Standard*, SEI/ASCE 7-05.

CEN. *Eurocode 8*, Design of Structures for Earthquake Resistance—Part 1: general rules, seismic actions and rules for buildings. EN 1998-1: 2004. Comité Européen de Normalisation, Brussels.

Constantinou MC. Design and Applications of Sliding Bearings. In: Soong TT, Costantinou MC, editors. *Passive and Active Structural Vibration Control in Civil Engineering*. New York: Springer, Wein 1994; 111-135.

Constantinou M, Mokha A, Reinhorn A. Teflon Bearing in Base Isolation II: Modeling. *Journal of Structural Engineering* 1990; 116(2): 455-473.

E.I. du Pont de Nemours & Co. *Teflon: Mechanical design data*. Wilmington, DE; 1981.

Gazetas G, Garini E, Anastasopoulos I, Georgarakos T. Effects of near-fault ground shaking on sliding systems. *ASCE Journal of Geotechnics and Geoenvironmental Engineering* 2009; 135(12): 1906–1921.

Hall JF, Heaton TH, Halling MW, Wald DJ. Near-source ground motion and its effects on flexible buildings. Earthquake Spectra 1995; 11(4): 569–605.

Heaton TH, Hall JF, Wald DJ, Halling MV. Response of high-rise and base-isolated buildings in a hypothetical Mw 7.0 blind thrust earthquake. Science 1995; 267: 206–211.

Igarashi A, Sato T, Shinohara M, Katou Y, Uno H, Adachi Y, Takahashi T. Uplifting Slide Bearing (1) – Characterization of Dynamic Properties. *34th IABSE Symposium on Large Structures and Infrastructures for Environmentally Constrained and Urbanised Areas*, Venice, Italy 2010; 1-8.

Igarashi A, Sato T, Shinohara M, Katou Y, Uno H, Adachi Y. Uplifting Slide Bearing (2) – Verification of Seismic Response by Tests. *34th IABSE Symposium on Large Structures and Infrastructures for Environmentally Constrained and Urbanised*

Areas, Venice, Italy 2010; 47-54.

Igarashi A, Sato T, Shinohara M, Katou Y, Uno H, Adachi Y. Uplifting Slide Bearing (3) – Development of the Analytical Model. *34th IABSE Symposium on Large Structures and Infrastructures for Environmentally Constrained and Urbanised Areas*, Venice, Italy 2010; 55-62.

Igarashi A, Sato T, Shinohara M, Katou Y, Uno H, Adachi Y. Uplifting Slide Bearing (4) – Application for a 3-Span Steel Girder. *34th IABSE Symposium on Large Structures and Infrastructures for Environmentally Constrained and Urbanised Areas*, Venice, Italy 2010; 24-30.

Jangid RS, Kelly JM. Base isolation for near-fault motions. *Earthquake Engineering and Structural Dynamics* 2001; 30: 691–707.

Kalkan E, and Kunnath SK. Relevance of absolute and relative energy content in seismic evaluation of structures. *Advances in Structural Engineering* 2008; 11 (1):1-18.

MathWorks. MATLAB, The Language of Technical Computing, version 7.4.0.287 (R2007a). *The Math Works*, Inc.

Meirovitch L., *Dynamics and Control of Structures*, Wiley , New York, 1990.

Mokha A, Constantinou M, Reinhorn A. Teflon Bearing in Base Isolation I: Testing. *Journal of Structural Engineering* 1990; 116(2): 438-454.

Paresh M, Ravi Sinha. VFPI: an isolation device for aseismic design. Earthquake *engineering and structural dynamics* 2000; 29: 603-627.

Panchal VR, Jangid RS. Variable friction pendulum system for near-fault ground motions. *Structural Control and Health Monitoring* 2008; 15(4): 568-584.

Wang Y-P, Chung L-L, Liao W-H. Seismic response analysis of bridges isolated with friction pendulum behavior. *Earthquake Engineering and Structural Dynamics* 1998;27:1069–93.

Yang YB, Lee TY, Tsai IC. Response of multi-degree-of-freedom structures with sliding supports. *Earthquake Engineering and Structural Dynamics* 1990; 19: 739-752.

Yang JN, Agrawal AK. Semi-active hybrid control systems for nonlinear building against near-fault earthquakes. *Engineering Structures* 2002; 24(3):271-80.

Yan Xu, Lee GC. Traveling wave effect on the seismic response of a steel arch bridge subjected to near fault ground motions. *Earthquake Engineering and Engineering Vibration* 2007; 6(3): 245-257.

Chapter 5

Numerical modeling of UPSS and comparison with experimental data

The five chapter of this dissertation intends to verify the actual behavior of the UPSS through both the component test and the shake table test. Two analytical models are presented in this chapter to simulate the behavior of the UPSS namely; the simplified model and spring model. The verification analysis to the shaking table experiment results was done. As a result, it was confirmed that the analytical result and the outcome of an experiment showed a good agreement.

5.1 Model validation by component test

In order to show the validity of the model of the bearing presented in the previous chapter, behavior of the assumed numerical model is compared with past experiments on set of sliders and sliding plates with configuration similar to the UPSS bearing (Igarashi et al 2010, Oiles Corporation 2008), except that the location of the PTFE sliders and stainless steel sliding plates are inverted Fig. 5.1.

Figure 5.1 Lower component of the test specimen with PTFE pads

The tests apparatus for the tests is shown in Fig. 5.2. A weight of 18 kN is installed on the top of the upper component. The PTFE dimensions used are 100x100 mm and 50x200 mm for the horizontal and inclined surfaces, respectively, and the clearance of 180 mm is used for all cases. Sinusoidal displacements of amplitude 250 mm with various velocity rates are applied to the lower component of the specimen.

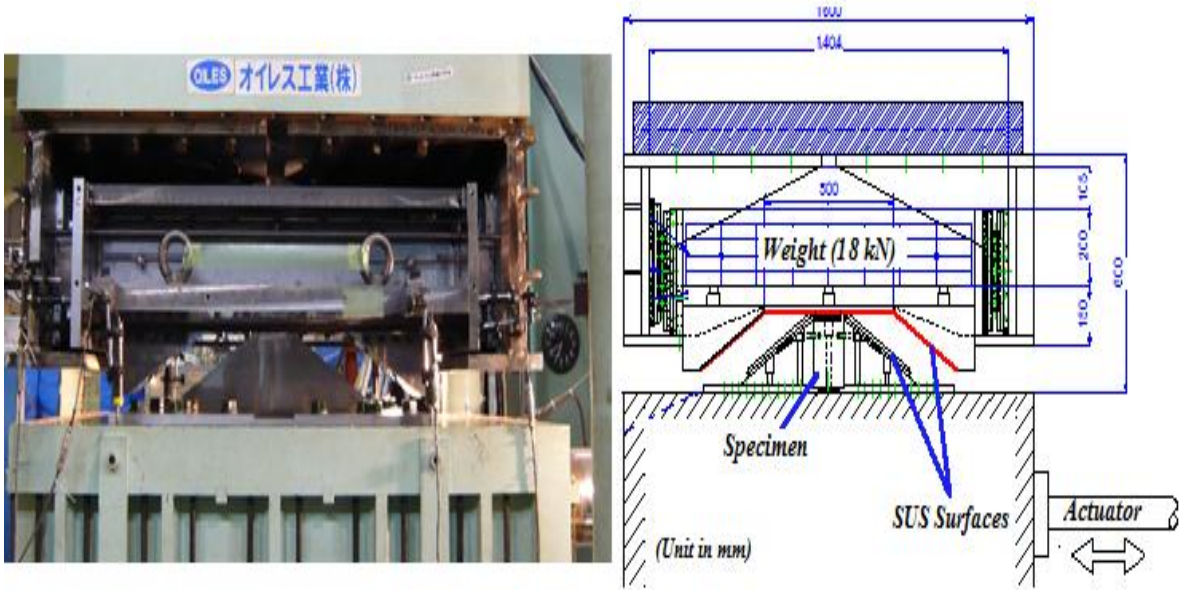

Figure 5.2 Details of test experiment

Fig. 5.3 shows the hysteresis behavior of the specimen with inclination angle θ=30° at velocity rate of 1.6 cm/s. The specimen of θ=30° during sliding is shown in Fig. 5.4.

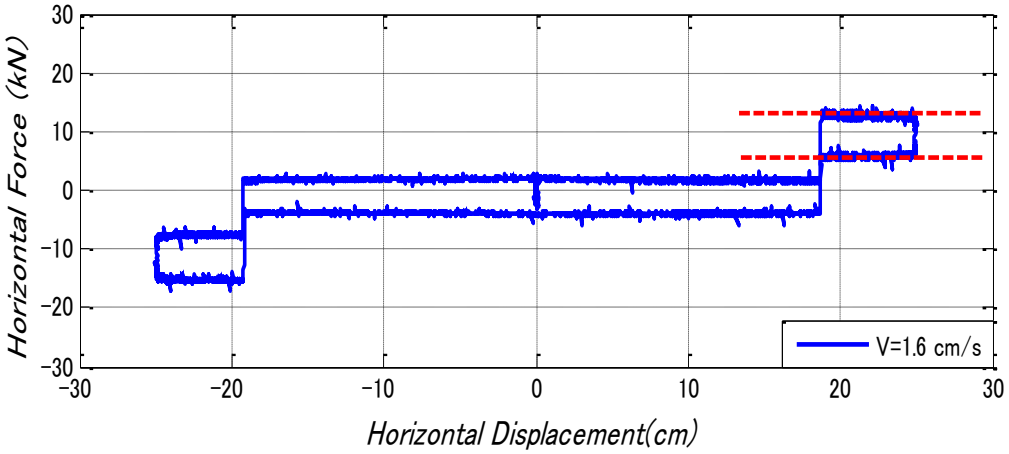

Figure 5.3 Hysteresis behavior of bearing with θ=30°

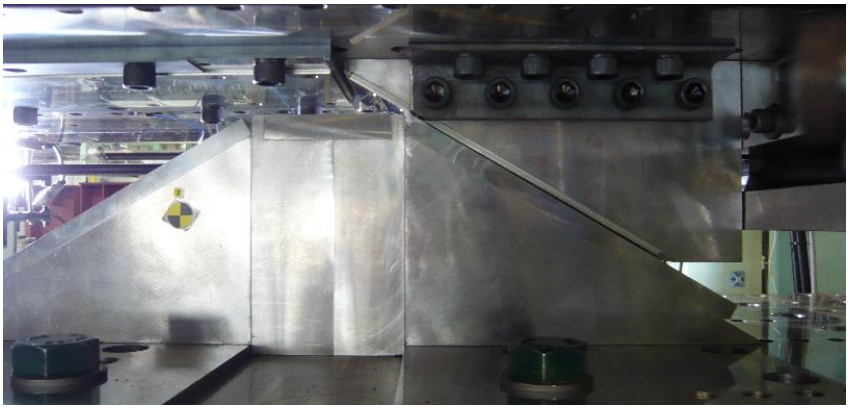

Figure 5.4 Test specimen with θ=30° during sliding

It is obvious that the hysteresis behavior resembles the simplified proposed model in Fig. 4.2. Applying Eq. 4.3 with μ about 0.14, the lower and upper bound of the horizontal forces generated at the inclined surfaces i.e. 14 kN and 7 kN are found similar to the force level shown by the dashed lines and these confirm the right formulation of the displacement-force relationship.

The effect of excitation at higher velocity is illustrated in Fig. 5.5 for θ=15°.

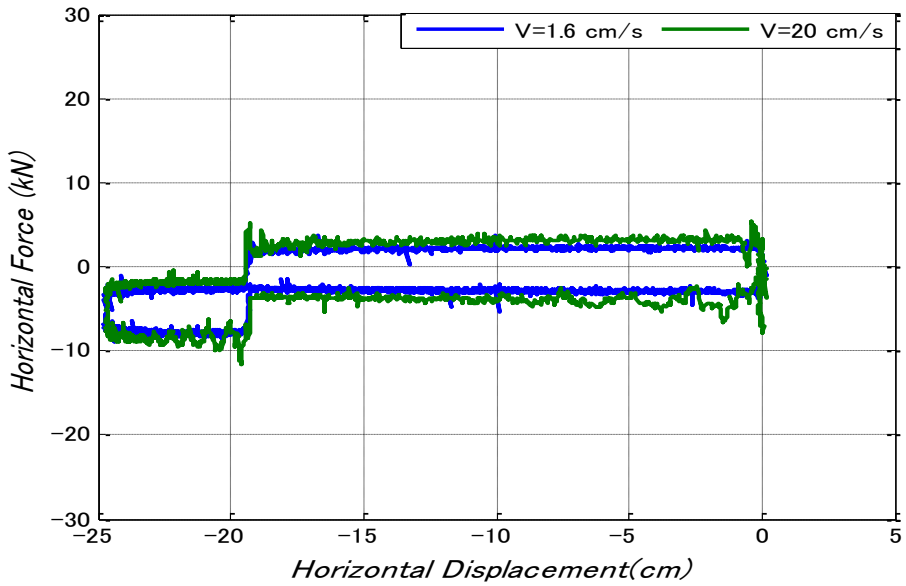

Figure 5.5 Hysteresis behavior of bearing with θ=15° at different velocity rate

It can be concluded from Fig. 5.5 that there are some differences especially in cases

where excitation velocity is high due to impact forces that are generated at the transition point between sliding surfaces. Fig 5.6 shows the same observation for the same case in Fig. 5.3 but with higher velocity rate of 18.5 cm/s. The test results indicate that higher θ generates higher impact force, see Fig 5.7.

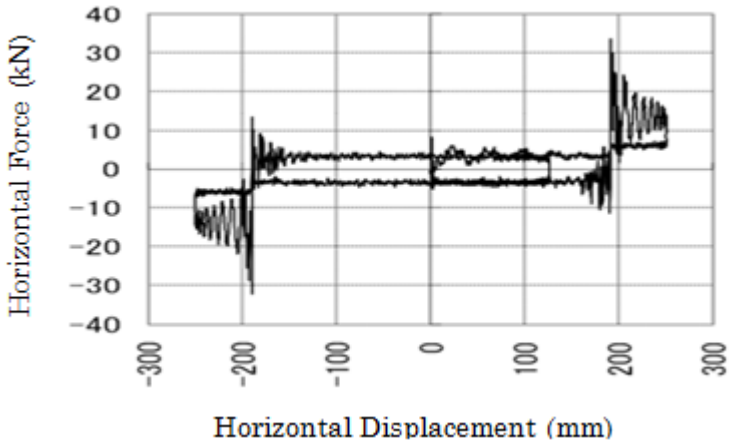

Figure 5.6 Hysteresis behavior of bearing with θ=30° at velocity rate of 18.5 cm/s (Uno et al 2009)

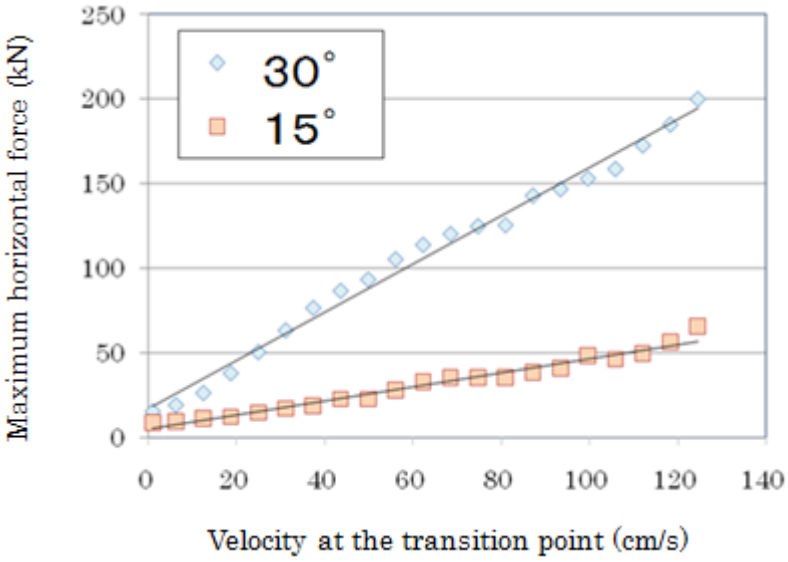

Figure 5.7 Relation between maximum impulse horizontal force and the velocity at the transition between the horizontal and inclined planes (Uno et al 2009)

As mentioned earlier, the hysteresis curve shown in Fig. 4.3 is still regarded as a good approximation that covers the essential characteristics of the device, and is used in the response analysis of the system in this study to simplicity of the analysis.

5.2 Shaking table test

An extensive series of shaking table tests were performed at Disaster Prevention Research Institute of Kyoto University, a facility that was found after the Kobe earthquake 1995 capable of producing a maximum acceleration up to 1.0g and 0.3[m] horizontal displacement. The main purpose of these tests is to capture the real dynamic behavior of multiple-slider bearing with different properties under various types of excitations including both harmonic and earthquake waves. A sample of these excitation waves is selected to compare the displacement time history between analytical and experimental results. A detailed study for these tests is found in reference (Morimoto 2009).

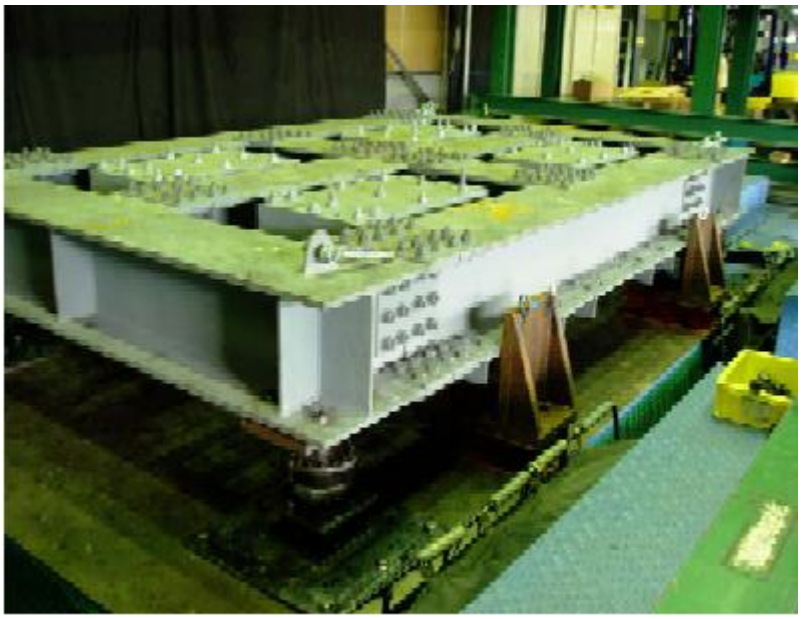

Figure 5.8 Experimental setup

In this experiment, a 4.15m × 2.65m rigid steel frame was supported on two multiple-slider bearing and two rubber bearings as shown from Fig 5.8 and Fig 5.9. The

total weight of the raised floor was 107.8 kN. The excitation was carried on only in one horizontal direction. Rubber bearing stiffness was chosen to produce an isolation period of 1.25 s with effective damping ratio 4.28%. The specifications used for the isolators were θ= (30°, 15°), L= (30, 42) mm and μ≈0.1.

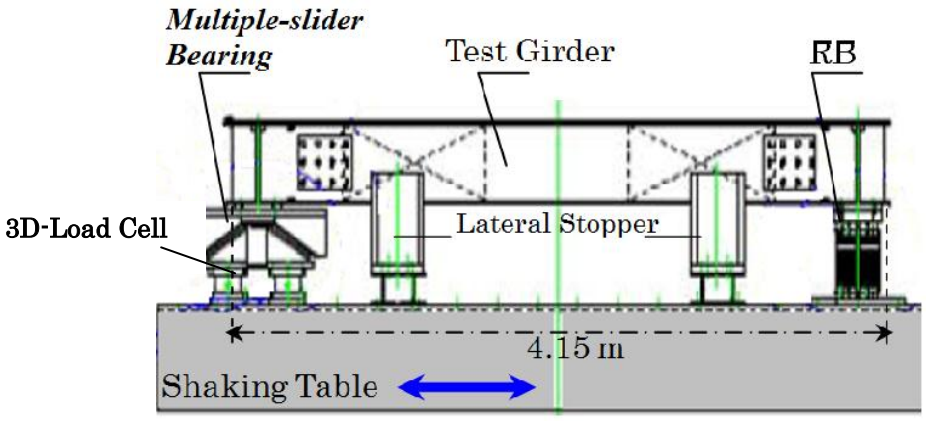

Figure 5.9 Details of test experiment

Besides the UPSS bearing, pure friction slider (PF) was also used for comparison purposes with μ≈0.1. The PF and UPSS bearings are shown in Fig 5.10 and Fig 5.11.

Figure 5.10 Uplifting sliding bearing

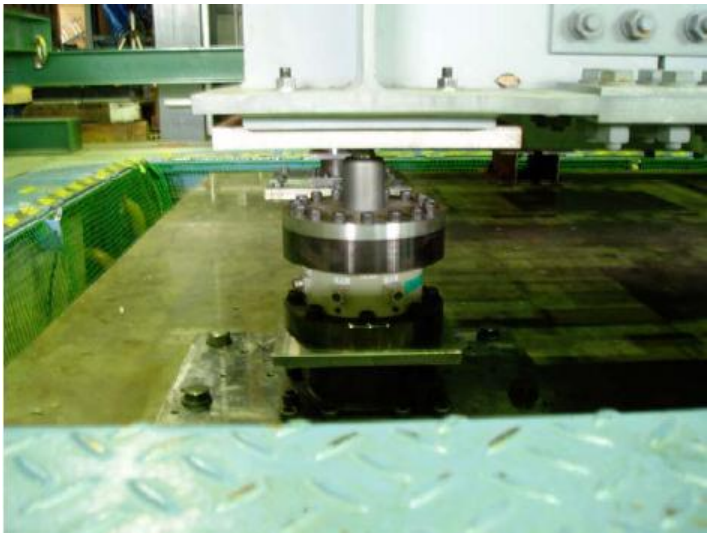

Figure 5.11 Pure friction bearing

Figure 5.12 shows a comparison between the experimental and analytical results for a sinusoidal excitation with intensity taken as 1 m/s^2 and period of excitation as 1.0 s.

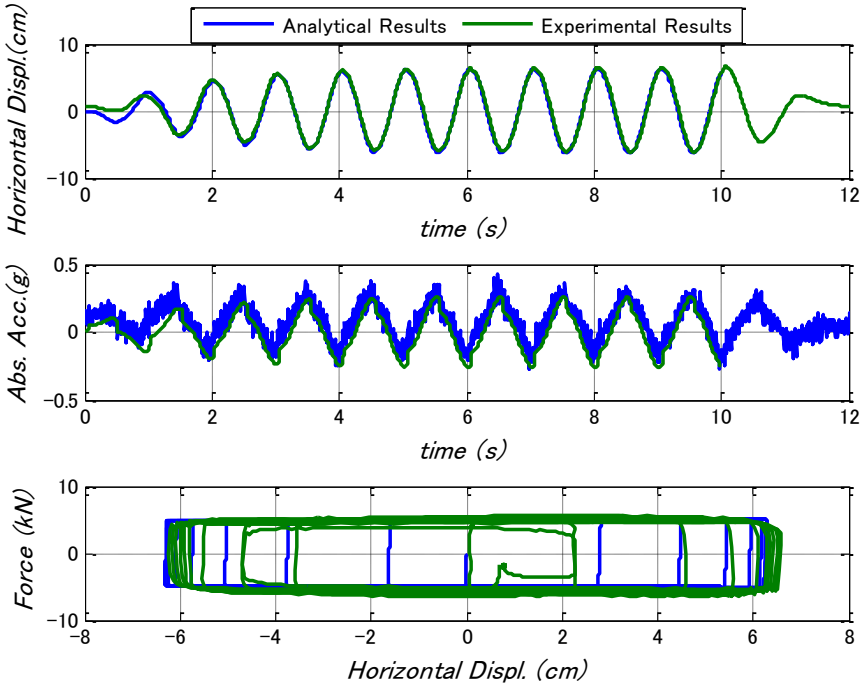

Figure 5.12 Response quantities for PF subjected to sinusoidal excitation

Fig 5.13 also shows the comparison of response with Hanaore earthquake. The name Hanaore comes from the name of the fault extending north-northeastward for some 45 km from the northeastern part of the urban area of Kyoto to Imazu Town, Shiga Prefecture in Japan. This earthquake is scaled to give PGA equal to 0.387g, see Fig 5.14.

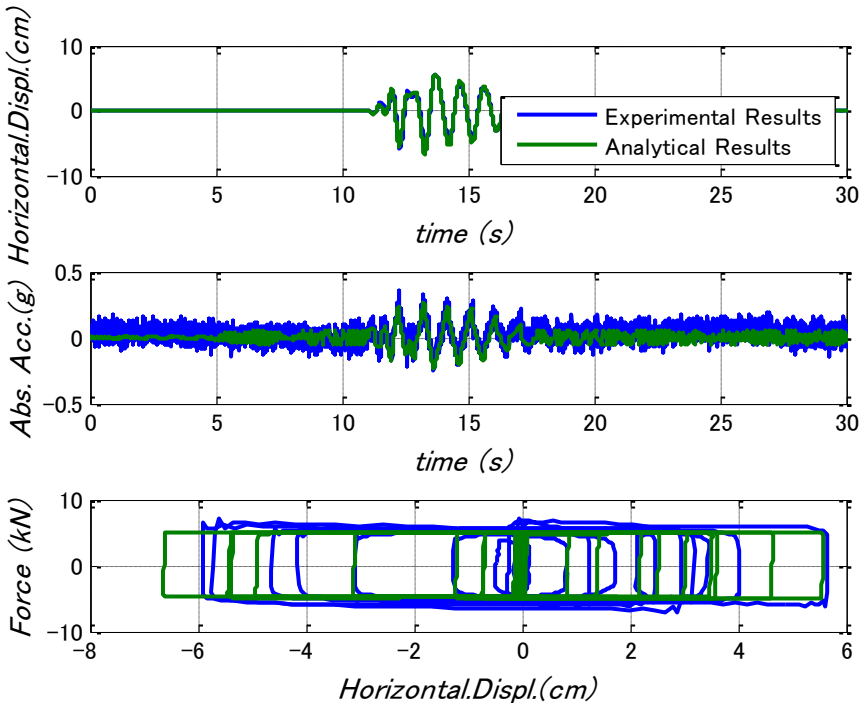

Figure 5.13 Response quantities for PF subjected to Hanaore earthquake

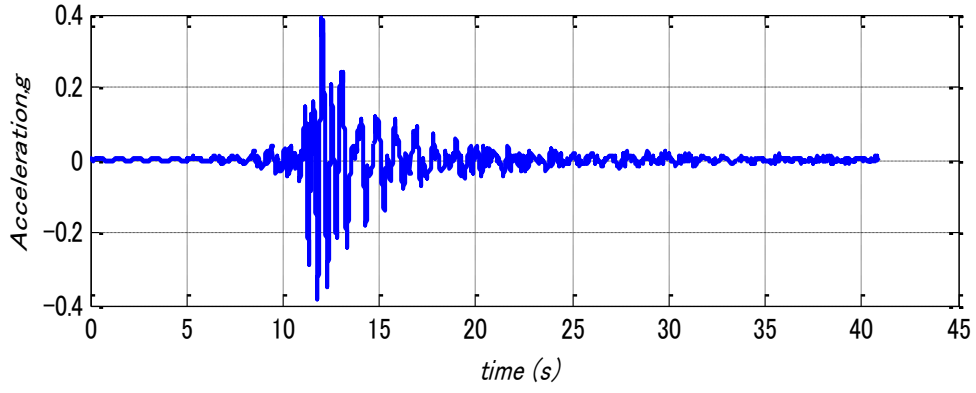

Figure 5.14 Acceleration record for Hanaore earthquake (longitudinal component)

In view of the fact that bearing displacement can be accurately obtained by modeling the superstructure as a rigid body in a base isolated structure (Kulkarni and Jangid 2002), the time history nonlinear analysis was carried on by assuming a rigid body motion.

Two models are considered for the numerical simulation of the raised floor girders supported on both the UPSS and rubber bearings. The two models are the simplified model and the spring model. The proceeding sections explain these models and present the simulation results.

5.2.1 Simplified model

This model is explained thoroughly in chapter 4. The idealized force-displacement relationship of UPSS bearing is used for simulation. A sample of results is presented here. Fig. 5.15 and Fig. 5.16 show a comparison between the experimental and analytical results for two different UPSS subjected to different sinusoidal excitations.

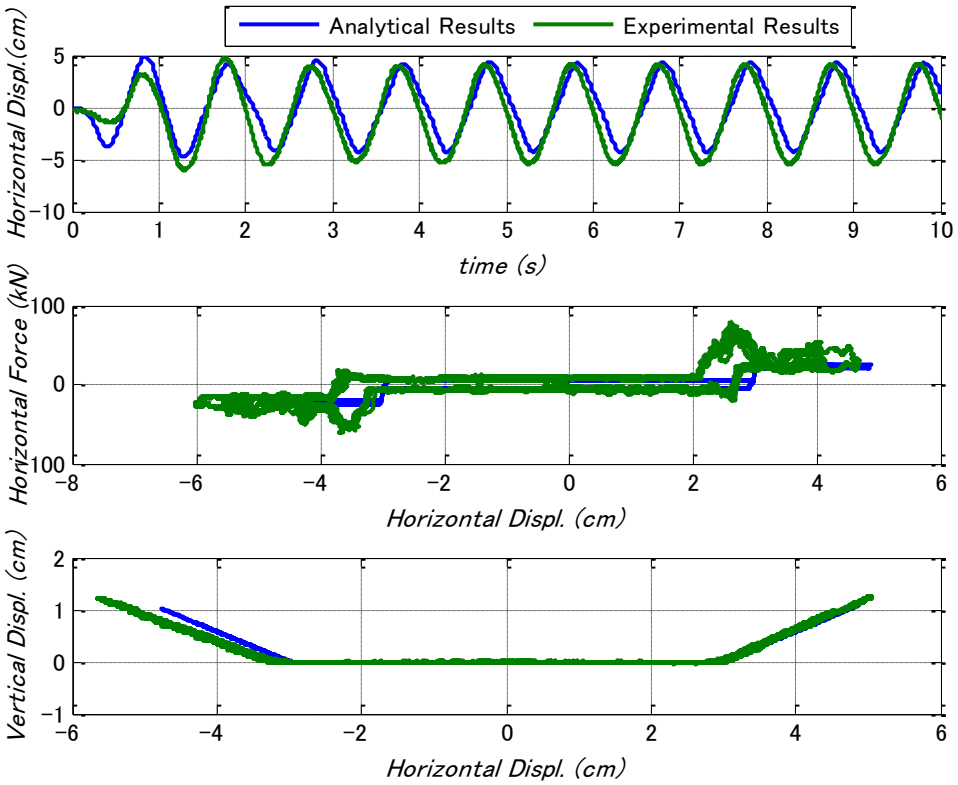

Figure 5.15 Time variation of response quantities for UPSS; 2.0 m/s^2 sin 1Hz, L=30mm, θ=30°

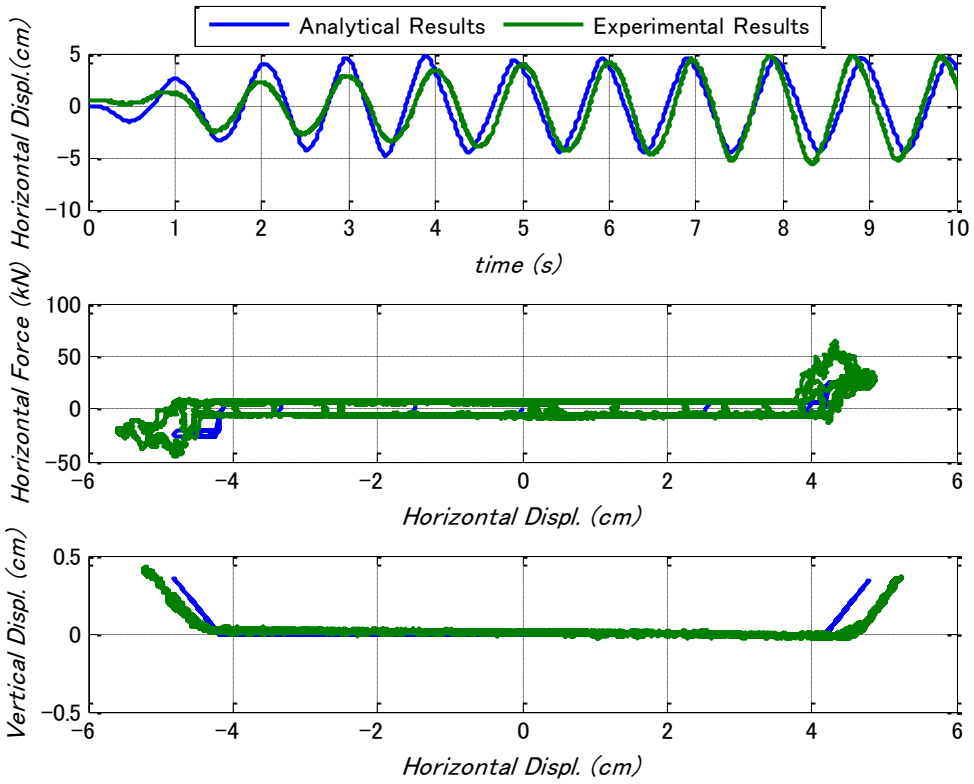

Figure 5.16 Time variation of response quantities for UPSS; 1.0 m/s^2 sin 1Hz, L=42mm, θ=30°

Figure 5.17 also shows the comparison between numerical model and experimental results when the raised floor girder is subjected to earthquake excitation. Despite the use of simplified mathematical modeling for the UPSS bearing, the results still shows a good agreement as can be noticed from Figs. 5.15,16 and 17. Additional displacement history response results are shown in Fig. 5.18 for various types of excitation and UPSS characteristics.

Therefore, the above formulated equations can safely predict the maximum displacement response during seismic excitation. However, it has been noticed that the dynamic behavior at the transition between horizontal and inclined surfaces is extremely random and nonlinear. Small shock impulses are formed in some strong excitation motions.

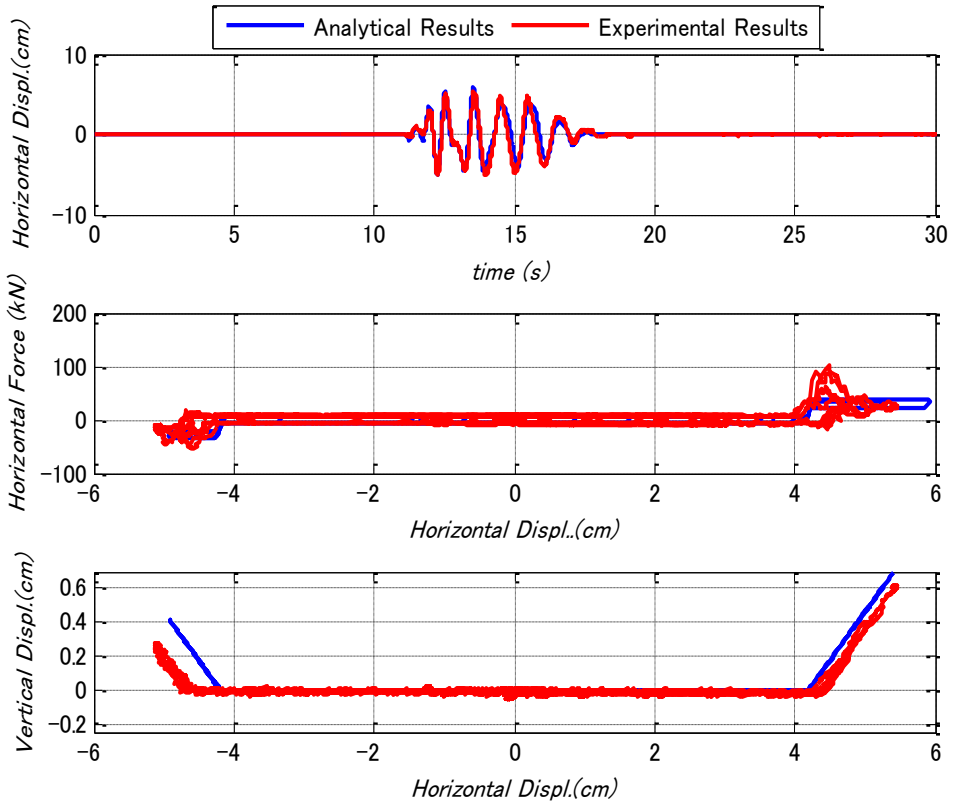

Figure 5.17 Time variation of response quantities for multiple-slider bearing; Hanaore EQ (0.378g), L=42 mm and θ=30°

Test results show the relationship of these impulse loads and the velocity at impact is almost linearly proportional. The maximum displacement of the UPSS bearing isolator can be optimized and reduced by a sensitivity analysis for a better selection of the three main parameters that define the bearing which are L, θ and μ.

Fig. 5.19 shows an example of a sensitivity analysis for a various combination of inclination angle and clearance length under various excitation frequencies. The trend shows clearly that the higher inclination angle is effective in reducing the horizontal displacement for any frequency range and smaller clearance is more preferable in adding more reduction to the horizontal displacement.

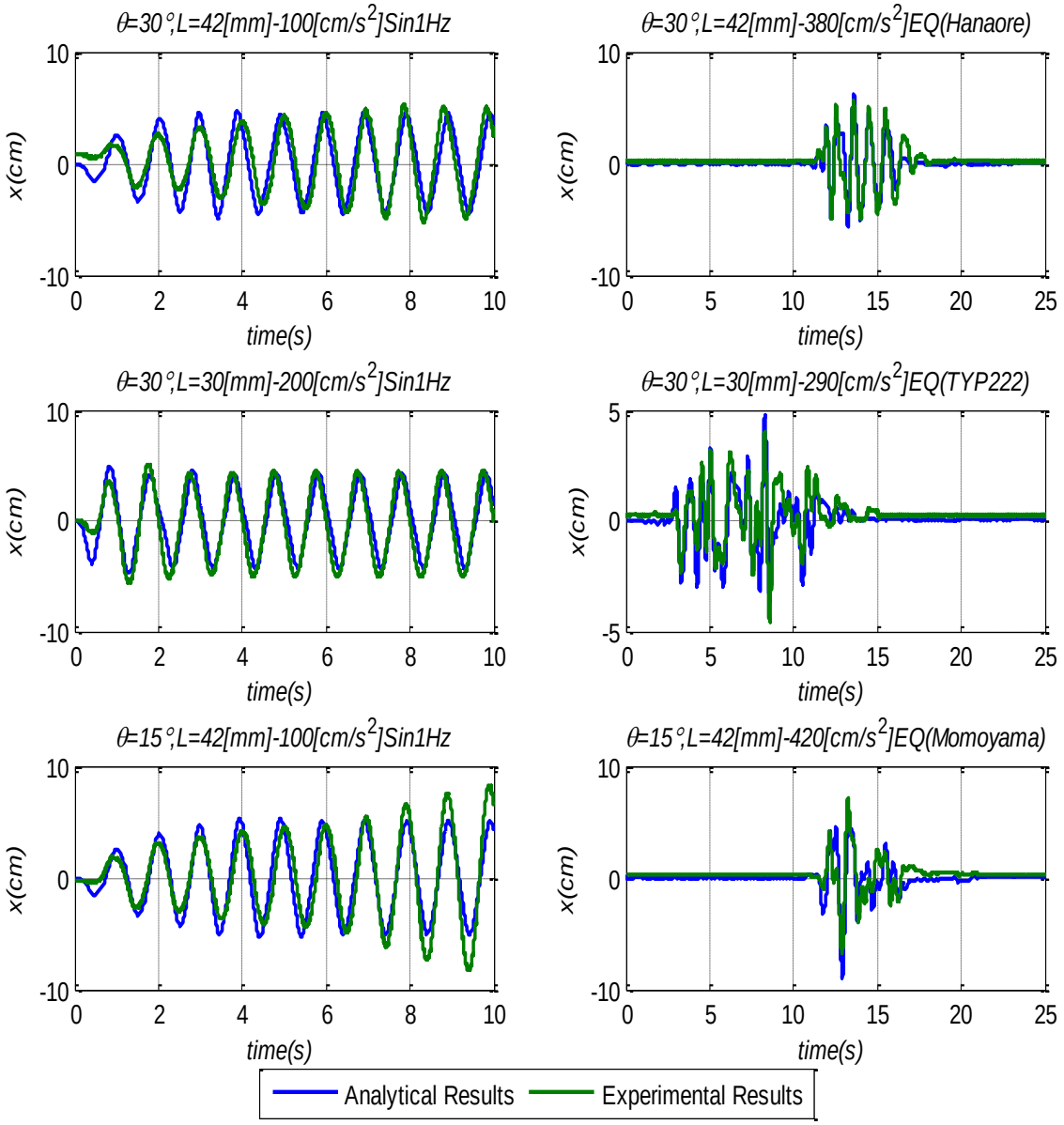

Figure 5.18 Displacement history response comparisons for various type of excitation

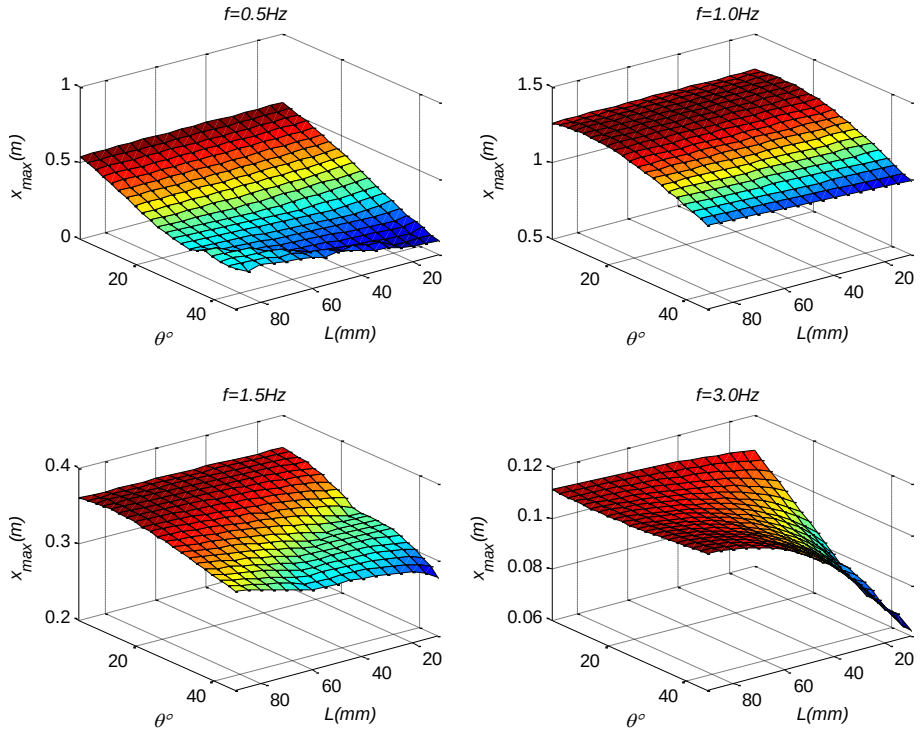

Figure 5.19 Maximum horizontal displacement subjected to harmonic excitation with various excitation frequencies; μ=0.1 and intensity 0.1g

5.2.2 Spring model

A more accurate model which takes into account the effect of both the horizontal and vertical motions is developed to simulate the behavior of UPSS. The UPSS model is defined as a set of non-linear springs as shown in Fig 5.20.

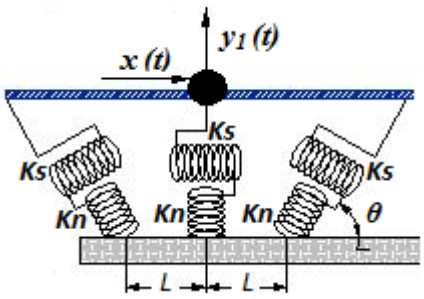

Figure 5.20 UPSS spring model

The analytical results using the spring model are compared to the experimental results obtained from the shaking table test. The complete analytical model is shown in Fig. 5.21.

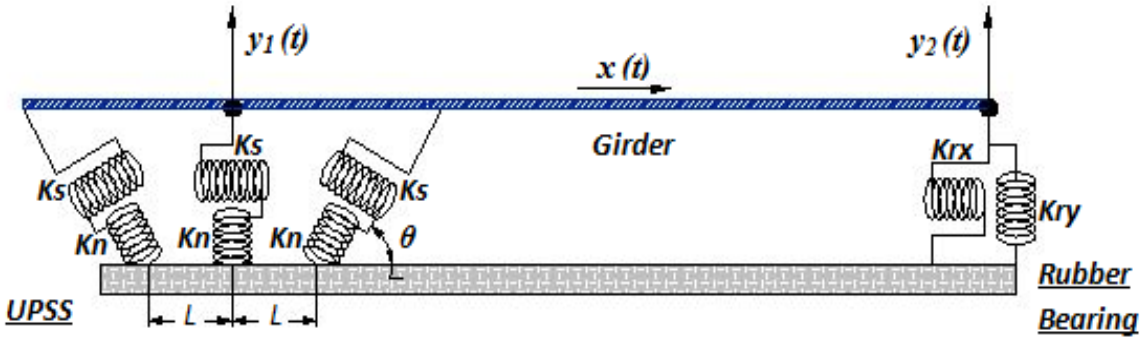

Figure 5.21 Shaking table test analytical model

Three degree of freedom in global coordinate system is assumed in this model as shown in Fig. 21: $x\ (t)$, y_1 (t), y_2 (t). Each sliding surface is modeled by two springs: K_s is the friction spring stiffness in the horizontal direction. The hysteresis behavior of the friction interface can be approximated as an elasto-plastic curve as shown in Fig. 5.22. f_s and u_s are the force and displacement parallel to the sliding surface respectively.

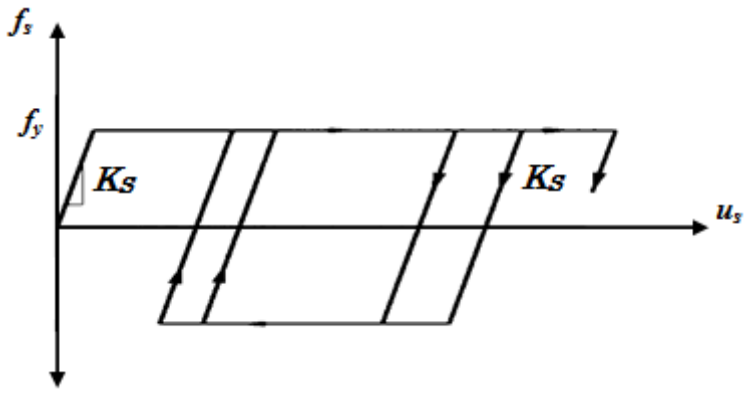

Figure 5.22 Friction spring hysteresis model

K_n is the normal spring stiffness perpendicular to the sliding surface. The behavior of the normal spring is shown in Fig. 5.23 where f_n and u_n are the force and displacement normal to the sliding surface respectively.

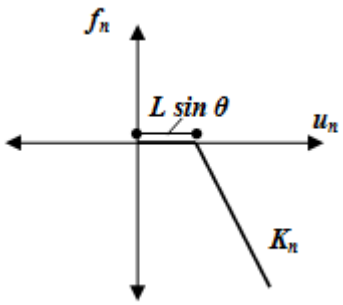

Figure 5.23 Normal spring

The yielding force f_y is defined by the multiplication of μ and f_n. Therefore, f_y changes by the change in f_n. However, when a force perpendicular to the sliding surface f_n reaches in tension, a force along the sliding surface f_s is 0. K_n is determined by compression test on PTFE sample and is found to be equal to 62.7 kN/mm as shown in Fig. 5.24.

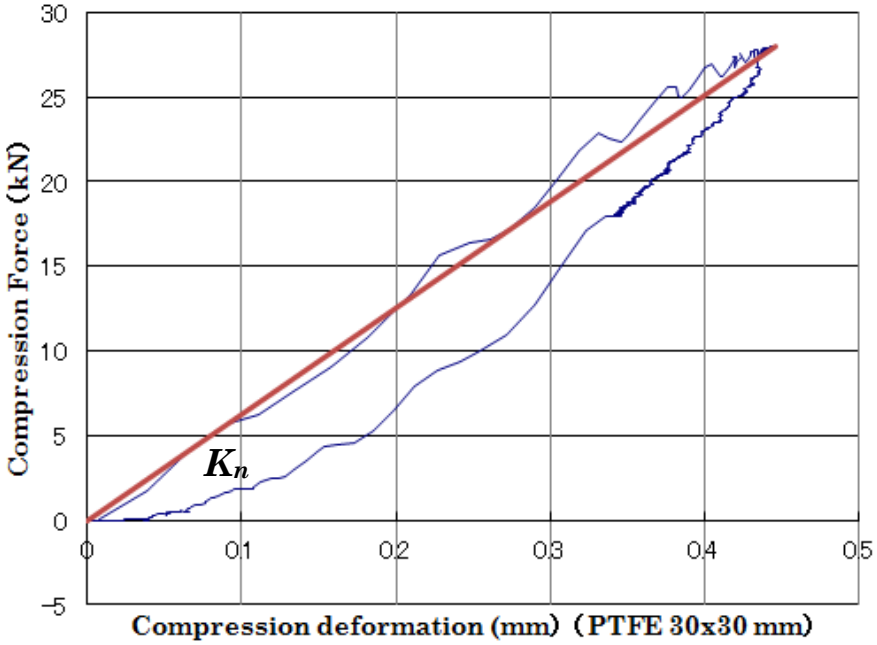

Figure 5.24 Compression test for PTFE sample

The stiffnesses of rubber in the horizontal and vertical directions used in the experement are 2700 kN/m and 128 kN/m respectively with damping ratio of 5%. Friction coefficient is taken as 0.14.

In the analatyical model f_s is calculated from the following expression:

$$f_s = \mu f_n \frac{v_s}{|v_s| + \varepsilon} \tag{5.1}$$

where v_s is the velocity parallel to the sliding surface and ε is a constant defines the sharpness of yielding point taken as 0.0009. In this study nine cases are considered for comparison purposes. Those cases are selected with various loading conditions and different UPSS characteristics. The nine cases are summarized in Table 5.1. Figs. 5.25 to 33 show the results of this comparison.

Table 5.1 Cases used in comparison with the experimental results

Cases	***θ°***	***L (mm)***	***Loading***	***Amplitude (m/s²)***
1	30	42	Sin (1.0Hz)	1.0
2	30	42	EQ-HanaoreP7	3.7
3	30	30	Sin (1.0Hz)	2.0
4	30	30	EQ-TYP2-2-2	2.9
5	15	42	Sin (1.0Hz)	1.0
6	15	42	EQ-MomoyamaP7	4.2
7	15	42	Sin (0.8Hz)	1.4
8	15	42	EQ-HanaoreP7	4.0
9	15	42	EQ-TYP2-2-2	3.0

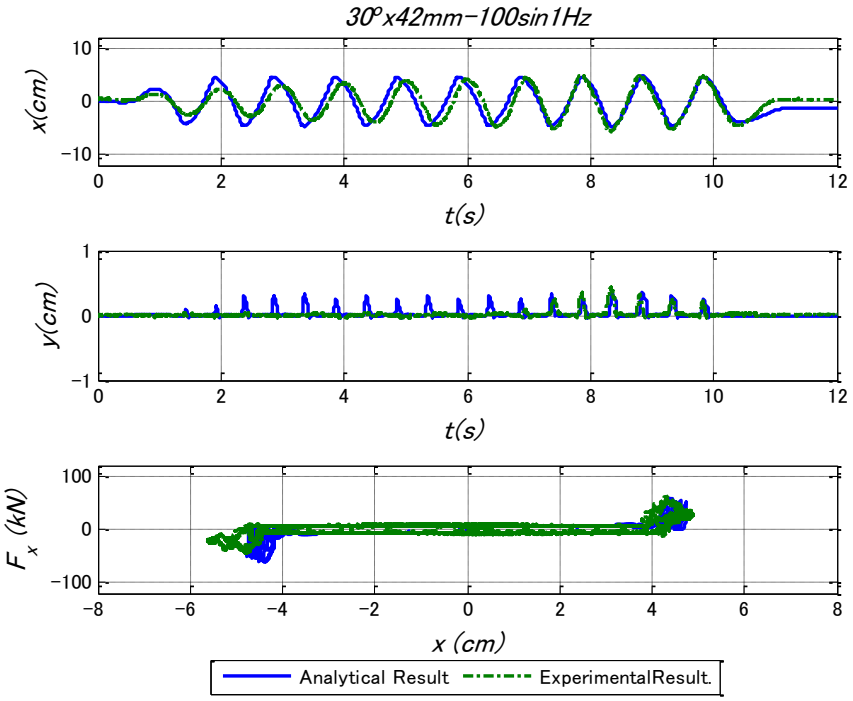

Figure 5.25 Time variation of response quantities for UPSS case #1

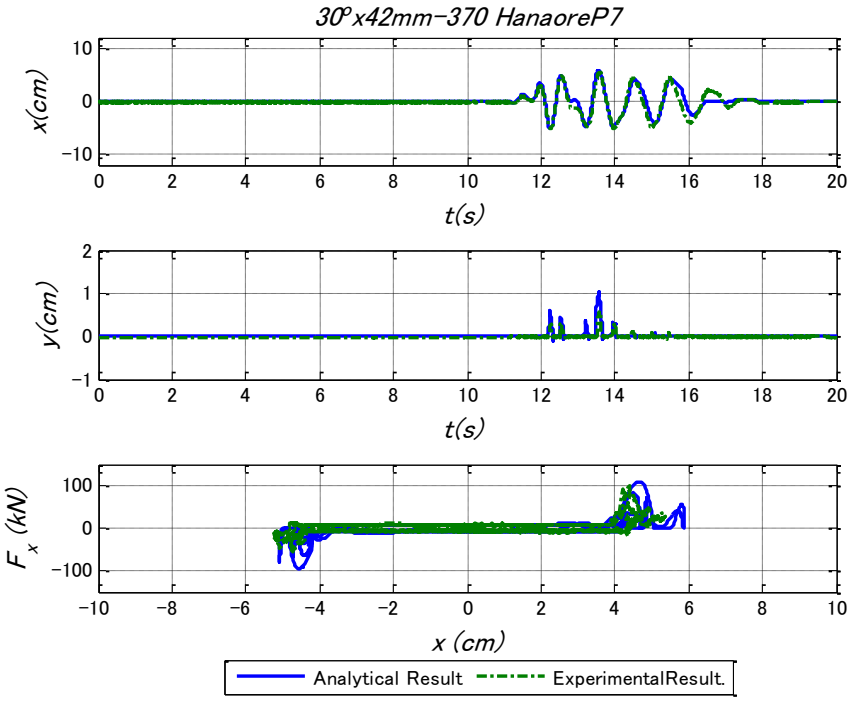

Figure 5.26 Time variation of response quantities for UPSS case #2

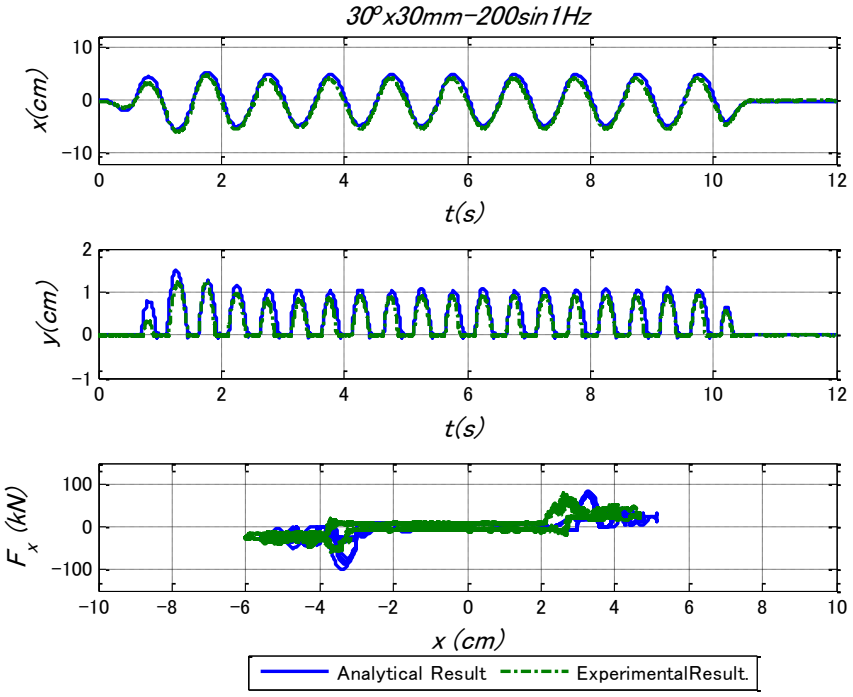

Figure 5.27 Time variation of response quantities for UPSS case #3

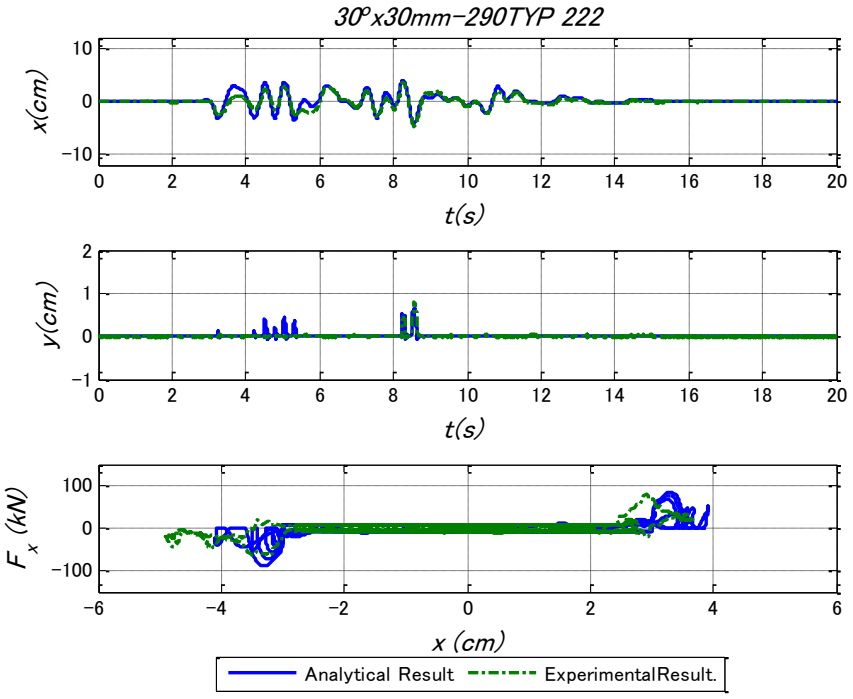

Figure 5.28 Time variation of response quantities for UPSS case #4

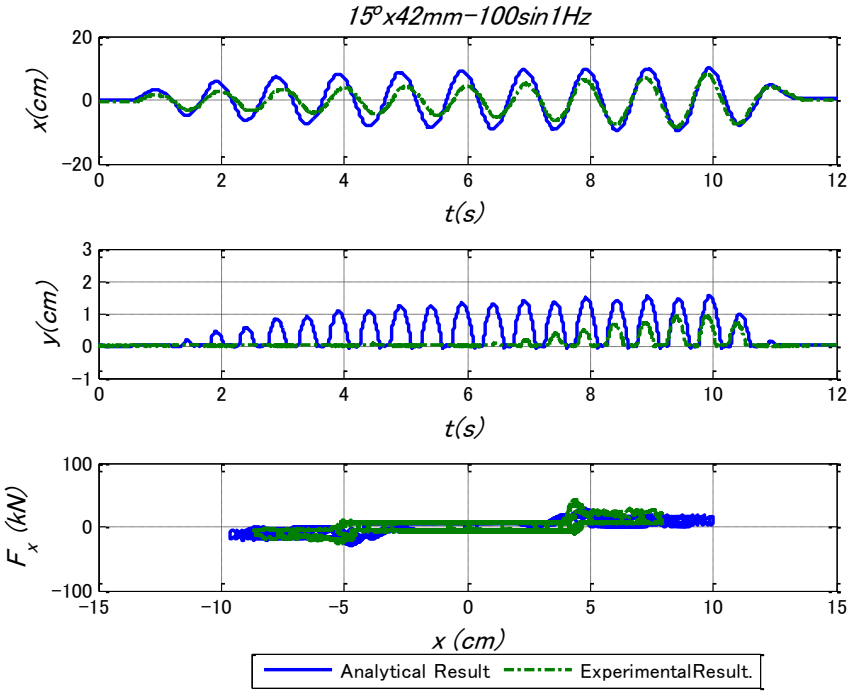

Figure 5.29 Time variation of response quantities for UPSS case #5

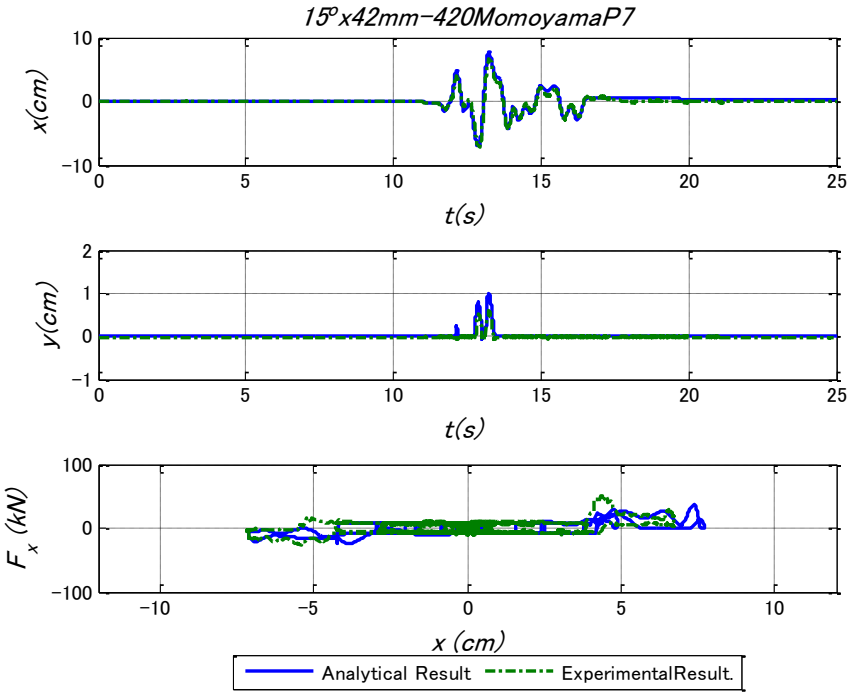

Figure 5.30 Time variation of response quantities for UPSS case #6

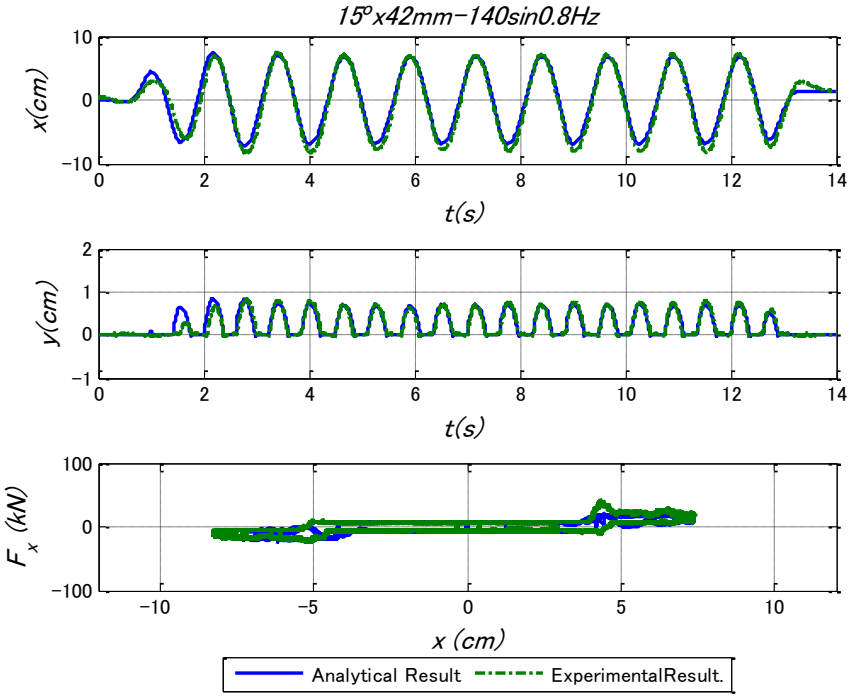

Figure 5.31 Time variation of response quantities for UPSS case #7

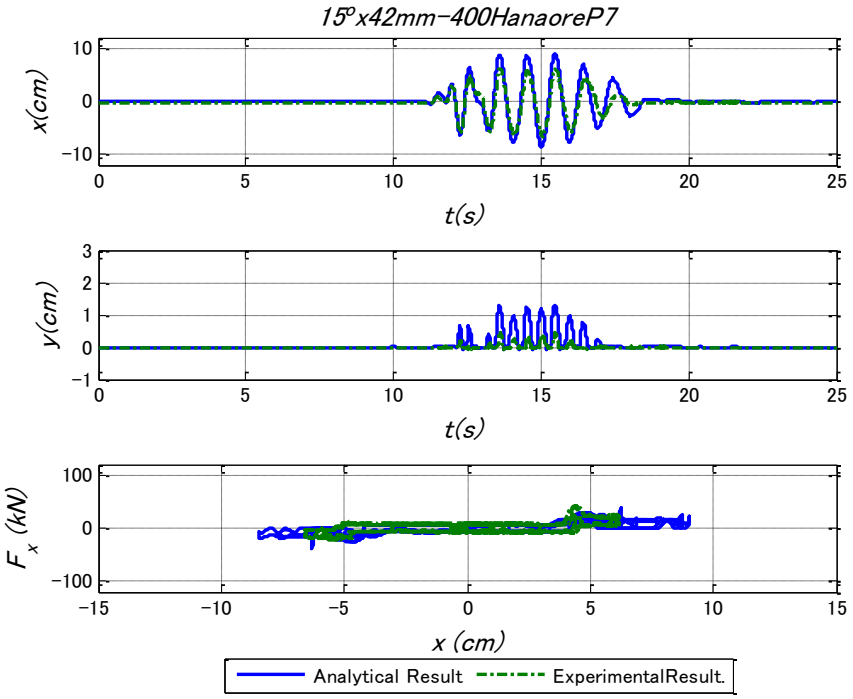

Figure 5.32 Time variation of response quantities for UPSS case #8

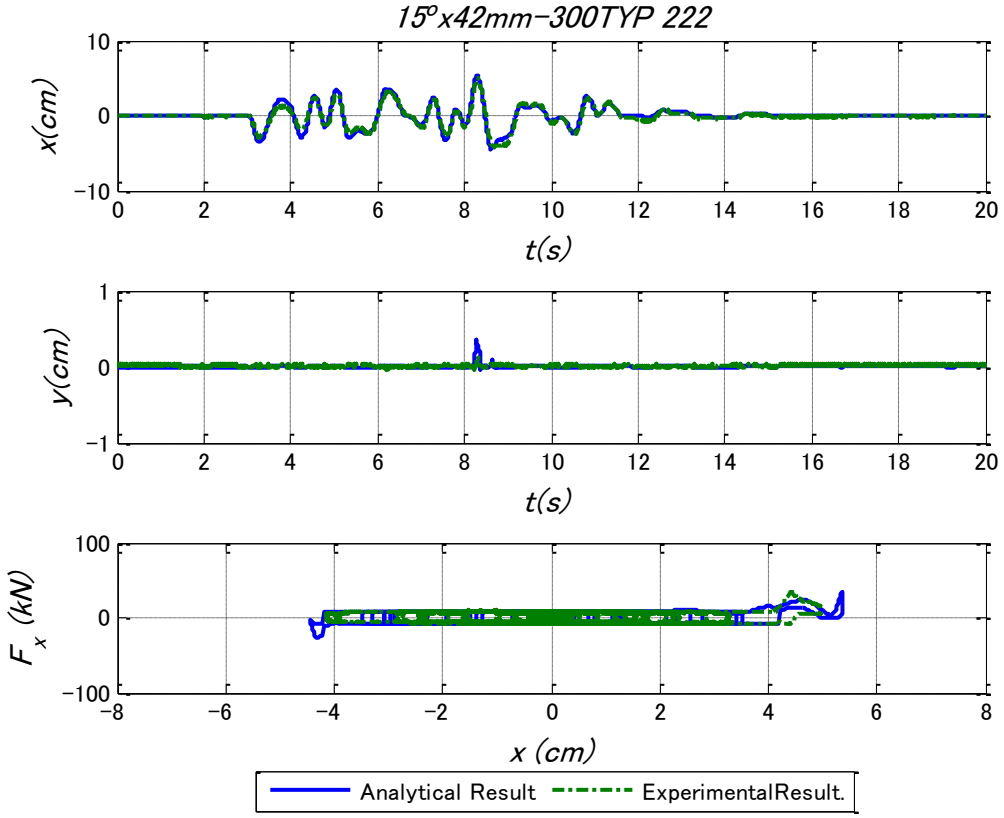

Figure 5.33 Time variation of response quantities for UPSS case #9

The above graphs show some variations between the two results. It might be due to the experimental girder rotation, or/and the time lag of the measuring sensors, or/and using Coulomb friction type or/and springs' stiffness values were not accurate enough. However, the results from the analytical spring model still indicate good agreement with the experimental results. The displacement time history obtained for both the horizontal and vertical directions in most simulation cases are found to be almost exact. The main error comes mainly from the pulse forces that are generated at the transition point between the horizontal and inclined sliding surfaces. These pulses are extremely random in both direction and magnitude which make the modeling more difficult.

5.3 Conclusion

The actual behavior of UPSS bearing under various types of excitations has been examined and verified. The component test results show a good agreement with the proposed idealized force-displacement relationship. However, at high velocity rate pulses are generated causing some variation in the hysteresis loop.

The shake table experiment has been modeled using two models. The first model is the simplified technique which depends on the essential characteristics of UPSS bearing and the second model is the spring model which depends on a set of non-linear springs to model the horizontal and vertical motion.

It has been found that both model can still be regarded as a good approximation that covers the essential characteristic of the device.

References

Igarashi A, Sato T, Shinohara M, Katou Y, Uno H, Adachi Y. Uplifting Slide Bearing (2) – Verification of Seismic Response by Tests. *34th IABSE Symposium on Large Structures and Infrastructures for Environmentally Constrained and Urbanised Areas*, Venice, Italy; 2010.

Kulkarni J, Jangid R. Rigid Body Response of Base-Isolated Structures. *Journal of Structural Control* 2002; 9:171-188.

Oiles Corporation, Document No. EKS-487-02, 2008 (in Japanese).

Morimoto S. The dynamic behavior of diagonally sliding bearing by shaking table test. *Master's thesis* 2009, Kyoto University, Japan, (in Japanese).

Uno H, Igarashi A, Adachi Y, Katou Y, Shinohara M, Matsuda H. Uplifting slide bearing - A seismic response control device for multi-span continuous bridges. *11th World Conference on Seismic Isolation, Energy Dissipation and Active Vibration Control of Structures*, Guangzhou, China, Nov. 17-21; 2009.

Chapter 6

UPSS bearing for seismic retrofitting of frame structures with soft first stories

UPSS bearing is proposed in this chapter to retrofit existing buildings with inadequate soft stories as well as new structures to be constructed with soft first story intended for architectural or functional purposes. The seismic interface is an assembly of bearings set in parallel on the top of the first story columns; the UPSS bearings and rubber bearings. A numerical example of five-story reinforced concrete shear frame with a soft first story is considered and analyzed to demonstrate the efficiency of the proposed isolation system in reducing the ductility demand and damage in the structure while maintaining the superstructure above the bearings to behave nearly in the elastic range with controlled bearing displacement. Comparative study with the conventional system as well as various isolation systems such as rubber bearing interface and resilient sliding isolation is carried out. Moreover, an optimum design procedure for the UPSS bearing is proposed through the trade-off between the maximum bearing displacement and the first story ductility demand ratio. The results of extensive numerical analysis verify the effectiveness of the multiple-slider bearing in minimizing the damage from earthquake and preserving the soft first story from excessively large ductility demand.

6.1 Introduction: Literature review

Despite structures with soft first story are inherently vulnerable to collapse during

earthquakes, it is still in demand especially in urban areas. Soft first story offers for architects an attractive model by allowing a sense of floating and bright spaces. The famous architect Le Corbusier was one of the pioneers who utilizes the idea of soft first story by lifting the structure off the ground, supporting it by pilotis (or piers), establishing the leading principle of the modern architecture: the "pilotis-story" (Mezzi 2006). A prime example is Le Corbusier's Villa Savoye in Poissy, France, see Fig 6.1.

Figure 6.1 View of the west and south facades of the Villa Savoye

The soft first story might be functionally or commercially desirable by providing parking spaces, allowing for a grand entrance or ballrooms as in hotels and permitting a desirable continuous windows for display for stores located in first story. In addition, such a building help in raising the inhabitants space in the building above typical storm surge levels in hurricane-prone areas.

Current design guidelines such as the International Building Code (International Code Council 2003) classify the structure as a "soft story" if the lateral stiffness of that story is less than 70% of that in the story immediately above it, or less than 80% of the average stiffness of the three stories above it . Moreover, the code also defines the “extreme soft story” when the lateral stiffness of that story is less than 60% of that in the story immediately above it, or less than 70% of the average stiffness of the three stories above it. Based on the ductility design concept that utilizes inelastic behavior to increase the flexibility of the structure by lengthening the fundamental period and generate energy-absorption, some structural engineers introduced the concept of flexible first story (Bednarski 1906, Green 1906, Martel 1929, Jacobsen 1938). Later on, this idea was modified leading to the concept of shock-absorbing soft story method (Fintel and Khan 1969). This system renders all the inelastic deformation to take place

in the first soft story columns while the above superstructure is designed to remain in the elastic range. The shock-absorbing soft first story contains neoprene layers placed on top of stability walls with separating the wall from the slab above as shown in Fig. 6.2.

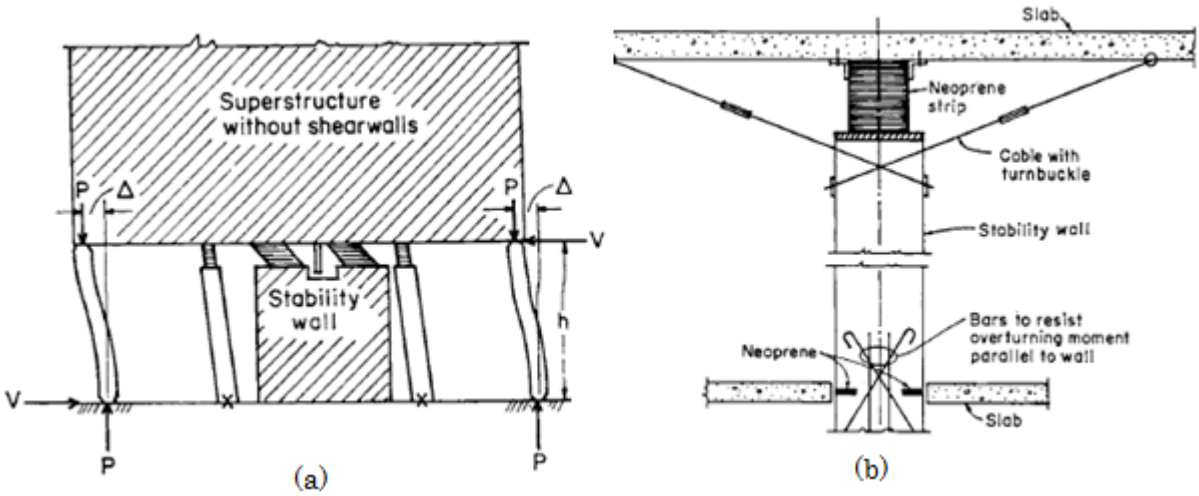

Figure 6.2 (a) Deflected shock-absorbing soft story (b) Detail of shock-absorber

However, this attempt to reduce forces on structure by allowing the first story columns to yield during an earthquake and produce energy-absorbing action is no longer an appealing idea for structural engineers due to the excessive drifts in the first story coupled with P-Δ effects on the yielded columns, increasing the risk to develop a collapse mechanism known as soft story failure (Chopra et al 1973). Such mode of failure was observed clearly during many earthquakes in the past; one example is the damage due to the 1995 Kobe earthquake. Many reinforced concrete buildings were severely damaged and most of them were buildings with soft story (Yoshimura 1997).

Figure 6.3 Soft story failure (Kobe earthquake, January 17, 1995, magnitude 6.9)

Additional example is the case of California's Loma Prieta Earthquake of 1989. The soft story failure was responsible for nearly half of all the homes that became uninhabitable.

Another modification to the soft first story concept was proposed by introducing additional energy dissipation capacity in order to reduce drift and providing a mechanism to reduce P-Δ effects (Chen and Constantinou 1990). In this system, Teflon sliders are placed at top of some of the first story columns while the rest of the first story columns are designed with reduced yield strength and ductile behavior in order to accommodate large drifts as shown in Fig.6.4.

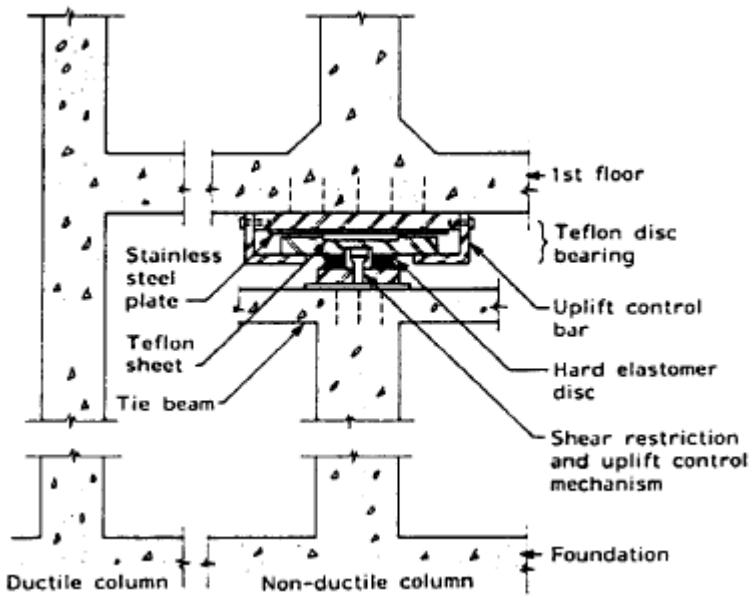

Figure 6.4 Chen and Constantinou proposed modification of first soft story

A similar concept with the difference that the first story shear walls are fitted with Teflon sliders was also proposed (Mo and Chang 1995) as in Fig. 6.5. A further extension of the concept was proposed similar to the above philosophy with additional steel dampers to enhance the energy dissipation during earthquakes (Iqbal 2006).

Todorovska proposed another variation of the soft story concept using inclined rubber base isolators or inclined soft first story columns (Todorovska 1999). The system behaves as a physical pendulum pivoted above the center of mass and is more stable than the standard system. Briman and Ribakov have developed a method for retrofitting soft story buildings by replacing weak conventional columns with seismic

isolation columns (Briman and Ribakov 2009). The seismic isolation device is based on a friction pendulum principle. The proposed seismic isolation column is a kinematic system. Its main joint has high load carrying capacity as well as all properties of a three-dimensial hinge connection as in Fig. 6.6.

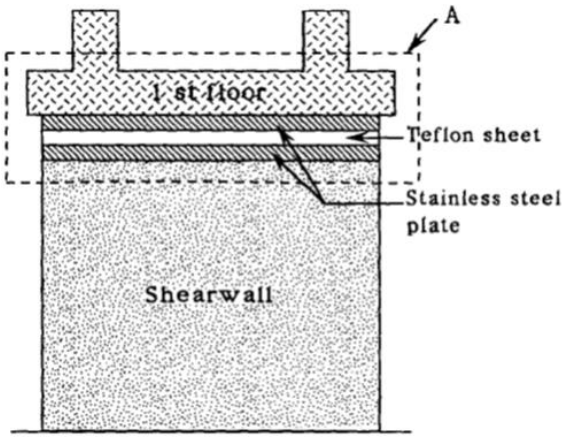

Figure 6.5 Mo and Chang proposed modification of first soft story

Figure 6.6 The middle part of the seismic isolation column

Past earthquake damage examples have proven that the performance of conventionally designed columns in soft story structures is unsatisfactory due to the high uncertainty in the ductility design concept. Although structures with soft stories may survive during

earthquakes, excessive drifts and formation of plastic hinges at critical sections could make it difficult to repair. For that reason, more effective and reliable techniques are needed to enhance the structural safety and integrity for such special type of structures. It can be noticed from the previous studies that seismic isolation is one of the prominent alternatives that can overcome the dilemma between the need for soft story and its vulnerability to collapse.

In this chapter, the seismic performance of soft first story frame structures is upgraded by installing the UPSS bearings on the top of first story columns to effectively prevent the first story damage by reducing its ductility demand and maintaining the superstructure to behave nearly in the elastic range at the same time. The mechanism and efficiency of the proposed system are illustrated using a nonlinear time history analysis of moment resisting concrete frame subjected to seismic excitation. Comparative study with the conventional system and with various isolation systems such as the rubber bearing interface and the resilient sliding isolation is carried out. Finally, an optimum design procedure for the UPSS bearing is proposed.

6.2 Proposed system concept

The need for controlling displacement of the isolators to a minimum level is a vital issue especially in big and crowded cities where buildings are often built closely to each other because of the limited availability and high cost of the land. This leads to cause pounding of adjacent buildings due to the insufficient or inadequate separation and can be a serious hazard in seismically active area. Accommodating such large displacement responses by the conventional rubber bearing is costly and may cause instability.

The proposed seismic retrofit scheme for soft-first-story frame structures to solve this problem is shown in Figure 6.7. Isolation between soft first story columns and the rest of the superstructure is incorporated by installing the UPSS bearings on the top of interior columns and rubber bearings at the top of edge columns. The first story columns are tied together by tie beams to insure stability and enhance the safety. The orientation of the multiple-slider bearing is chosen as shown in Figure 6.7 to divert P-Δ moments from weak elements below the isolation interface which resemble the orientation mechanism of FPS (Almazan and Llera 2003, Earthquake Protection

Systems 2003, Eroz and DesRoches 2008).

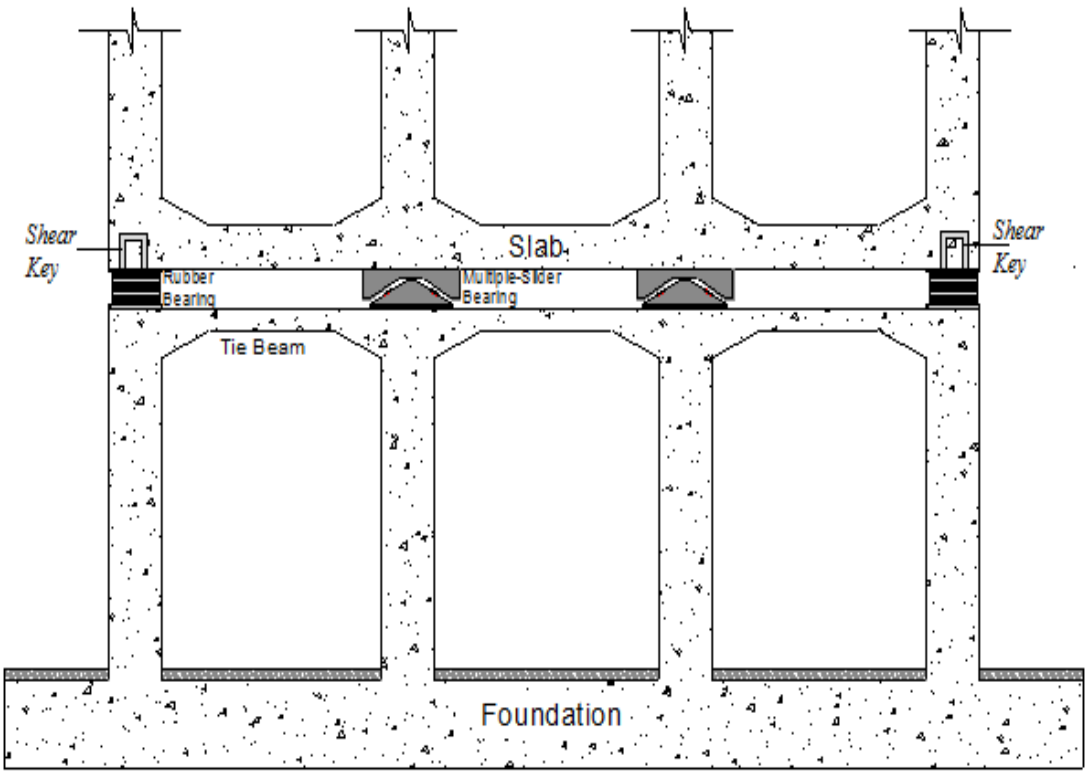

Figure 6.7 Set up arrangement of the UPSSS bearings in soft-first-story frame structure

The proposed system also offers a feasible solution for seismic retrofitting of existing buildings with soft stories in area where clearance between adjacent buildings is limited. Commonly, the seismic rehabilitation can be carried out simply by transmitting the load acting on the column temporary to jacks, then column is cut from the top at first story level and the isolation device is inserted and connected to the adjacent structural elements before the removal of the temporary jacks. Nevertheless, more neat and reliable methods without using lifting equipment also exist (Kawamura et al 2000). The UPSS bearing is vertically stiff, minimizing the vertical deflections of columns that occur during bearing installation in retrofit application avoiding damage to architectural finishes in upper stories. It is worth pointing out that the isolator provides an architecturally flexible and aesthetic solution in term of integration into the structural system.

6.3 Seismic response of five-story frame structure with first soft story

A five-story reinforced concrete shear frame with soft first story Figure 6.8 is considered to demonstrate the efficiency of the proposed isolation system in reducing the ductility demand and damage in the structure. The system is also examined and compared with the conventional frame structure.

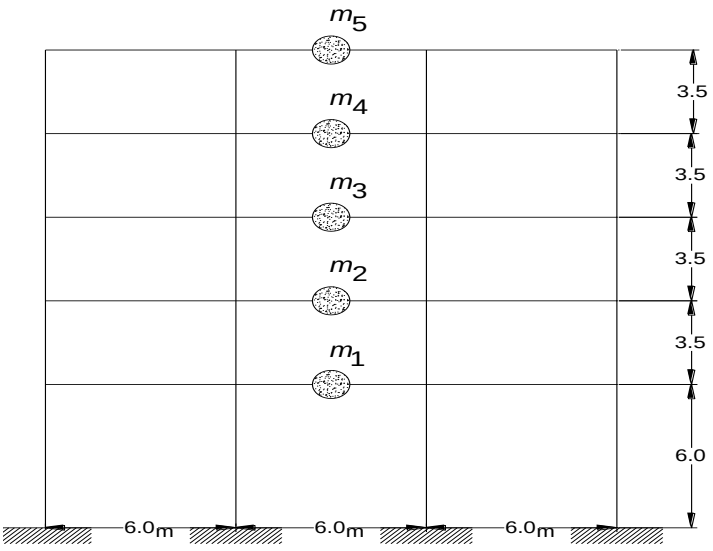

Figure 6.8 Five-story shear frame structure with soft story

Table 6.1 Presents the story initial stiffness (K_i) and the story yield strength to total weight (V_y/W).

Table 6.1 Properties of five-story frame structures

Story	K_i (kN/m)	V_y/W
1	41137	0.1451
2	154220	0.5344
3	133500	0.4572
4	96127	0.3488
5	60997	0.2084

It is obvious that the first story property implies sharp discontinuities in strength and stiffness relative to the above stories. In this example, the foundation connected to the structure is assumed to be rigid. Girders and floor systems are assumed to be rigid bodies and the columns do not deform axially. The fundamental natural period (T_1) is equal to 0.56 s for this frame structure with equal lumped floor masses (m) equal to 45.34 t for each story. Rayleigh damping in the structure with damping ratio of 5% for the first two modes is assumed.

To account for the continually varying stiffness and energy absorbing characteristics of the columns under cyclic loading, the modified Clough bilinear stiffness degrading model is used to represent the hysteretic behavior of the columns, see Figure 6.9. Five percentage post to pre-yielding stiffness ratio and 10% degradation stiffness rate (α) are used for columns hysteretic model. The ground motions used in simulations are: 1940 El Centro record NS component (0.32g) and 1995 Kobe JMA NS record (0.82g). Only unidirectional excitation is considered.

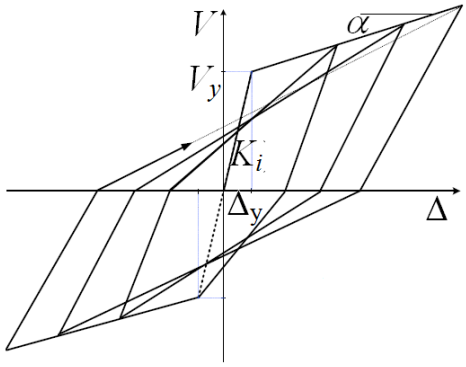

Figure 6.9 Modified Clough Degradation Model

The UPSS bearing is chosen with L=10 mm in the case of El Centro earthquake and L=50 mm in the case of Kobe earthquake and θ=15^0 for both cases. The restoring force (F_b) of RB is modeled with linear force-displacement relationship with viscous damping and can be expressed as follows:

$$F_b = k_b x_b + c_b \dot{x}_b \tag{6.1}$$

$$c_b = \zeta_b \times \left(2\omega_b m_t\right) \tag{6.2}$$

where c_b is the effective viscous damping of RB; m_t is the total mass of the superstructure above the isolation level; ω_b is the angular isolation frequency=$2\pi/T_b$; ζ_b is the effective damping ratio=0.15. The period of isolation T_b is chosen to be 2.0 s. T_b is equal to:

$$T_b = 2\pi\sqrt{m_t / K_b} \tag{6.3}$$

The friction coefficient of the multiple-slider bearing for all the three sliding surfaces is assumed to be Coulomb's type μ=0.05 in the case of El Centro record and μ=0.15 in the case of Kobe earthquake. The peak response of structures subjected to earthquake excitation using a velocity dependent friction model was not significantly different from that predicted by a Coulomb friction model (Fan et al 1988, Clark and Kelly 1990).

The dynamic equation of motion for the shear type isolated building can be written as follows:

$$[M][\ddot{x}(t)] + [C][\dot{x}(t)] + \{f_s(t)\} = -[M][r_1]\{\ddot{x}_g(t)\} - [r_2]\{f_h(t)\} \tag{6.4}$$

where [*M*], [*C*] are the $n \times n$ mass and damping matrices, respectively. $[\dot{x}(t)]$ and $[\ddot{x}(t)]$ are $n \times 1$ relative velocity and acceleration vectors, respectively. $f_s(t)$ is the vector of restoring forces which are described by modified Clough model and $\ddot{x}_g(t)$ is the ground acceleration. $[r_1]$ and $[r_2]$ are the force distribution loading vectors. $f_h(t)$ is the horizontal nonlinear isolators forces. Numerical time integration is performed using Newmark β-method.

6.4 Simulation Results

The analysis results for seismic response of five-story frame structure with soft first story are presented in this section. The primary concern of these simulations is to show the effectiveness of the proposed system in significantly reducing the ductility demand and drift of the soft first story in comparison with the conventional structure. Figs. 6.10 and 6.11 illustrate the ability of the proposed system to reduce both drift and ductility demand in the first story columns without significant changes in upper

stories in comparison with the conventional design. The drift and ductility demand were reduced both considerably by 49% when subjected to the El Centro record and by 41% when subjected to Kobe earthquake.

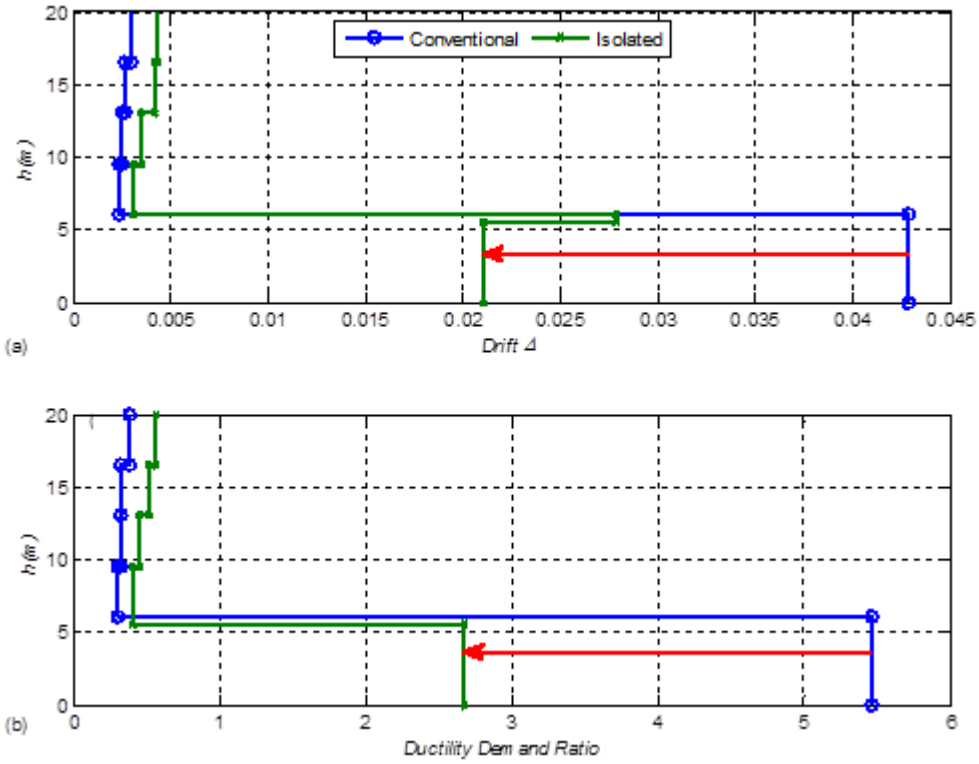

Figure 6.10 Comparison between conventional design and proposed isolation system subjected to El Centro record (a) max. story drift vs. story height (b) story ductility demand vs. story height

Figs. 6.12 and 6.13 show the force-displacement relationship for the UPSS bearings placed on the top of the first story columns and that for the first story. It is obvious that the presence of such isolation interface efficiently controls the transfer of the high concentrated energy and stresses from the soft first story columns to the isolation interface.

As shown in Figs. 12b and 13b, inelastic deformation of the first story columns is reduced, indicating a less energy being absorbed by these columns. It can be concluded that the proposed system is a practical cost-effective solution which can be adopted to retrofit existing buildings with soft stories and increase their seismic resistance.

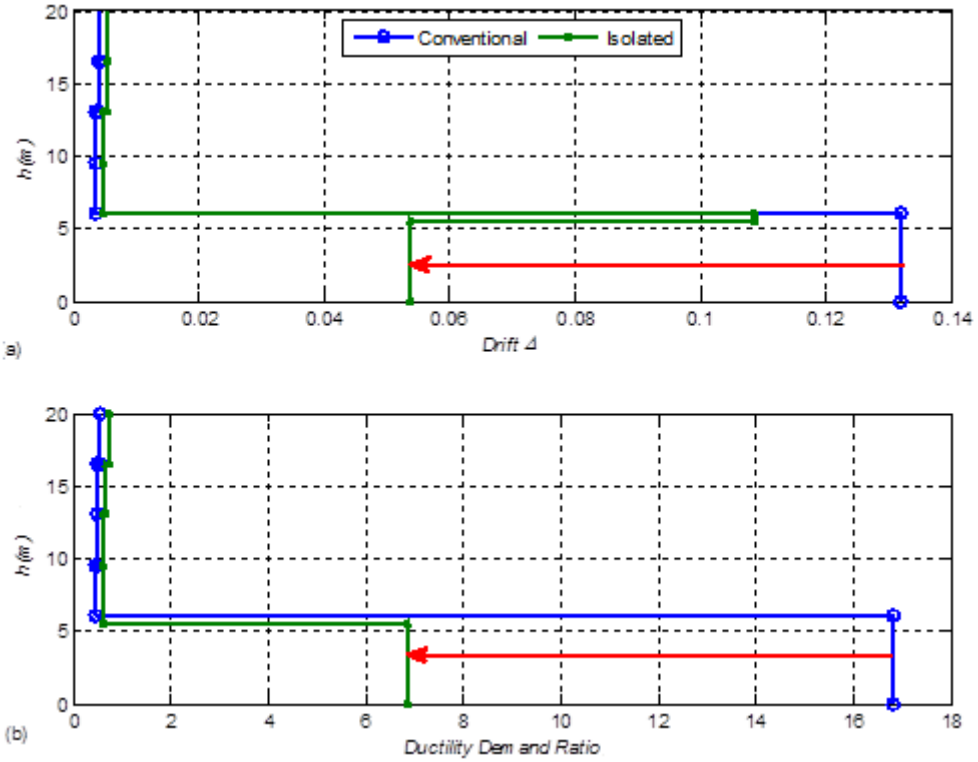

Figure 6.11 Comparison between conventional design and proposed isolation system subjected to Kobe record(a) max. story drift vs. story height (b) story ductility demand vs. story height

Installing the isolation on the top of columns rather than at the base level is a good solution to improve the seismic performance of the existing old building, especially for cases where installation at foundation level may be difficult or inaccessible. There exist examples of retrofit by a mid-story seismic isolation interface where it was difficult to put the isolators below the existing foundation stepwise along slope (Kawamura et al 2000).

Fig. 6.14 shows the layout of the building being retrofitted by a mid-story seismic isolation interface. 22 columns on the 8th story were cut at their mid-height and lead rubber bearings were installed.

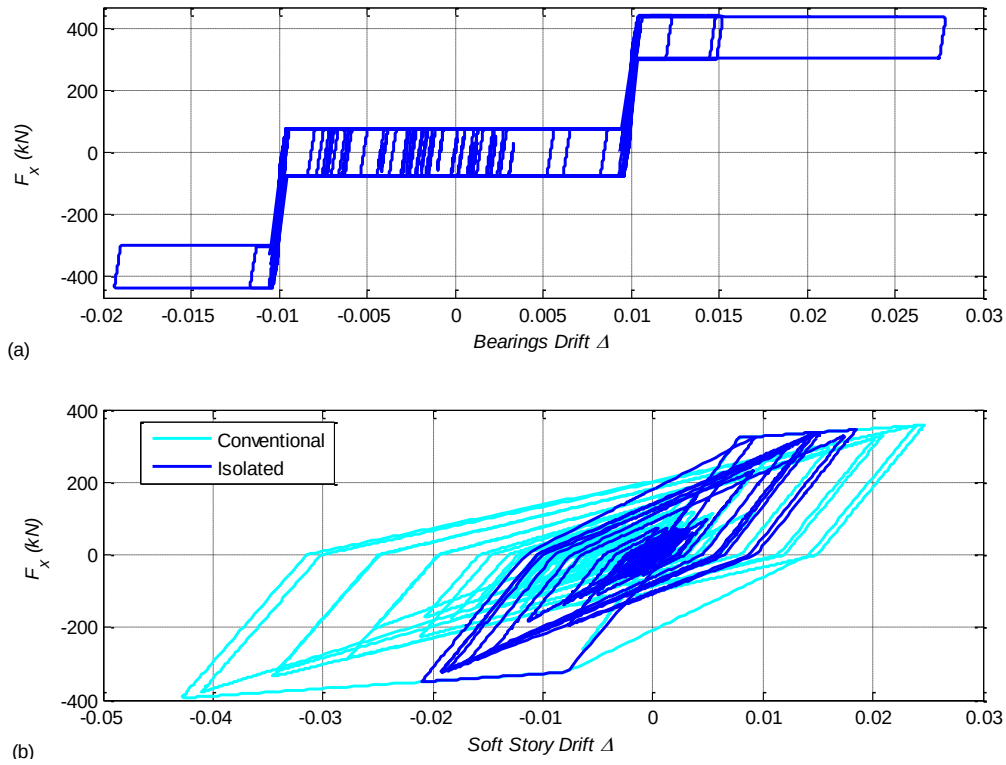

Figure 6.12 Hysteresis loop – El Centro record (a) the UPSS bearings (b) soft first story

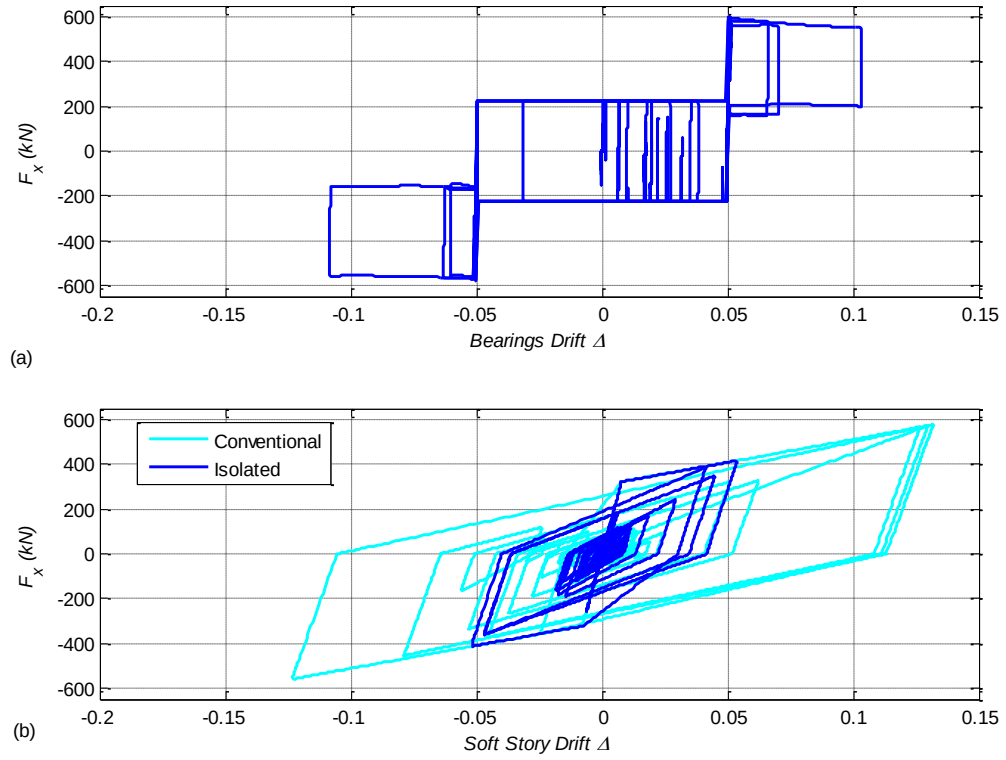

Figure 6.13 Hysteresis loop - Kobe record (a) the UPSS bearings (b) soft first story

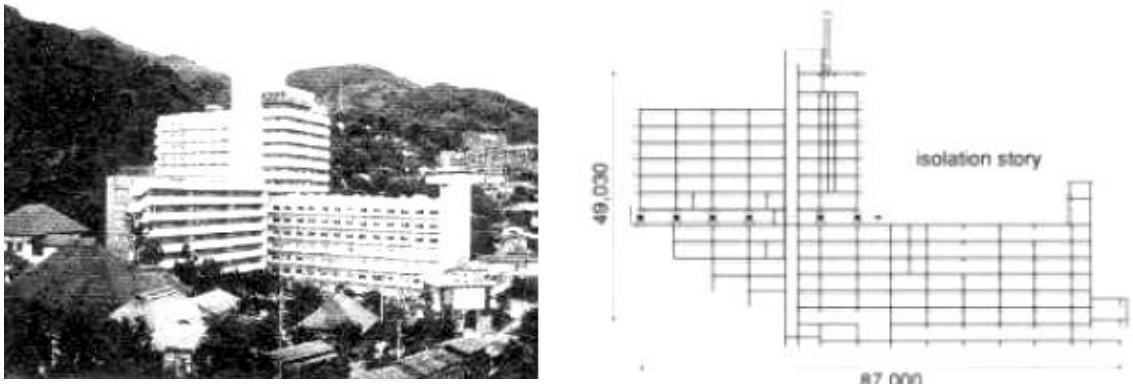

Figure 6.14 Whole view and section in the main retrofitted building of the personnel-training center of Taisei Corporation

Furthermore, the results of Figs 6.15 and 6.16 indicate that the seismic performance of the soft story frame structure in terms of ductility demand and story drift with the seismic interface on the top of the columns is superior to the case when the same interface is allocated at the base level.

The effect of inter-story isolation has been studied and analyzed by some researchers in which a seismic isolation system is installed at the middle story level (Murakami et al 2000, Sueoka et al 2004). It was shown in those research results that such type of concentrated response control systems reduces the response and improves the seismic performance of the entire building.

One example of the design of a building where a seismic isolation system is placed on its middle-story is the building located at Koraku 2-Chome, Bunkyo-ku, in Tokyo which is shown in Figs. 6.17 and 6.18. A seismic isolation system composed of 800mm diameter laminated natural rubber bearings and lead dampers is installed on the lower story of the 10th floor.

Another example is the Shiodome Sumitomo building, Fig. 6.19, with a height of 120m which considered a high-rise building in Japan since it is more than 60m. The middle story seismic interface is composed of 41 natural laminated rubber bearings located under columns, 100 lead dampers and 14 steel dampers.

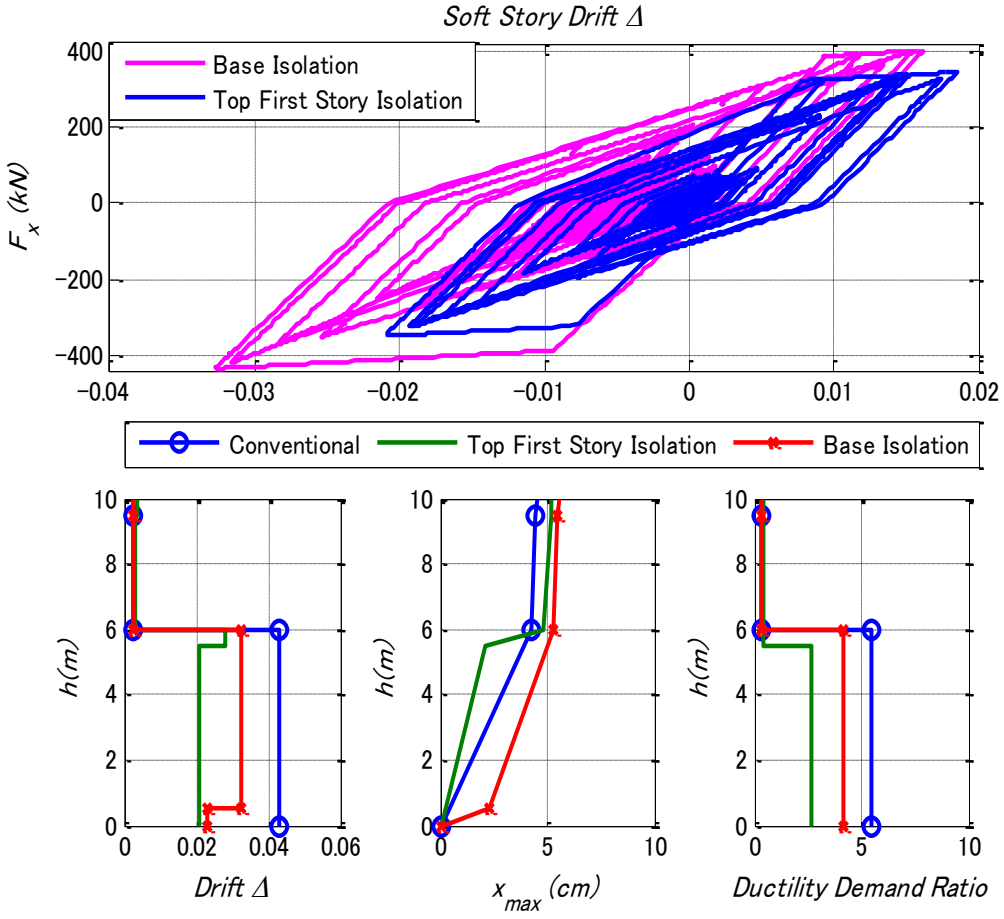

Figure 6.15 Comparison with base isolation case-El-Centro record (a) hysteresis loop of the UPSS (b) max. story drift vs. story height (c) max. displacement vs. story height (d) story ductility demand vs. story height

The proposed system in this chapter to introduce a seismic isolation interface on the top of first story columns has been recently used in the newly completed civil engineering research building of the National Taiwan University Fig 6.20. The isolation system, which is composed of 19 lead rubber bearings and 6 viscous dampers, is installed on the top of the first story (Chang et al 2008). The height of the isolation layer is designed to be 3.2m. The superstructure and substructure are designed to remain elastic under the design basis earthquake and the maximum considered earthquake.

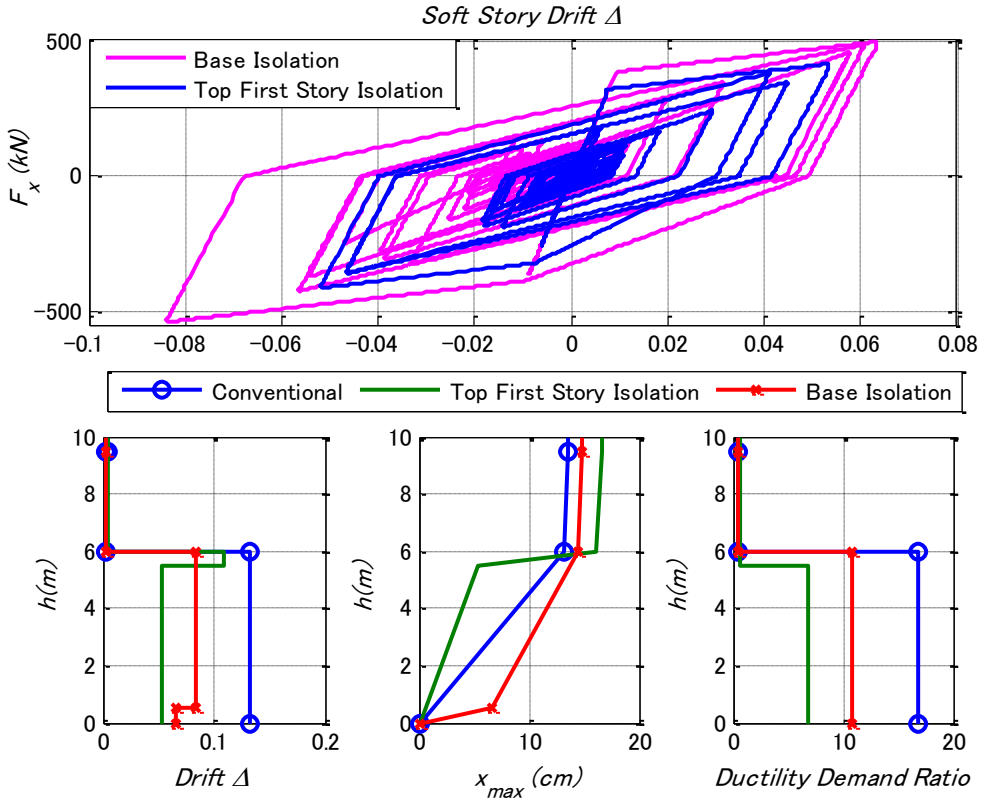

Figure 6.16 Comparison with base isolation case-Kobe record (a) hysteresis loop of the UPSS bearings (b) max. story drift vs. story height (c) max. displacement vs. story height (d) story ductility demand vs. story height

Figure 6.17 External view of the building constructed with mid-story seismic isolation (Murakami et al 2000)

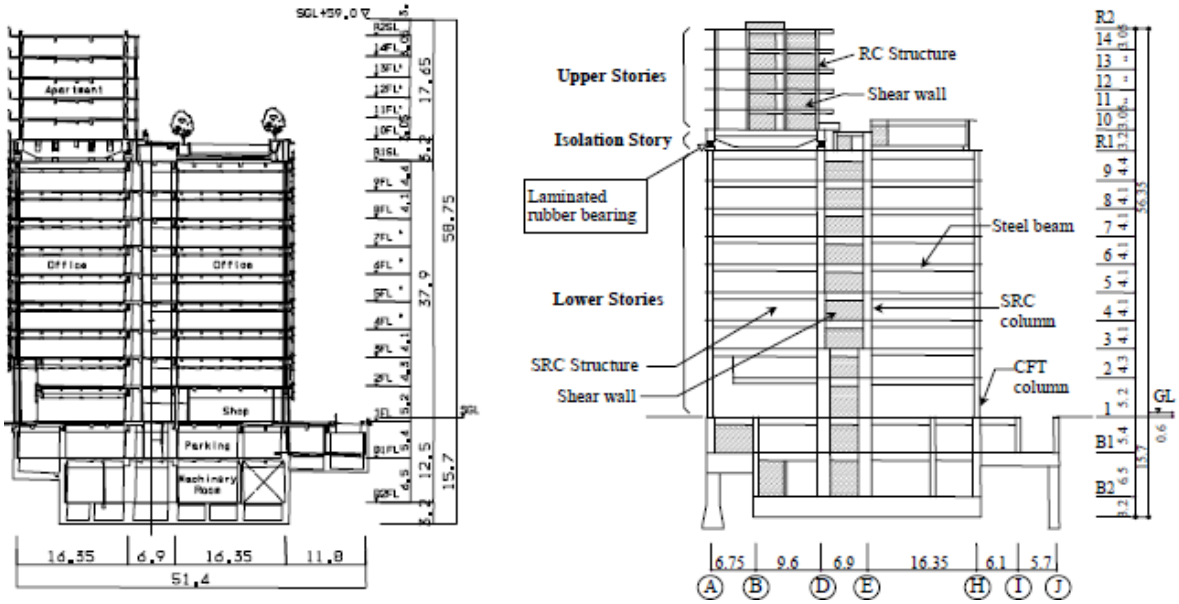

Figure 6.18 Sectional view and framing elevation of the mid story isolation building (Murakami et al 2000)

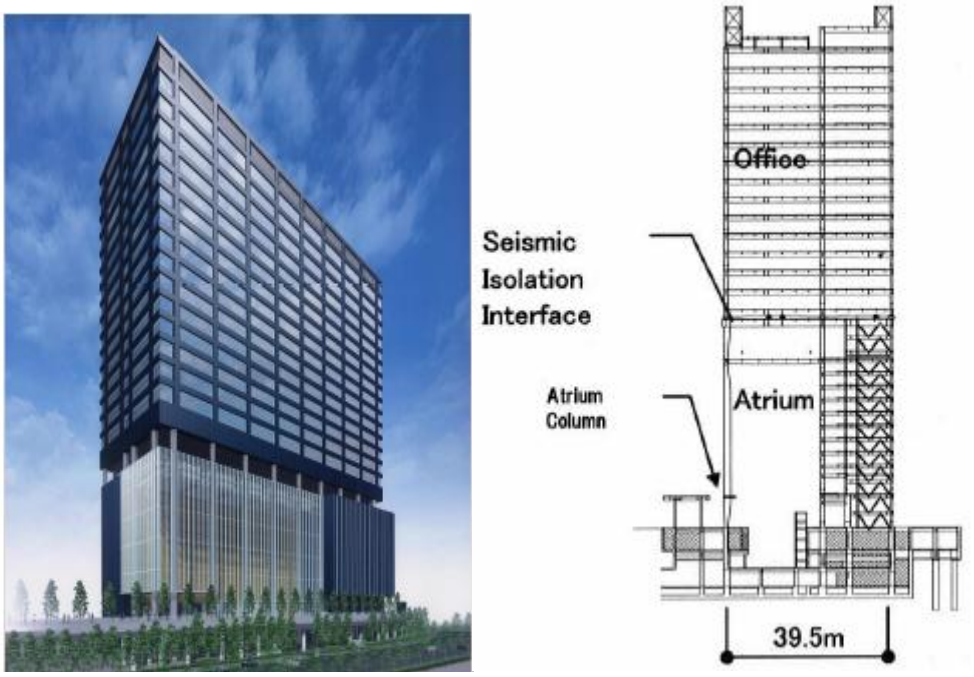

Figure 6.19 A 3D view of Shiodome Sumitomo building and framing elevation (Sueoka et al 2004)

(a)

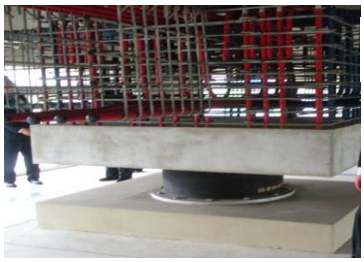

(b)

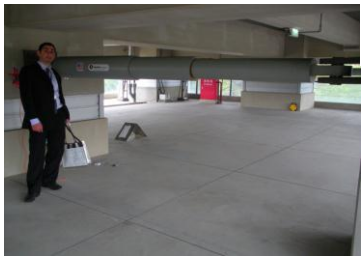

(c)

Figure 6.20 (a) Civil engineering research building of the National Taiwan University (b) Lead rubber bearing (c) Viscous damper

Seismic isolation requires modifications to some architectural features and services to accommodate the movements such as stairs, elevators, water and sewage pipelines. For example the pipelines used in the project above has been lengthened at the isolation interface to accommodate the horizontal movement and some have been cut as shown in Fig 6.21 that shows the flexible connections of non-structural components.

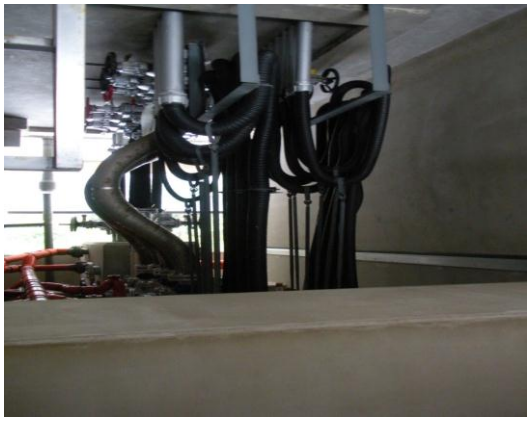

Figure 6.21 Non-structural components at the seismic isolation level

6.5 Optimum design for the Uplifting Sliding Bearing

As previously mentioned, one of the distinctive characteristics of the UPSS bearing is its capability to provide more freedom in the design process while defining the optimum parameters that are required to define the bearing to obtain the most efficient seismic performance. In this section, the optimum design for the UPSS bearing is adopted and discussed. This is accomplished by understanding the sensitivity of the bearing parameter selection and their effects in control of the structural response.

The most appropriate design is achieved by minimizing both the maximum bearing displacement and the ductility demand ratio for the soft story. However, the relation between these two quantities is inversely proportioned making it difficult to maintain the two values minimum at the same time. For this reason, the approach of optimum design is more appropriate through the trade-off between the maximum bearing displacement and the ductility demand ratio. Extensive analysis is carried out through various combination of variation of θ, L and μ.

The parameters used in these simulations are given in Table 6.2. A total of 441-case is considered in this study. The same example of the five-story frame structure is used again in the simulation.

Table 6.2 Parameters for the multiple-slider bearing

Parameters	*Value*
θ^o	*5, 10, 15, 20, 25, 30, 35*
L [mm]	*10, 20, 30, 40, 50, 60, 70, 80, 90*
μ	*0.05, 0.10, 0.15, 0.20, 0.25, 0.30, 0.35*

Figure 6.22 shows the relation between the UPSS bearing maximum horizontal displacement and soft first story ductility demand ratio with all the cases considered in Table 2 when the frame structure was subjected to Kobe earthquake.

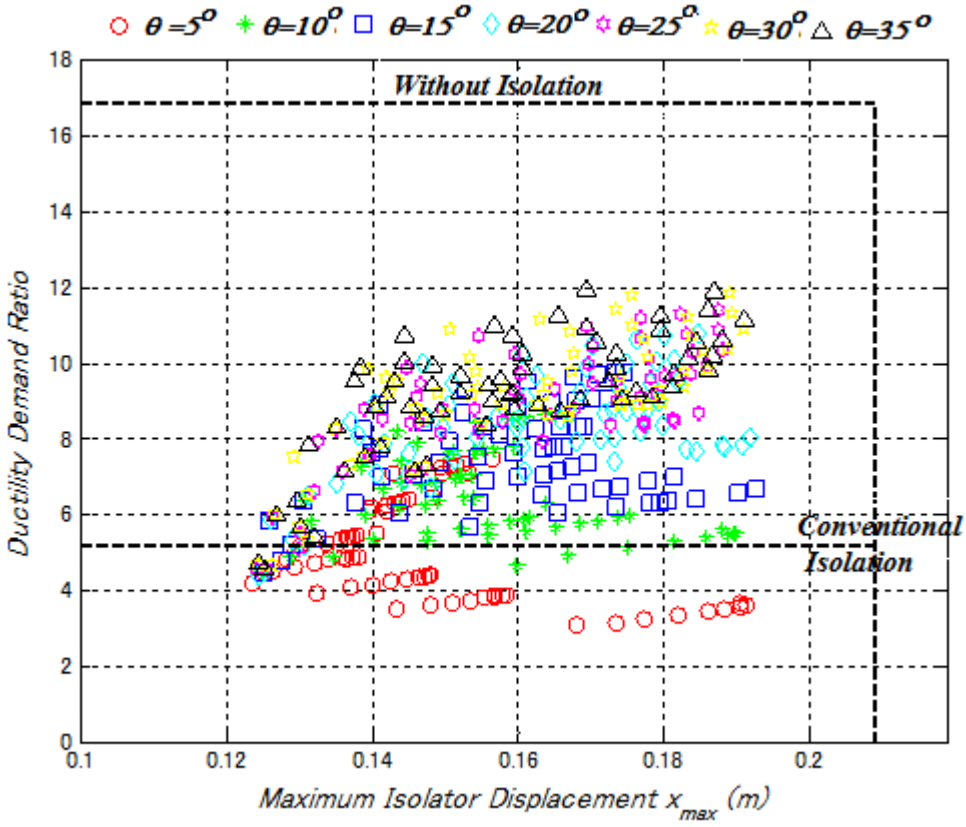

Figure 6.22 Various design combinations for the UPSS bearing

Generally speaking, any combination of θ, L and μ achieves a better seismic performance than conventional design in term of ductility demand ratio. The selection for the optimum design can simply be made by tracking the lowest points in the lower region which can be regarded as desirable in the sense that each point attains a minimum story ductility for a given isolator displacement as shown in the line connecting these optimum design candidates points which are also superior to the seismic performance of the conventional bearings.

Figure 6.23 shows response analysis result for another group of parameter combinations when the frame structure was subjected to El Centro record. The analysis here was carried out using μ value of 0.05 with all combinations of θ and L. In addition, a comparison with resilient sliding isolation (RSI), that is a combination of rubber and plane sliding bearings set in parallel, was also performed. It can be considered as a special case of the UPSS bearing when either θ is zero or L is very large.

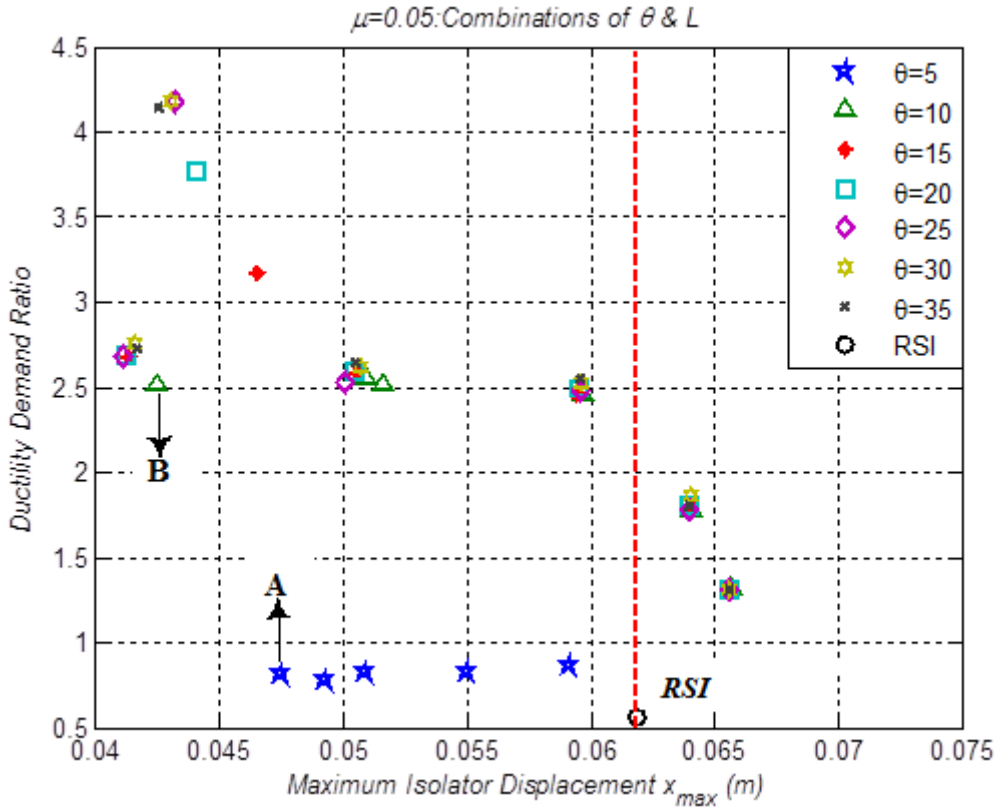

Figure 6.23 Comparison between UPSS bearing and RSI under various combinations

Although RSI provide in some cases a lower story ductility demand, the horizontal displacement is larger than many cases which can be achieved by the UPSS bearing. In this case study, selecting θ equal to 5° and L equal to 20 mm i.e. point A in Fig. 6.23, gives better results than RSI in term of horizontal displacement while still maintaining ductility demand ratio less than one that is the story first story columns have not reached to yield level.

As mentioned before, the maximum horizontal displacement is one of the crucial quantities in the process of design. Maintaining this displacement to a minimum value becomes a priority in case where the clearance to the neighboring structure is limited or when the expansion joints in the original construction turn out to be an issue for the choice of the most suitable isolator in retrofitting the structure. For example, if the maximum displacement shall not exceed 4.5 cm in this case study, Fig. 6.23 indicates that the UPSS bearing is applicable to achieve this criteria but with an increase in ductility demand ratio at points such as B, whereas RSI cannot be implemented and

its usage is limited.

6.6 Conclusion

Seismic retrofitting of soft-first-story frame structures by introducing a seismic interface on the top of first story columns proves its efficiency to enhance the structural safety and integrity for such special type of structures.

It has been shown that the UPSS bearing can be considered as one of the prominent cost effective solutions that can overcome the dilemma between the need for soft story and its vulnerability to collapse. Moreover, the proposed system also offers a feasible solution that is simple and practical to be implemented for seismic retrofitting of existing building with soft stories. The results indicate the ability of the proposed system to significantly reduce the ductility demand and excessive drift for the first story columns to the level the rubber bearing and resilient sliding isolation cannot achieve.

References

Almazan JC, Llera JCDL. Physical model for dynamic analysis of structures with FPS isolators. *Earthquake Engineering and Structural Dynamics* 2003; 32: 1157-1184.

Bednarski EJ. Discussion of Paper No. 1906, *Flexible 'First-Story' Construction for Earthquake Resistance. Transactions ASCE* 1935; 100: 657-660.

Briman V, Ribakov Y. Using seismic isolation columns for retrofitting buildings with soft stories. *The Structural Design of Tall and Special Buildings* 2009; 18: 507-523.

Chang, K.C. et al, "Experiments of Mid-Story Isolation Bearings in the New Research Building of Civil Engineering Department of National Taiwan University", *Report of National Center for Research on Earthquake Engineering (NCREE)*, NCREE-080-42, Taiwan, 2008. (In Chinese).

Chen YQ, Constantinou MC. Use of Teflon sliders in a modification of the concept of soft first storey. *Engineering Structures* 1990; 12: 243-252.

Chopra AK, Clough DP, Clough RW. Earthquake Resistance of Buildings with a 'Soft First Storey'. *International Journal of Earthquake Engineering and Structural Dynamics* 1973; 1: 347-355.

Clark PW, Kelly JM. Experimental testing of the resilient friction base isolation system, Rep. *UCB/EER~90/IO*, University of California, Berkeley, CA 1990.

Earthquake Protection Systems. *Technical Characteristics of Friction Pendulum Bearings. Vallejo*, California., USA, 2003.

Eroz M, DesRoches R. Bridge seismic response as a function of the Friction Pendulum System (FPS) modeling assumptions. *Engineering Structures* 2008; 30 (11): 3204-3212.

Fan FG, Ahmadi G, Mostaghel N, Tadjbakhsh IG. Performance analysis of aseismic base isolation systems for a multi-story building. *Rep. MIE-165*, Clarkson University, Potsdam,NY, 1988.

Green NB. Flexible 'First-Storey' Construction for Earthquake Resistance. *Transactions ASCE*, 100, Paper No. 1906, 1935; 644-674.

International Code Council. *International Building Code* 2003. Falls Church, Va, 2003.

Iqbal A. Soft First Story with Seismic Isolation System, *Proceedings of the Annual Conference of New Zealand Society for Earthquake Engineering* 2006; Napier, New Zealand.

Jacobsen LS. Effects of a Flexible First Story in a Building Located on Vibrating Ground. *S. Timoshenko, 60th Anniversary Vol. Macmillan Co.*, New York, 1938; 93-103.

Kawamura S, et al. Seismic isolation retrofit in Japan. *Proceedings of the 12th World Conference on Earthquake Engineering* 2000; Auckland, New Zealand.

Martel RR. The Effects of Earthquake on Buildings with a Flexible First Storey. *Bulletin of the Seismological Society of America* 1929; 19 (3): 167-178.

Murakami K, Kitamura H, Ozaki H, Teramoto T. Design analysis of a building with the middle story isolation structural system. *Proceedings of the 12th World Conference on Earthquake Engineering*, 2000.

Mezzi M. Enhancing the Seismic Performance of Existing "Pilotis" Configurations. *IABSE Conference, Responding to Tomorrow's Challenges in Structural Engineering* 2006; Budapest. Hungary.

Mo YL, Chang YF. Application of base isolation concept to soft first story buildings. *Computers & Structures* 1995; 55(5): 883-896.

Sueoka T, S Torii, Y Tsuneki. The Application of Response Control Design Using Middle-Story Isolation System to High-Rise Building. *Proceedings of the 13th World Conference on Earthquake Engineering*, 2004.

Todorovska MI. Base isolation by a soft first storey with inclined columns, *Engineering*

Mechanics, ASCE 1999; 125(4): 448-457.

Yoshimura M. Nonlinear analysis of a reinforced concrete building with a soft story collapsed by the 1995 Hyogoken-Nanbu Earthquake. *Cement and Concrete Composites* 1997; 19(3): 213-221.

Chapter 7

Performance-based design of seismically isolated frame structures by the UPSS bearing based on building code in Japan

In this chapter of this dissertation a design procedure is proposed for seismically isolated frame structures by the UPSS bearings. This design procedure is based on the basic concepts of performance-based seismic and structural code introduced by the Japanese Building Research Institute (BRI). The reliability of the simplified design procedure evaluated using equivalent linearization system is assessed and validated through nonlinear time history analysis. In addition, modified deign procedure is proposed to take into account the effect of vertical damping.

7.1 Introduction

In recent years researchers and engineers worldwide become more aware of the excellent performance of seismically isolated structures recognizing the isolation systems as a promising technique toward building an earthquake resilient society. During the 1995 Hyogoken-Nanbu earthquake in Japan, the performance of seismically isolated buildings have been tested and proven to be effective in mitigating the damage by maintaining both the safety and functionality of the structures.

The affirmative results of the analysis of seismographic records for seismic isolated buildings from recent earthquakes in Japan and the streamlined process of design lead

to a significant increase in the number of isolated structures. With two decades of experience in designing and constructing isolated structures, Japan now has the world's highest number of seismically isolated structures (Kani 2009, Nakashima et al. 2004, Becker et al. 2010). An overview of seismically isolated buildings in Japan is summarized in Table 7.1.

Table 7.1 An overview of seismically isolated buildings in Japan (Kani 2009)

Total number	2,000	1983-2007
Ratio of condominiums (%)	45	
High-rise condominiums (%)	6	Increased from 2000
Ratio of Kanto-area buildings (%)	45	Tokyo has the highest ratio at 20%.
Ratio of retrofitting (%)	4	
Annual number of isolators	6,000	Manufactured in 2004-2007
Annual number of dampers	1,200	Manufactured in 2004-2007
Total number of seismically isolated residences	3,000	1996-2007

The seismic isolation has also flourished to include retrofit of existing structures and tall buildings. Recent statistics show that 5% of seismic isolated buildings in Japan are retrofit of existing buildings (Okamoto et al. 2002).

Even though dynamic response time history analysis is recommended by most of design building codes, still simplified design procedure based on static nonlinear analysis is recognized and allowed under certain conditions. The design by the simplified method often results in more conservative design than the dynamic analysis due to several safety factors being used in the method. The most popular static nonlinear analysis is the capacity spectrum method that uses the intersection of the capacity or pushover curve and a reduced response spectrum to estimate maximum displacement. This procedure is an effective tool that helps designers to acquire a better understanding of how structure may response during major earthquakes through a visual representation assessment curves between capacity and demand which may also be helpful tool in various retrofit strategies. Many earthquake resistant design codes have implemented guidelines toward a simplified nonlinear static procedure to evaluate the performance state of structure under ground motion excitations such as ATC40 (ATC 1996) and FEMA 273/274 (FEMA 1997) which issued a further improvement on the equivalent linearization procedure in the FEMA-440 guidelines (FEMA 2005). The applicability of the simplified equivalent linearization procedures differs from country to another. The variation is shown clearly in the code

limitations which are summarized in Table 7.2.

Table 7.2 Applicability of the equivalent linear analysis method in the five different codes (Feng et al 2006)

Code / Structure	Japan	China	USA	Italy	Taiwan
Limitation on site seismicity	—	—	$S_1 < 0.6$g	—	—
Limitation on soil class	1,2	I,II,III	A,B,C,D	—	1,2
Maximum plan dimension	—	—	—	50m	—
Maximum height of superstructure	60m	40m	19.8m	20m	—
Maximum number of stories	—	$T_f \leq 1$s	4	5	—
Location of devices	Base only	Base only	—	—	—
Maximum mass-stiffness centers eccentricity	3%	—	—	3%	—
K_v/K_e	—	—	—	≥ 800	—
Tension in isolator	Not allowed	Not allowed	Allowed	Not allowed	—
Yield strength	$> 0.03W$	—	—	—	—
Period range of T_e	$T_2 > 2.5$s	—	$3T_f$~3.0s	$3T_f$~3.0s	≤ 2.5s
Maximum value of Tv	—	—	—	< 0.1s	—

Where T_f is the natural period of fixed-base superstructure, T_2 is the period of the isolation system considering only the stiffness of rubber bearings, T_e is the equivalent period of the isolation system, and T_V is the period of the isolation system in vertical direction.

In recent years, several methods have been proposed for the analysis and design of base isolated structures. One of these procedures is N2 method that was first proposed for fixed based structures as a frame work that connects pushover analysis with the response spectrum approach (Fajfar and Gaspersic 1996, Fajfar 2000) and being employed in Eurocode-8 (CEN 2005). N2 method was later extended to include the analysis of base-isolated structure through a three-linear idealization of the capacity curve based on the first yielding point of superstructure obtain by the pushover analysis (Kilar and Koren 2010).

Other method is the direct displacement-based design for seismic isolated reinforced concrete framed buildings (Cardone et al. 2010), which an approach firstly proposed by Priestley (Priestley 1993) recognizing the fact that damage for seismic isolation systems in term of displacements is better correlated than forces. The seismic

performance of the designed isolated building is governed by the designer selection of both the base displacement and maximum inter-story drift. In this method a target profile should be specified by assigning suitable displacement pattern and target displacement amplitude to obtain a structure which will respond according to this profile when subjected to earthquakes compatible with a reference response spectrum.

7.2 Equivalent Linear Analysis Method in the Japanese Building Code

The seismic design building code in Japan was also revised in 2000 to adopt a performance-based design approach. The Japanese code specifies two performance levels of buildings: the life safety corresponds to maximum earthquake motions and damage limitation corresponds to once in a lifetime earthquake motions (Midorikawa et al. 2003). The new provisions of seismically isolated buildings are also introduced where a simplified seismic evaluation method is allowed under certain conditions ($MLIT_a$ 2000). These new provisions are formulated based on equivalent single degree of freedom system, equivalent linearization and response spectrum analysis.

The scope of this method is not extended to building with height more than 60 m and not applicable where seismic isolation layer is not at ground layer or liquefaction is expected at this level. The proposed evaluation procedure is simple and realistic to predict maximum structural response without the use of time history analysis.

The earthquake design ground motion can be classified mainly into two levels each have different probability of occurrence as shown in Fig. 7.1. Level 1 ensures the superstructure to behave elastically aiming to prevent and control damage with maximum story drift of 0.005. Level 1 has a return period of 30-50 years and peak ground velocity of 0.25 m/s. On the other hand, Level 2 allows a limited yielding to occur in the superstructure but plastic hinges must be prevented. Level 2 has a return period of 500 year and peak ground velocity of 0.5 m/s. Up to the designers and owners discretion additional performance may be performed to check safety margin at a 50% increase in Level 2 ground motion (AIJ 2001).

The basic ground motion is defined first at the engineering bedrock based on Level 2 ground motion. The bedrock is assumed at soil layer where shear wave velocity is equal or more than 400 m/s. The standard acceleration response spectrum (S_o) (m/s^2) of

5% damping at engineering bedrock in the revised Japanese resistant Design Code is given by:

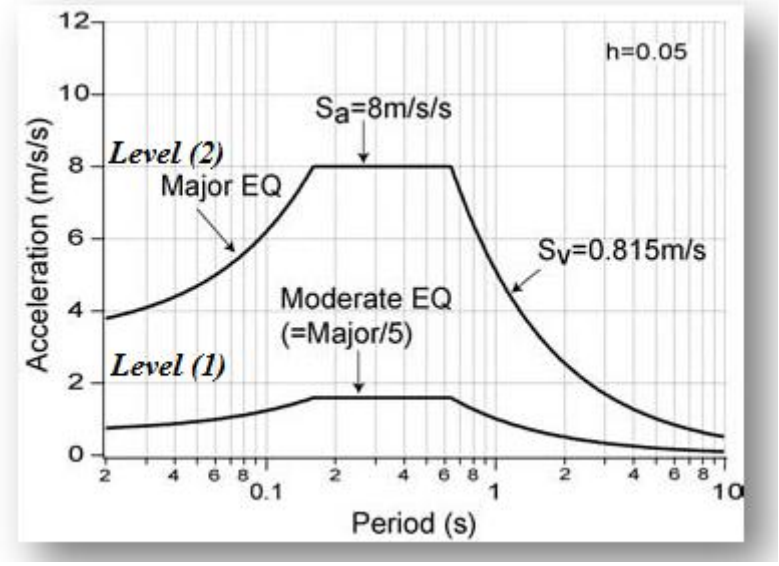

Figure 7.1 Basic design earthquake acceleration response spectra at exposed engineering bedrock

$$S_0(T) = \begin{cases} 3.2 + 30T, & T < 0.16 \\ 8.0, & 0.16 \leq T \leq 0.64 \\ 5.12/T, & 0.64 \geq T \end{cases} \tag{7.1}$$

where T is the period in seconds. The design earthquake ground motion (S_a) is expressed as:

$$S_a(T) = Z \cdot G_s(T) \cdot S_0(T) \tag{7.2}$$

where Z is seismic zone factor takes values from 0.7 to 1.0, G_s is soil amplification factor based on soil properties above engineering bedrock determined either by an accurate or simplified procedure (MLIT$_b$ 2000).

The accurate method uses the wave propagation procedure based on shear wave velocity and damping of the soil. When the soil properties are not precisely defined simplified method can be used based on a three given classification of soil i.e. stiff, medium stiff and soft soil. The two methods are plotted in Fig. 7.2.

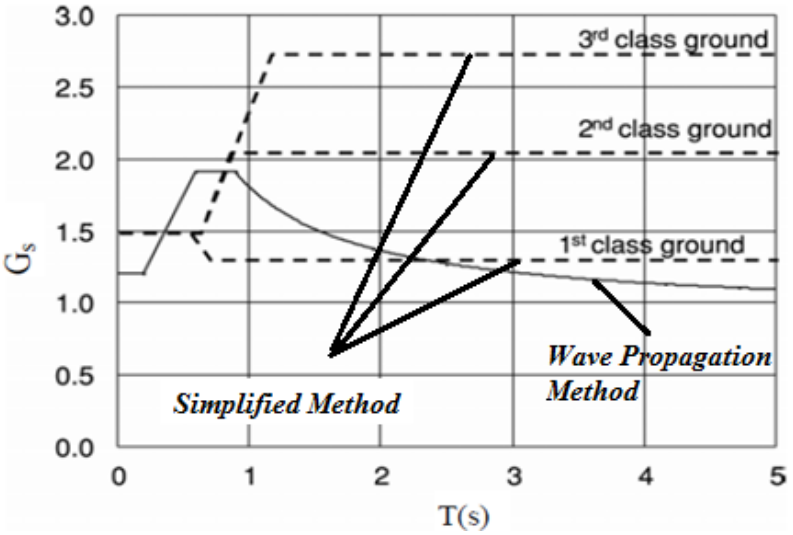

Figure 7.2 Amplification factor G_s in subsurface layers

The following equations are used to solve for G_s using the accurate methods:

$$G_s = G_{s2}\frac{T}{0.8T_2}, \quad T \le 0.8T_2 \tag{7.3}$$

$$G_s = \frac{G_{s1}-G_{s2}}{0.8(T_1-T_2)}T + G_{s2} - 0.8\frac{G_{s1}-G_{s2}}{0.8(T_1-T_2)}T_2 \quad , \quad 0.8T_2 < T \le 0.8T_1 \tag{7.4}$$

$$G_s = G_{s1} \quad , \quad 0.8T_1 < T \le 1.2T_1 \tag{7.5}$$

$$G_s = \frac{G_{s1}-1}{\frac{1}{1.2T_1}-0.1}\cdot\frac{1}{T} + G_{s1} - \frac{G_{s1}-1}{\frac{1}{1.2T_1}-0.1}\cdot\frac{1}{1.2T_1} \quad , \quad 1.2T_1 \le T \tag{7.6}$$

where Gs_1 is Gs value at the period of T_1, Gs_2 is G_s value at the period of T_2, T is natural period (s), T_1 is the predominant period of surface soil layers for the first mode (s), T_2 is predominant period of surface soil layers for the second mode (s). The minimum value of G_s is 1.2 for $T \le 1.2T_1$ and 1.0 for $1.2T_1 < T$. T_1, T_2, Gs_1 and Gs_2 are calculated based on an equivalent surface soil layer and are obtained by the following equations:

$$T_1 = \frac{4H}{V_{se}} \tag{7.7}$$

$$T_2 = \frac{T_1}{3} \tag{7.8}$$

$$G_{s1} = \frac{1}{(1.57h_{se} + \alpha)} \tag{7.9}$$

$$G_{s2} = \frac{1}{(4.71h_{se} + \alpha)} \tag{7.10}$$

$$\alpha = \frac{\rho_e V_{se}}{\rho_b V_{sb}} \tag{7.11}$$

where V_{sb} is the shear wave velocity of engineering bedrock (m/s), ρ_b is the mass density of engineering bedrock (kg/m^3) and α is the wave impedance ratio. H is the total thickness of surface soil layers (m), V_{se} is the equivalent shear wave velocity of surface soil layers (m/s) and ρ_e is the equivalent mass density of surface soil layers (kg/m^3). H, V_{se} and ρ_e are estimated as follows:

$$H = \Sigma d_i \tag{7.12}$$

$$V_{se} = \frac{\Sigma V_{si} d_i}{H} \tag{7.13}$$

$$\rho_e = \frac{\Sigma \rho_i d_i}{H} \tag{7.14}$$

where d_i is the thickness of soil layer i (m), V_{si} is the shear wave velocity soil layer i (m/s) and ρ_i is the mass density of surface soil layer i (kg/m^3).
h_{se} is the viscous damping ratio of the equivalent surface soil layer which is calculated as:

$$h_{se} = 0.8\frac{\Sigma h_i W_{si}}{\Sigma W_{si}} \tag{7.15}$$

where h_i is the viscous damping ratio of soil layer i and W_{si} is the potential energy of soil layer i. This method requires iteration due to the nonlinear behavior of soils. In addition, the soil profile properties and standard penetration test (SPT) are needed to

determine the predominant natural period of the surface soil layers.

In the equivalent linear analysis method, the seismic isolated building is considered as an equivalent degree of freedom system with spring and damper at the isolation level. The target displacement is set by the designer to ensure specified seismic performance level. The response shear and response displacement are obtained at the intersection of the demand and capacity spectra. The code requires that the maximum displacement response demand at the isolation interface (δ_d) should be less than the following:

$$\delta_d \leq \left(\frac{\delta_s}{1.1 \times \gamma} \right) \tag{7.16}$$

where δs is the design displacement limit at the base isolation level and is determined as the minimum value of the ultimate deformation (δ_u) for all the components at the isolation interface multiplied by a safety factor (β) based on empirical knowledge resulting from experimental data obtained in Japan. For example, the β for sliding and roller bearing such as the multiple-slider bearing is taken as (0.9) (Midorikaw et al. 2004). γ is safety factor for temperature dependent stiffness, dispersion of manufactures and aging with minimum value of (1.2). The value (1.1) is considered to take into account the accidental eccentricity. The horizontal isolation gap should be also designed larger than 1.25 times the design response displacement or 0.2 m plus the design response displacement.

The basic design shear force (Q_d) at the isolation interface is calculated as:

$$Q_d = M \cdot F_h \cdot S_a(T) \tag{7.17}$$

where M is the total mass above the isolation system level, F_h denotes reduction factor of acceleration response due to damping of the isolation system not less than 0.4 given based on the summation of hysteretic damping ratio (h_d) and fluid damping ratio (h_v) at δ_d as:

$$F_h = \frac{1.5}{1 + \left(10 \times \left(h_d + h_v\right)\right)} \tag{7.18}$$

The ratio of the hysteretic damper is defined as:

$$h_d = \frac{0.8}{4\pi} \cdot \frac{\sum \Delta W_i}{\sum W_i} \tag{7.19}$$

where ΔWi is the energy dissipated and W_i is the maximum strain energy of the isolator. The value (0.8) is introduced to account for the difference between steady and non-steady state of vibration.

7.3 Evaluation of Performance Point of Seismically Isolated Building with the UPSS Bearing

The distinctive hysteretic behavior of the UPSS Bearing provides simplicity and allows a direct evaluation through a simple iteration presented by a graphical presentation to find the point on the isolation system capacity spectrum (load-deformation relation) that also lies on the appropriate demand response spectrum, reduced by reduction factor for damping effects as shown in Fig 7.3 in shear force-displacement response spectra format.

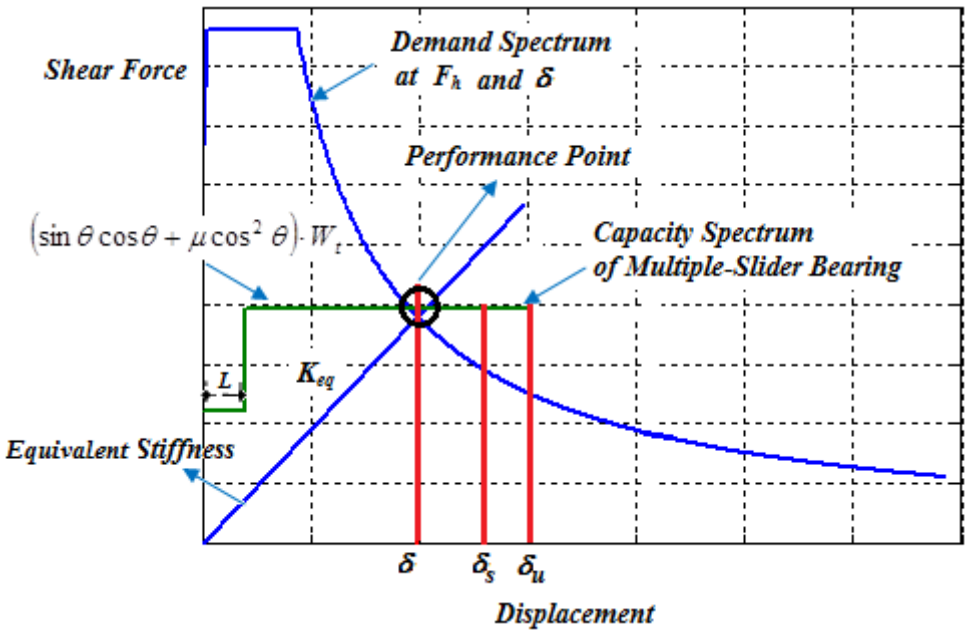

Figure 7.3 Demand spectrum and capacity spectrum of the isolation interface

In should be noted that designing the UPSS bearing requires the determination of three parameters: clearance length (L) i.e. the specified distance prior to the diagonal sliding, the inclination angle (θ) and the friction coefficient (μ).

The quasi-static hysteretic behavior shown in Fig. 7.4 is used to evaluate the equivalent damping ratio of the UPSS bearing based on the well-known Jacobsen's approach.

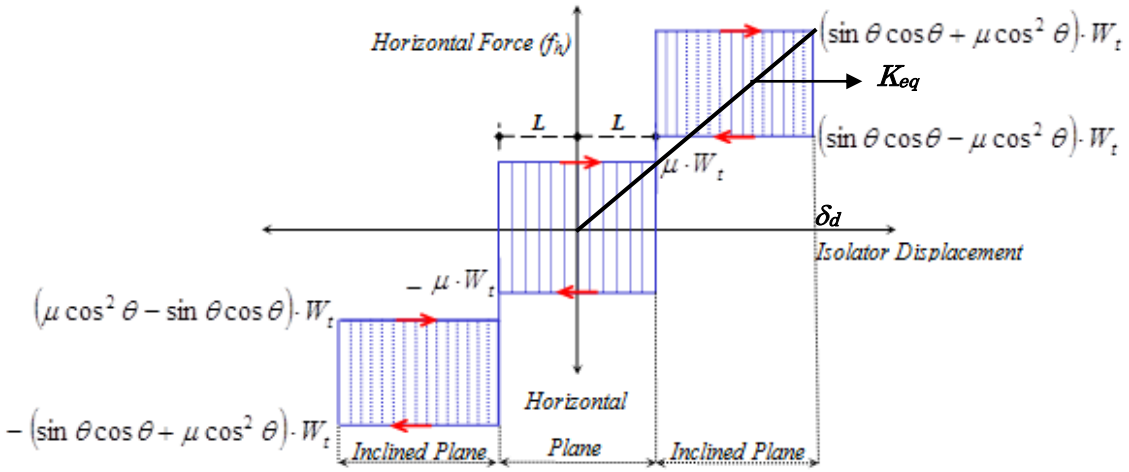

Figure 7.4 Idealized force-displacement relationship of UPSS bearing for a quasi-static cycle

The first step is to calculate h_d which is the ratio of the absorbed energy of the damper to the potential energy of the isolated and damper as defined in Eq. 7.19. The maximum strain energy of the UPSS can be expressed as:

$$\sum W_i = 0.5\times\delta_d\times f_{\max} \Rightarrow \sum W_i = 0.5\times\delta_d\times\left(\sin\theta\cos\theta+\mu\cos^2\theta\right)\times W_t \tag{7.20}$$

and the ΔW_i is the energy dissipated is expressed as:

$$\sum\Delta W_i = 4\times\mu\times W_t\times\left(\delta_d\times\cos^2\theta+L\times\sin^2\theta\right) \tag{7.21}$$

Therefore, the equivalent damping ratio h_d of the UPSS Bearing can be derived as:

$$h_d = \frac{1.6}{\pi}\cdot\frac{\mu\times\left(\delta_d\times\cos^2\theta+L\times\sin^2\theta\right)}{\delta_d\times\left(\sin\theta\cos\theta+\mu\cos^2\theta\right)} \tag{7.22}$$

For practical design, the upper and lower values for L, θ, and μ are taken as: θ^{o}= (5-30), μ = (0.05-0.3), L(mm) = (20-100). The design of the UPSS Bearing is achieved by determining the quantities (L, θ, μ) that provide a desirable performance level. After the building to be isolated is defined in term of geometry and basic characteristics, the UPSS offers for the designer the freedom to select simultaneously both the desirable design ultimate displacement (δ_u) and the maximum shear to weight ratio (α) which is defined as:

$$\frac{f_{\max}}{W_t} = \alpha = \left(\sin\theta\cos\theta + \mu\cos^2\theta\right) \tag{7.23}$$

It should be noted that α depends basically on θ and μ only. Examining the range of α within the practical upper and lower values of θ, and μ, the value of α is found to be varied from 0.14 up to 0.66 as shown in Table 7.3. It is clear that the higher the inclination angle or the friction coefficient, the higher the maximum shear to weight ratio.

Table 7.3 Variation of maximum shear to weight ratio (α)

		μ																									
		0.05	**0.06**	**0.07**	**0.08**	**0.09**	**0.1**	**0.11**	**0.12**	**0.13**	**0.14**	**0.15**	**0.16**	**0.17**	**0.18**	**0.19**	**0.2**	**0.21**	**0.22**	**0.23**	**0.24**	**0.25**	**0.26**	**0.27**	**0.28**	**0.29**	**0.3**
	5	***0.14***	0.15	0.16	0.17	0.18	0.19	0.20	0.21	0.22	0.23	0.24	0.25	0.26	0.27	0.28	0.29	0.30	0.31	0.32	0.33	0.33	0.34	0.35	0.36	0.37	0.38
	6	0.15	0.16	0.17	0.18	0.19	0.20	0.21	0.22	0.23	0.24	0.25	0.26	0.27	0.28	0.29	0.30	0.31	0.32	0.33	0.34	0.35	0.36	0.37	0.38	0.39	0.40
	7	0.17	0.18	0.19	0.20	0.21	0.22	0.23	0.24	0.25	0.26	0.27	0.28	0.29	0.30	0.31	0.32	0.33	0.34	0.35	0.36	0.37	0.38	0.39	0.40	0.41	0.42
	8	0.19	0.20	0.21	0.22	0.23	0.24	0.25	0.26	0.27	0.28	0.28	0.29	0.30	0.31	0.32	0.33	0.34	0.35	0.36	0.37	0.38	0.39	0.40	0.41	0.42	0.43
	9	0.20	0.21	0.22	0.23	0.24	0.25	0.26	0.27	0.28	0.29	0.30	0.31	0.32	0.33	0.34	0.35	0.36	0.37	0.38	0.39	0.40	0.41	0.42	0.43	0.44	0.45
	10	0.22	0.23	0.24	0.25	0.26	0.27	0.28	0.29	0.30	0.31	0.32	0.33	0.34	0.35	0.36	0.36	0.37	0.38	0.39	0.40	0.41	0.42	0.43	0.44	0.45	0.46
	11	0.24	0.25	0.25	0.26	0.27	0.28	0.29	0.30	0.31	0.32	0.33	0.34	0.35	0.36	0.37	0.38	0.39	0.40	0.41	0.42	0.43	0.44	0.45	0.46	0.47	0.48
	12	0.25	0.26	0.27	0.28	0.29	0.30	0.31	0.32	0.33	0.34	0.35	0.36	0.37	0.38	0.39	0.39	0.40	0.41	0.42	0.43	0.44	0.45	0.46	0.47	0.48	0.49
	13	0.27	0.28	0.29	0.30	0.30	0.31	0.32	0.33	0.34	0.35	0.36	0.37	0.38	0.39	0.40	0.41	0.42	0.43	0.44	0.45	0.46	0.47	0.48	0.49	0.49	0.50
	14	0.28	0.29	0.30	0.31	0.32	0.33	0.34	0.35	0.36	0.37	0.38	0.39	0.39	0.40	0.41	0.42	0.43	0.44	0.45	0.46	0.47	0.48	0.49	0.50	0.51	0.52
θ°	**15**	0.30	0.31	0.32	0.32	0.33	0.34	0.35	0.36	0.37	0.38	0.39	0.40	0.41	0.42	0.43	0.44	0.45	0.46	0.46	0.47	0.48	0.49	0.50	0.51	0.52	0.53
	16	0.31	0.32	0.33	0.34	0.35	0.36	0.37	0.38	0.39	0.39	0.40	0.41	0.42	0.43	0.44	0.45	0.46	0.47	0.48	0.49	0.50	0.51	0.51	0.52	0.53	0.54
	17	0.33	0.33	0.34	0.35	0.36	0.37	0.38	0.39	0.40	0.41	0.42	0.43	0.44	0.44	0.45	0.46	0.47	0.48	0.49	0.50	0.51	0.52	0.53	0.54	0.54	0.55
	18	0.34	0.35	0.36	0.37	0.38	0.38	0.39	0.40	0.41	0.42	0.43	0.44	0.45	0.46	0.47	0.47	0.48	0.49	0.50	0.51	0.52	0.53	0.54	0.55	0.56	0.57
	19	0.35	0.36	0.37	0.38	0.39	0.40	0.41	0.42	0.42	0.43	0.44	0.45	0.46	0.47	0.48	0.49	0.50	0.50	0.51	0.52	0.53	0.54	0.55	0.56	0.57	0.58
	20	0.37	0.37	0.38	0.39	0.40	0.41	0.42	0.43	0.44	0.45	0.45	0.46	0.47	0.48	0.49	0.50	0.51	0.52	0.52	0.53	0.54	0.55	0.56	0.57	0.58	0.59
	21	0.38	0.39	0.40	0.40	0.41	0.42	0.43	0.44	0.45	0.46	0.47	0.47	0.48	0.49	0.50	0.51	0.52	0.53	0.54	0.54	0.55	0.56	0.57	0.58	0.59	0.60
	22	0.39	0.40	0.41	0.42	0.42	0.43	0.44	0.45	0.46	0.47	0.48	0.48	0.49	0.50	0.51	0.52	0.53	0.54	0.55	0.55	0.56	0.57	0.58	0.59	0.60	0.61
	23	0.40	0.41	0.42	0.43	0.44	0.44	0.45	0.46	0.47	0.48	0.49	0.50	0.50	0.51	0.52	0.53	0.54	0.55	0.55	0.56	0.57	0.58	0.59	0.60	0.61	0.61
	24	0.41	0.42	0.43	0.44	0.45	0.46	0.46	0.47	0.48	0.49	0.50	0.51	0.51	0.52	0.53	0.54	0.55	0.56	0.56	0.57	0.58	0.59	0.60	0.61	0.61	0.62
	25	0.42	0.43	0.44	0.45	0.46	0.47	0.47	0.48	0.49	0.50	0.51	0.51	0.52	0.53	0.54	0.55	0.56	0.56	0.57	0.58	0.59	0.60	0.60	0.61	0.62	0.63
	26	0.43	0.44	0.45	0.46	0.47	0.47	0.48	0.49	0.50	0.51	0.52	0.52	0.53	0.54	0.55	0.56	0.56	0.57	0.58	0.59	0.60	0.60	0.61	0.62	0.63	0.64
	27	0.44	0.45	0.46	0.47	0.48	0.48	0.49	0.50	0.51	0.52	0.52	0.53	0.54	0.55	0.56	0.56	0.57	0.58	0.59	0.60	0.60	0.61	0.62	0.63	0.63	0.64
	28	0.45	0.46	0.47	0.48	0.48	0.49	0.50	0.51	0.52	0.52	0.53	0.54	0.55	0.55	0.56	0.57	0.58	0.59	0.59	0.60	0.61	0.62	0.63	0.63	0.64	0.65
	29	0.46	0.47	0.48	0.49	0.49	0.50	0.51	0.52	0.52	0.53	0.54	0.55	0.55	0.56	0.57	0.58	0.58	0.59	0.60	0.61	0.62	0.62	0.63	0.64	0.65	0.65
	30	0.47	0.48	0.49	0.49	0.50	0.51	0.52	0.52	0.53	0.54	0.55	0.55	0.56	0.57	0.58	0.58	0.59	0.60	0.61	0.61	0.62	0.63	0.64	0.64	0.65	***0.66***

The design equivalent period of an isolated building (T_{eq}) is expressed as:

$$T_{eq} = 2\pi \cdot \sqrt{\frac{M}{K_{eq}}} \tag{7.24}$$

where K_{eq} is the equivalent stiffness of the UPSS at the isolation interface level defines as:

$$K_{eq} = \frac{\alpha \cdot W_t}{\delta_d} \tag{7.25}$$

The simple step by step design procedure of the Uplift Sliding Bearing is described in Fig. 7.5.

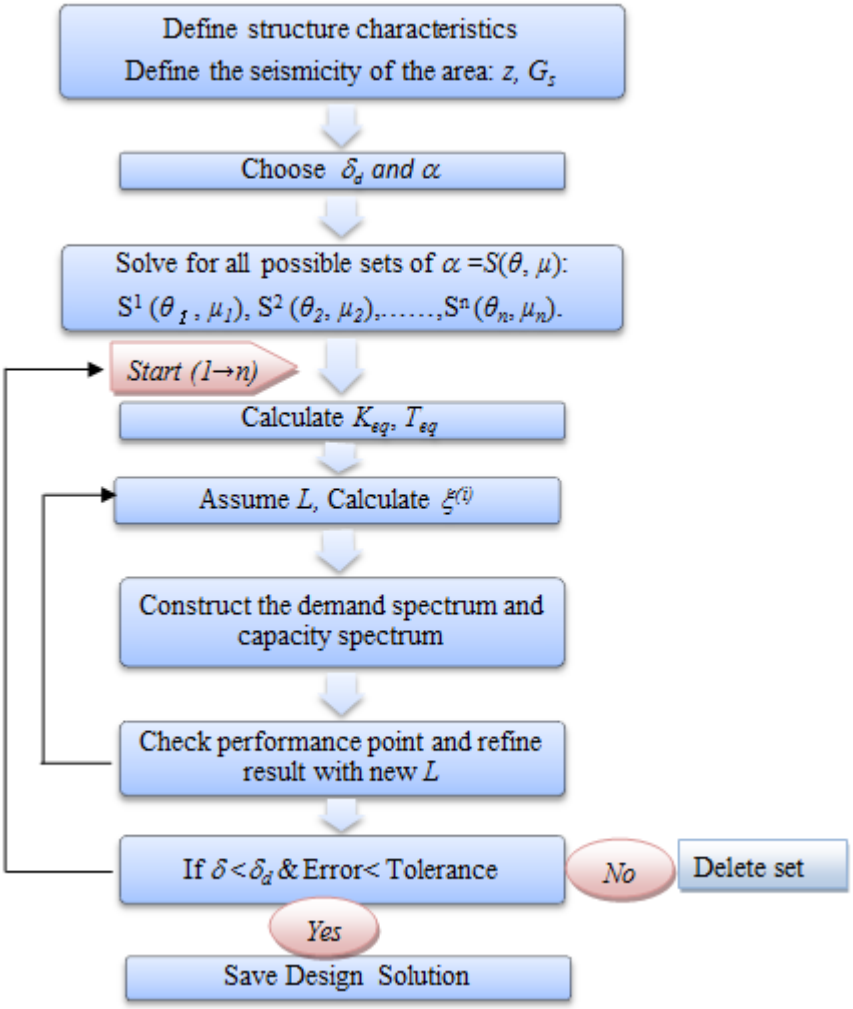

Figure 7.5 Flow Chart of design procedure for seismically isolated building with UPSS

7.4 Verification of the Proposed Procedure

In order to assess and validate the reliability of the proposed design procedure, a typical six-story reinforced concrete shear frame is designed with UPSS Bearings shown in Fig. 7.6. The design parameters of the UPSS Bearing are validated through a non-linear time history analysis. In this section, two design examples are considered.

The properties of the model are chosen with equal story masses of $m_{1\text{-}6}$=100 t. The mass of foundation m_b is taken equal to story masses. The stiffness for all stories are set equal to $k_{1\text{-}6}$=188700 kN/m. The fundamental period of the fixed base building T_1 is 0.6 s. Rayleigh Damping is used to formulate the damping matrix. It has been assumed that the damping ratios for the first two modes of vibration equal to 5%. The rubber bearing shown in Fig. 7.6 is a mean of providing a displacement restrain.

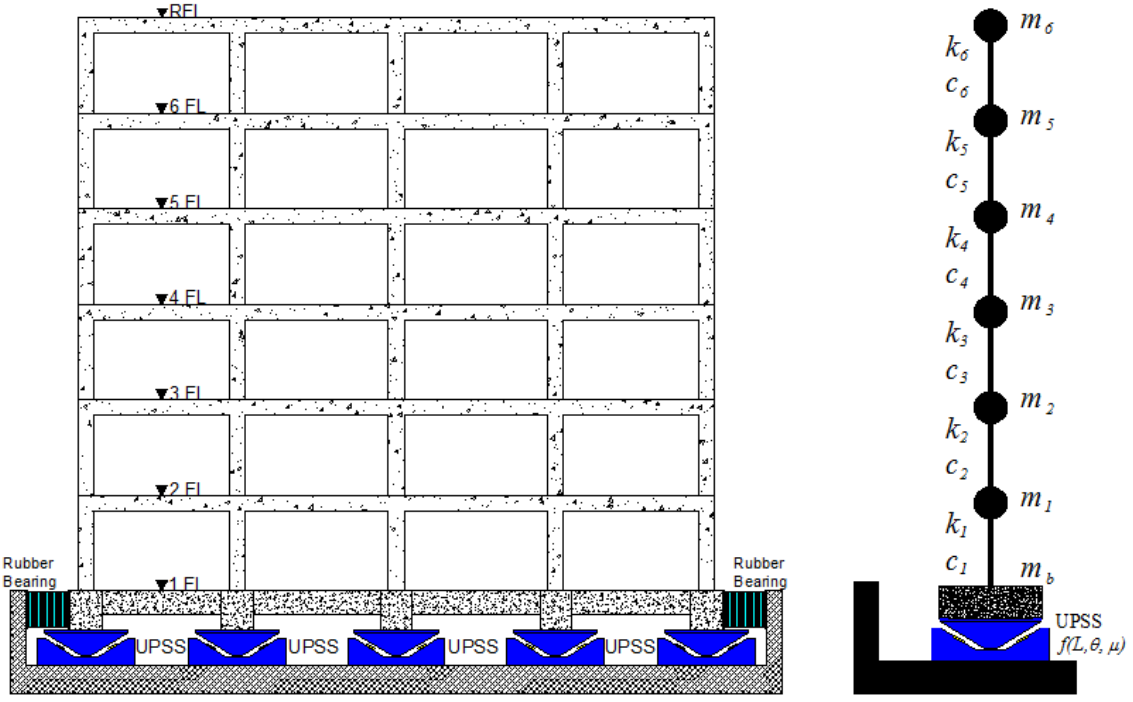

Figure 7.6 Elevation view of six-story reinforced concrete shear frame and the lumped mass model

The building is located in seismic zone with z factor equal 1.0. 1st class ground is considered for the construction site in which subsurface layers are stiff enough and predominant period of the ground is 0.2 s or less. Thus, G_s is taken as 1.35. The ultimate deformation at the isolation interface is to be design for δ_u=0.15 m and with base shear

coefficient (α) equal to 0.2.

For dynamic response analysis, the lumped mass model is assumed to behave elastically linear and the overturning or tilting effect of the structure during sliding has been neglected and only unidirectional excitation is considered in this study.

The response quantities are obtained as the average of the nonlinear dynamic analysis results for the ensemble of seven spectrum-compatible natural and artificial accelerograms shown in Fig. 7.7. The design Japanese response spectrum of 5% damping is clearly compatible with the average response spectrum associated to the select set of accelerograms as can be seen from Fig. 7.8.

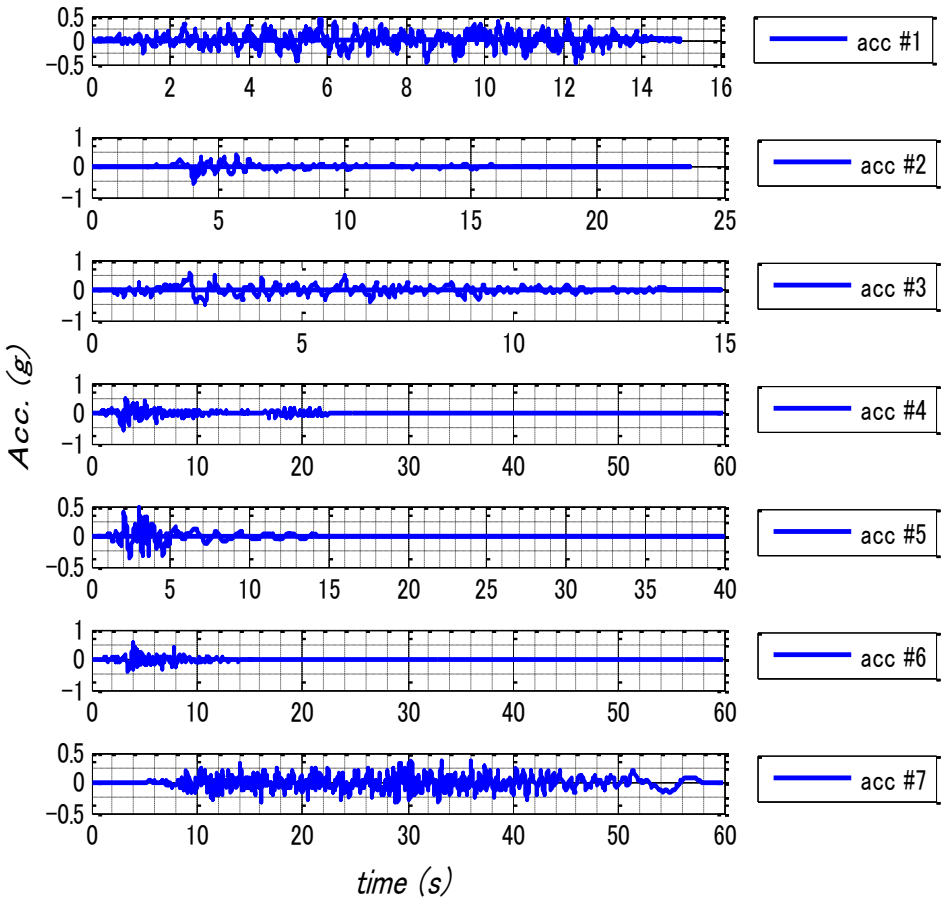

Figure 7.7 Set of accelerograms considered in the nonlinear time history analysis

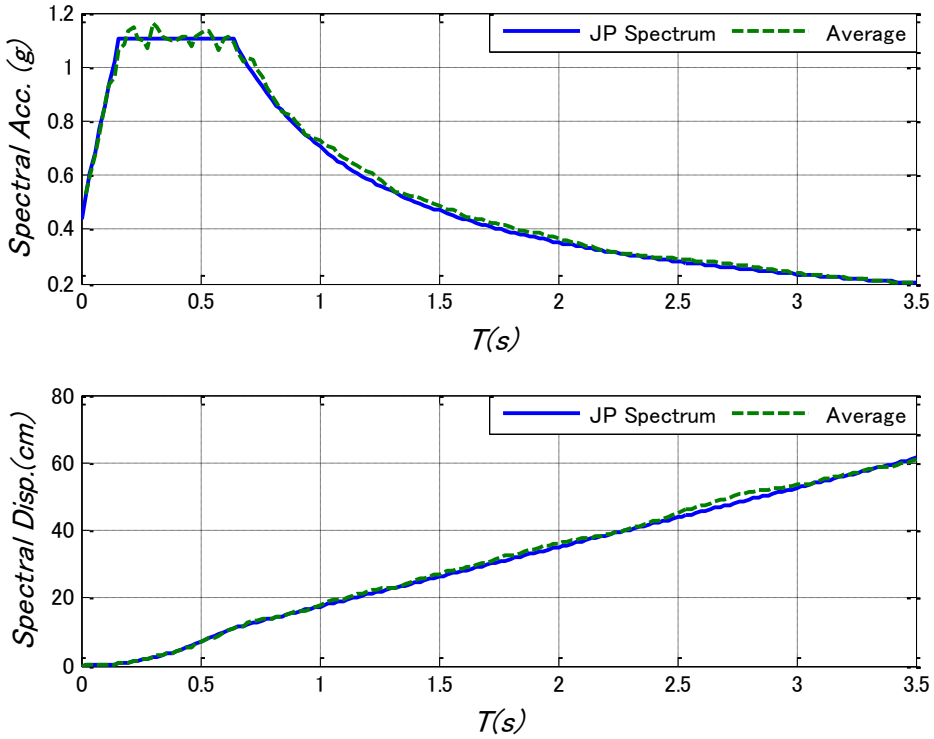

Figure 7.8 Comparison between target spectrum and the average response spectrum derived from the ensemble of seven accelerograms

The seven selected records have been scaled and adjusted to match the design Japanese response spectrum with the assistance of SeismoMatch application. The software uses the wavelets algorithm (Abrahamson 1992, Hancock et al 2006) to adjust earthquake accelerograms.

7.5 Design Results

The design of the seismic interface requires defining the parameters of the UPSS bearing. The number of bearing under each column is essentially selected to support the vertical loads transferred from the superstructure to the foundation level.

Based on the designed base shear coefficient i.e. 0.2, solution of Eq. 7.23 results in six sets $S^{1\to 6}(\theta, \mu)$ represented in Table 7.4.

Table 7.4 Preliminary design candidate parameters

	S^1	S^2	S^3	S^4	S^5	S^6
θ^o	5	5	6	7	8	9
μ	0.11	0.12	0.10	0.08	0.06	0.05

From Eqs. (7.24, 7.25), K_{eq} and T_{eq} at δ_d of the isolation interface are calculated as 13479 kN/m and 1.43 s, where δ_d is equal to 0.1023 m from Eq. 3. Iterations are carried out for every set of parameters and the performance point is checked and evaluated. For each set new values of h_d and F_h are computed since they are a function of θ, μ, and L. The solution is converged if the displacement at the intersection of the demand curve is less than δ_d and within the allowable tolerance of the displacement at the capacity spectrum. In this case study, the tolerance is selected as 5%. More than one design solution can be estimated.

These six candidates are examined as shown in Fig. 7.9. It is clear that sets S^1 and S^2 achieves the targets design values i.e. δ_u and α.

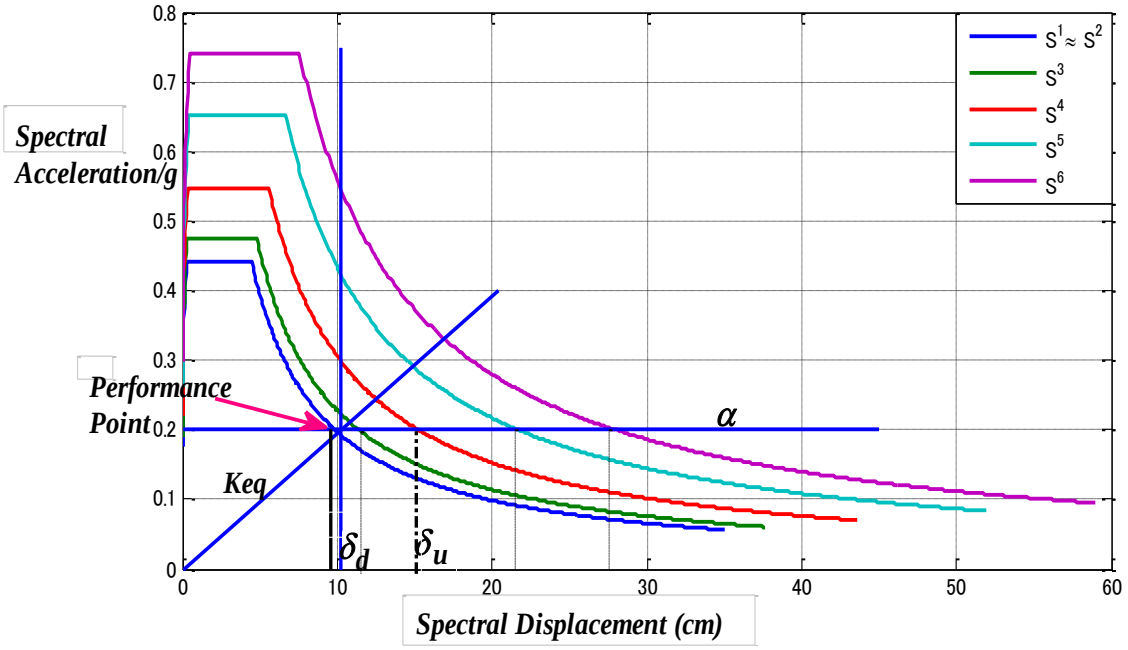

Figure 7.9 Demand spectrum and capacity curve intersect at performance point

Refinement of results is also done by varying L. It has been found that the effect of L on F_h is negligible. This observation is illustrated in Fig. 7.10 where the variation of L is plotted verses F_h for $\alpha=0.20$ to the three sets: S^1, S^2, and S^3.

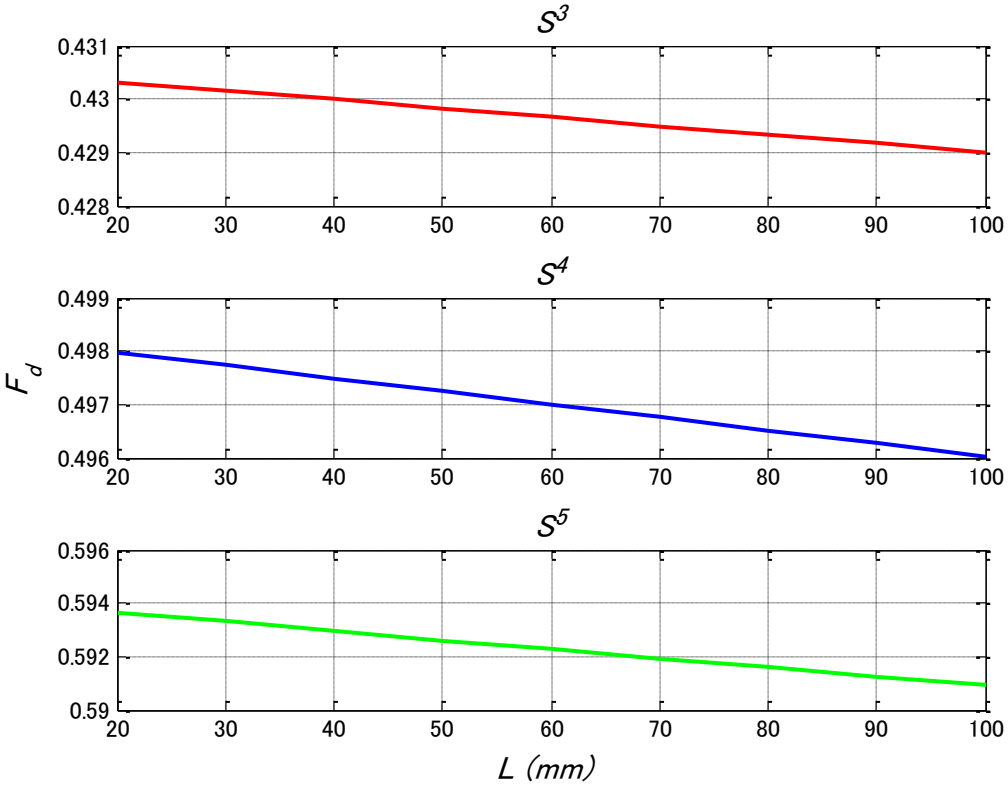

Fig. 7.10 Relationship between L and F_d for $\alpha=0.20$

The design solution for the UPSS bearing in the above example is determined as (θ=5°, μ=0.11, and L=2 mm). The difference between the displacement at the intersection of the demand and capacity is 0.77%. Fig. 7.11 illustrates the design solution graphically. It should be noted that α is also the maximum base acceleration in g unit. The common design rule is to limit the horizontal floor acceleration to 3.0 m/s^2 (Pan et al 2005).

In should be kept in mind that in the acceleration-displacement response spectrum such as Fig. 7.9, any lines radiates from the origin have a constant period. The period can be computed using the relationship:

$$T = 2\pi\left(\frac{S_d}{S_a}\right)^{0.5} \tag{7.26}$$

where S_a and S_d is the spectral acceleration and displacement respectively.

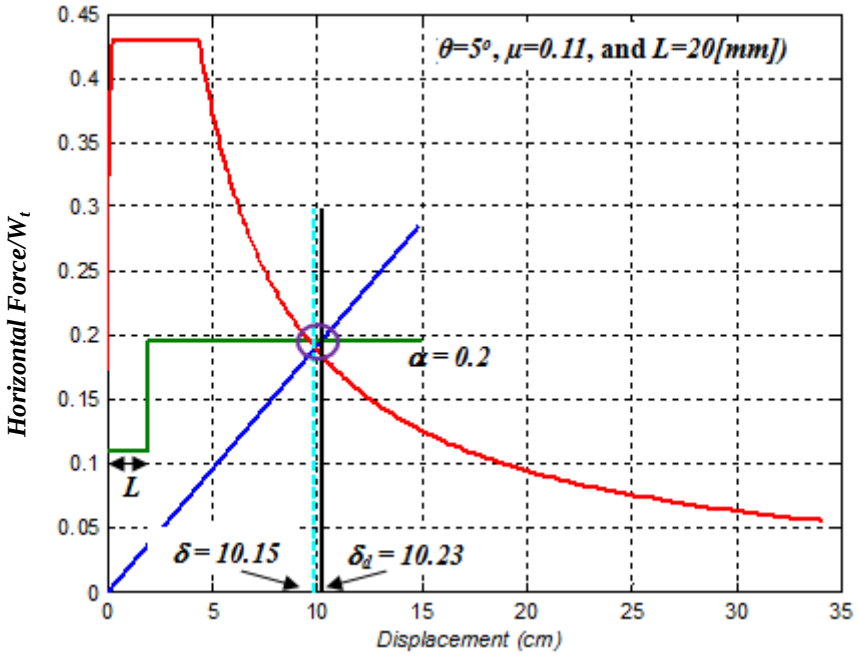

Figure 7.11 Demand spectrum and capacity curve intersect at performance point

The above result is validated through the non-linear time history analysis which is conducted on the six-story reinforced concrete shear frame shown in Fig. 7.6. The ensemble of seven accelerograms shown in Fig. 7.7 is considered in the simulation. The average displacement of the UPSS (θ=5°, μ=0.11, and L=2 mm) of the seven accelerograms are found to be δ_{avg}=11.09 cm. Fig. 7.12 shows the hysteresis loop for the UPSS bearings under the seven records. The design displacement obtained by the equivalent linearization is considered a good approximation to the non-linear time history.

The use of an average value for a set of simulated accelerograms is a common practice in design building codes. For example, the Eurocode-8 section 4.3.3.4.3 (CEN 2005) requires that if the response is obtained from at least 7 nonlinear time-history analyses with ground motions, the average of the response quantities from all of these analyses should be used as the design value. Otherwise, the maximum value of the response should be used. In the same manner the Uniform Building Code section 1631.6.1 (International Conference of Building Officials 1997) requires that if three time-history analyses are performed, then the maximum response of interest shall be used for design.

If seven or more time-history analyses are performed, than the average value of the response parameter of interest may be used for design.

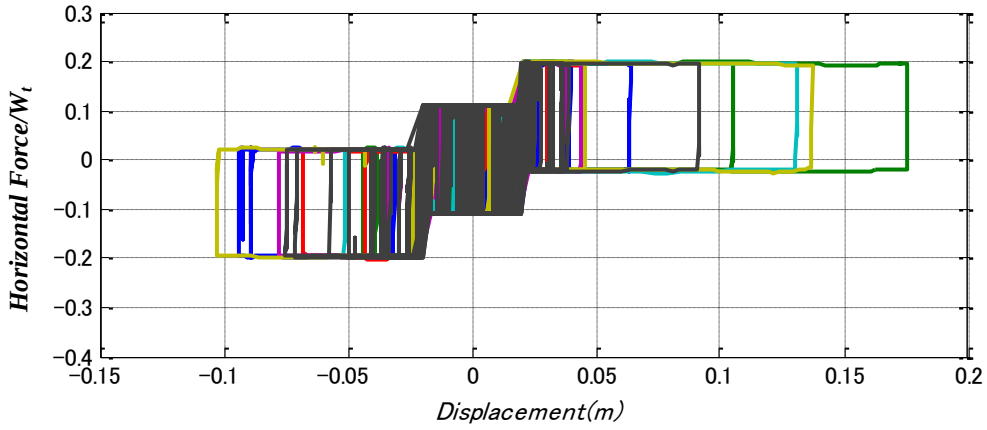

Figure 7.12 Hysteresis loop for the Uplifting Sliding Bearing

Checking the serviceability and comfort limits are important issues in design. Fig. 7.13 and Fig. 7.14 shows the drift and floor acceleration response at each story for the isolated six-story reinforced concrete shear frame with UPSS (θ=5°, μ=0.11, and L=2 *mm*). According to design building code such as the UBC 1997, the maximum inter-story drift ratio of the structure above the isolation system shall not exceed 0.01/R_I where R_I *is* a numerical coefficient related to the type of lateral-force resisting system above the isolation system in most cases taken as 2.0. In Japanese design code maximum inter-story drift ratio of 1/200 (AIJ, 2001). According to Fig. 7.13 the drift values satisfy both codes limitation.

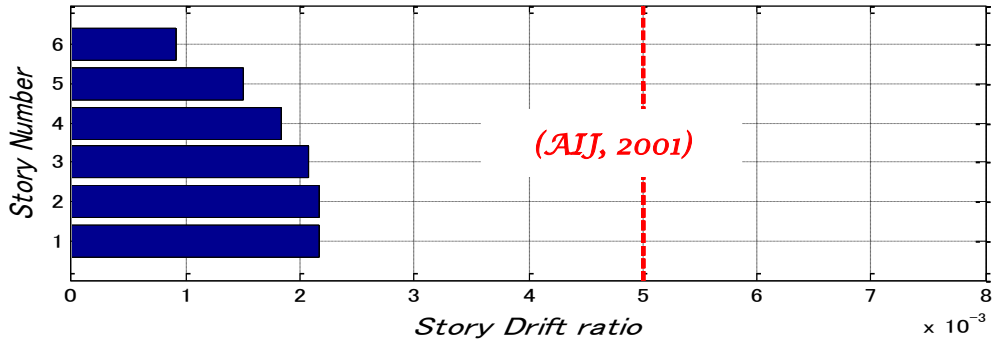

Figure 7.13 Story drift ratio at each story

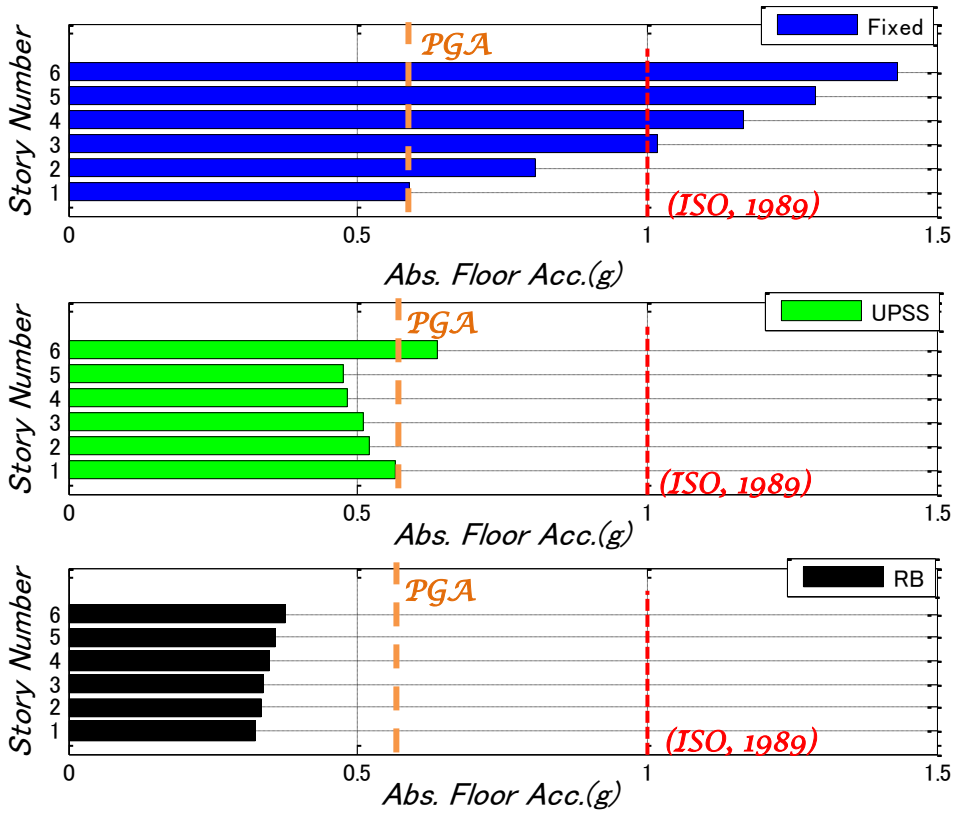

Figure 7.14 Absolute acceleration at each story

As for the maximum floor acceleration, the design codes usually don't specify a specific value. However, this value often determined based on the acceptable criteria for human comfort. Many criteria for human comfort have been proposed over the years. Acceleration limits as recommended by the International Standards Organization (International Standard ISO 1989) suggests limits in terms of root mean square acceleration as a multiple of the baseline line curve shown in Figure 7.15.

The multipliers for the proposed criterion, which is expressed in terms of peak acceleration, are 10 for offices, 30 for shopping malls and indoor footbridges, and 100 for outdoor footbridges. For design purposes, the limits can be assumed to range between 0.8 and 1.5 times the recommended values depending on. Figure 7.14 shows also the comparison with fixed base and isolation with conventional rubber bearing. The rubber bearing interface was selected to provide an isolation period of 1.5 sec and damping ratio of 10%. The responses are obtained by taking the average of the maximum values

for the seven earthquake records. It is clear that both isolation systems are effective in reducing floor acceleration. The figure also confirms the fact that friction based isolators often generate quit higher floor acceleration than elastomeric bearing on the account of reducing the horizontal displacement. However, according to the classification of Fig. 7.15, the absolute acceleration at each story shown in Fig. 7.14 satisfied also the human comfort for vibrations.

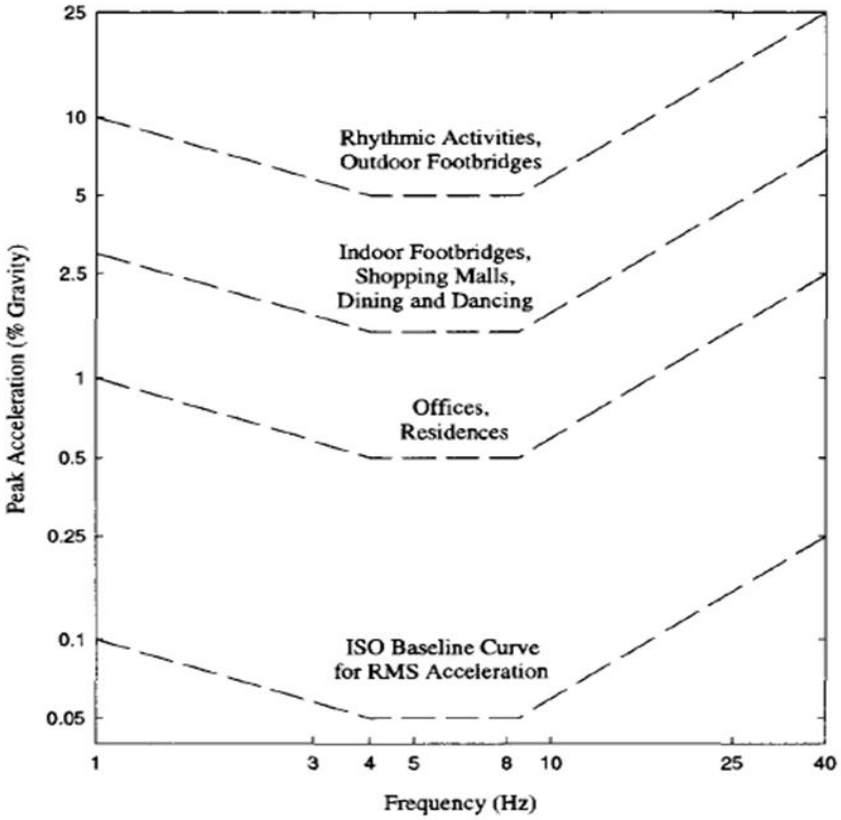

Figure 7.15 Recommended peak acceleration for human comfort for vibrations due to human activities (ISO 1989)

The second design example to be considered here considered the same building shown in Fig. 7.6. This time the design targets are taken as: δ_u=0.25 at the isolation interface and α equal to 0.30.

In the same procedure mentioned above, the design candidates are shown in Table 7.5. Fig. 7.13 illustrates the design solution graphically.

Table 7.5 Preliminary design candidate parameters

	S^1	S^2	S^3	S^4	S^5	S^6	S^7	S^8	S^9	S^{10}	S^{11}	S^{12}	S^{13}	S^{14}
θ^o	5	5	6	6	7	7	8	8	9	9	10	10	11	11
μ	0.21	0.22	0.19	0.2	0.18	0.19	0.16	0.17	0.14	0.15	0.13	0.14	0.11	0.12

	S^{15}	S^{16}	S^{17}	S^{18}	S^{19}	S^{20}	S^{21}	S^{22}
θ^o	12	12	13	13	14	14	15	15
μ	0.1	0.11	0.08	0.09	0.06	0.07	0.05	0.06

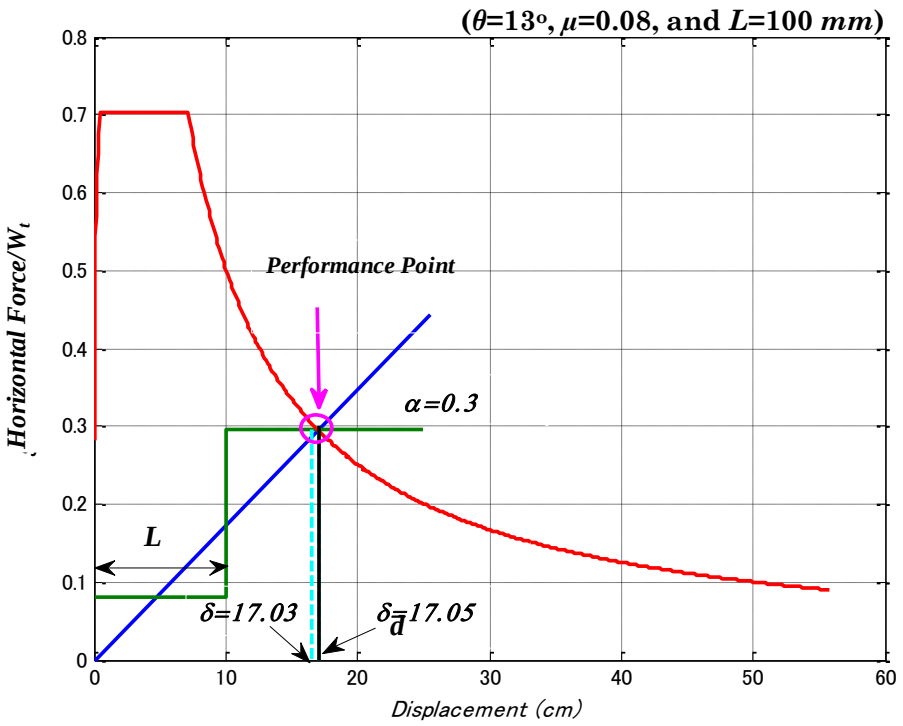

Figure 7.16 Demand spectrum and capacity curve intersect at performance point of δu=0.25 and α = 0.30.

Several design target cases are performed and compared with non-linear time history analysis. A summary of results are given in Table 7.6. Fig. 7.14 illustrates the relation between the results obtained by the equivalent linearization and non-linear time history. As expected, most of the results obtained by the equivalent linearization are

larger than the results from the non-linear time history. Since several safety factors have to be considered in the results of equivalent linear analysis, the non-linear time history analysis results in more economical designs (Feng et al 2006).

Table 7.6 Summary of design target cases

α	0.15		0.2			0.25				0.3					0.35			0.4
δ_u (cm)	30	40	15	20	25	15	20	25	30	10	12	20	25	30	12	20	25	15
δ_d (cm)	20.45	27.27	10.23	13.64	17.05	10.23	13.64	17.05	20.45	6.82	8.18	13.64	17.05	20.45	8.18	13.64	17.05	10.23
δ (cm)	20.26	26.58	10.15	12.39	16.15	9.94	13.01	16.81	20.06	6.7971	8.17	13.47	17.03	20.43	8.17	13.64	16.54	10.20
δ_{NLTH} (cm)	17.05	17.71	11.09	11.25	12.41	9.15	10.21	11.26	11.5	6.21	8.00	8.50	13.17	10.32	6.79	9.80	7.92	8.3554
θ^o	5	6	5	6	7	8	9	10	11	11	9	12	13	14	12	15	16	17
μ	0.06	0.05	0.11	0.1	0.08	0.12	0.1	0.08	0.07	0.17	0.14	0.1	0.08	0.07	0.15	0.1	0.09	0.13
L (mm)	20	20	20	20	20	20	20	20	20	30	40	20	100	30	20	70	20	70
F_d	0.49	0.57	0.40	0.43	0.4979	0.45	0.5	0.58	0.64	0.44	0.44	0.57	0.64	0.7053	0.48	0.62	0.67	0.57

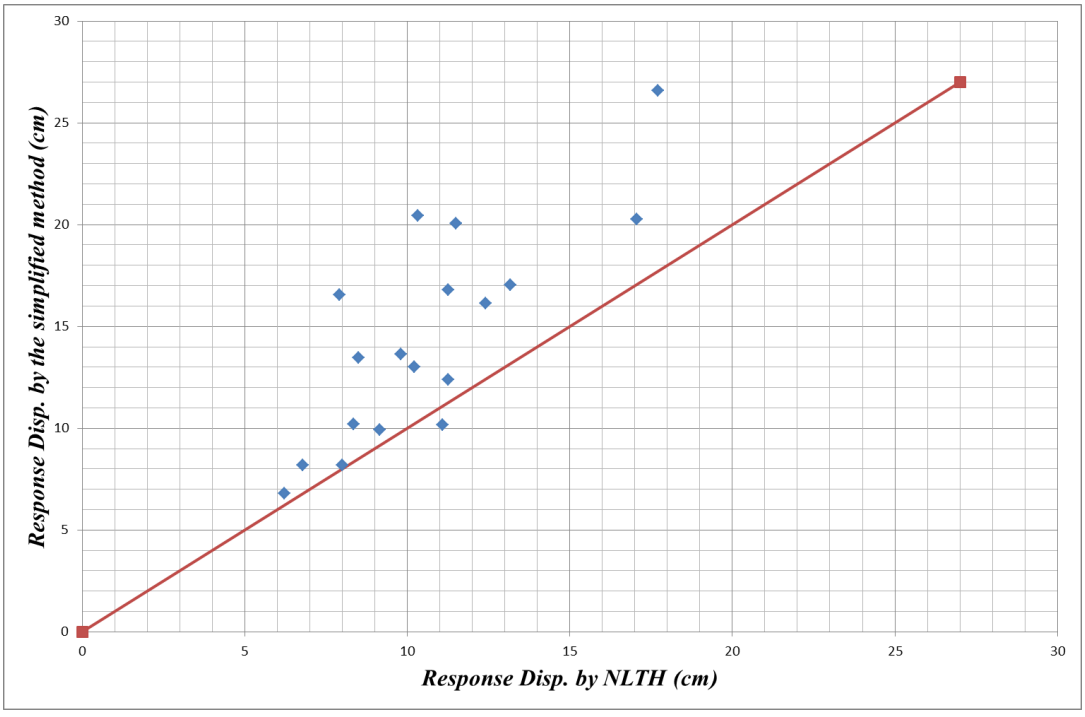

Figure 7.17 Comparison of response displacements obtained from simplified procedures and time history analysis

7.6 Modified design procedure including vertical motion

This section intends to take into account the effect of vertical damping in the process of design which is generated through the inclined sliding. The design procedure is only modified in the evaluation part of equivalent damping ratio h_d.

The validation for the effect of vertical motion requires the utilization of spring model discussed thoroughly in section 5.2.2 to carry out the time history nonlinear analysis on the six-story reinforced concrete shear frame. The lumped mass model with the UPSS spring model is shown in Fig. 7.15. Since a real data is not available in this example, the stiffness of the vertical spring K_n is assumed based on the value used in the shaking table test. This value is modified to take into account the new superstructure weight.

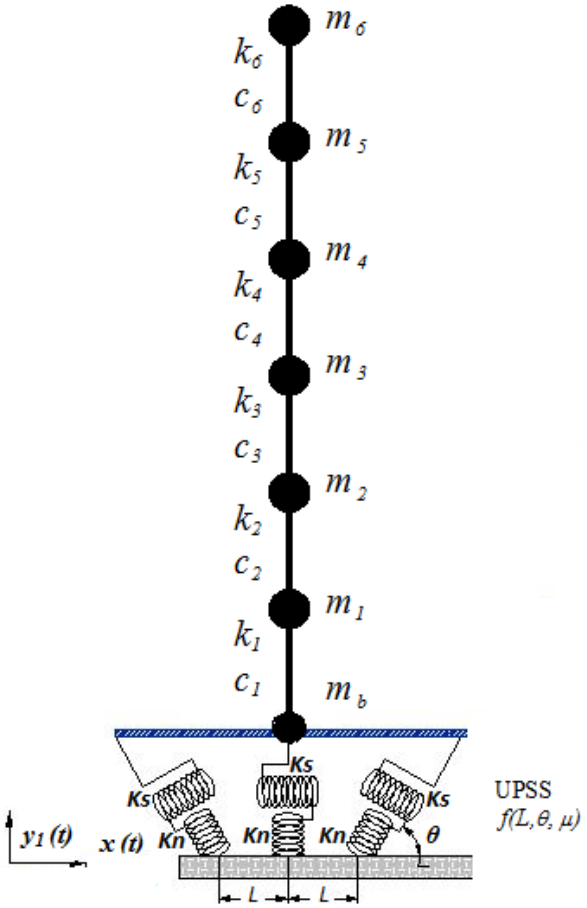

Figure 7.18 Analytical model using UPSS spring model for Non-linear time history

To evaluate the damping in the vertical direction, the relation between the vertical displacement and the vertical reaction should be considered first. The vertical reaction for an upward motion along the inclined surface can be expressed as:

$$F_v = W_t\left(\mu \sin\theta\cos\theta + \sin^2\theta\right) \tag{7.26}$$

In the same way, the vertical reaction for a downward motion can be expressed as:

$$F_v = W_t\left(\sin^2\theta - \mu \sin\theta\cos\theta\right) \tag{7.27}$$

Therefore, the relation between the relation between the vertical displacement and the vertical reaction can be plotted as shown in Fig. 7.16.

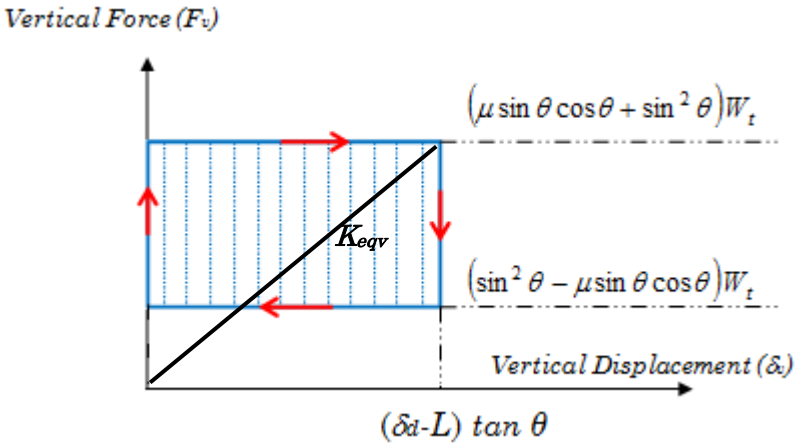

Figure 7.19 Idealized vertical hysteresis of UPSS bearing for a quasi-static cycle

Then, the ratio of the equivalent UPSS damping is redefined as:

$$h_d = \frac{0.8}{4\pi}\cdot\frac{\sum \Delta W_i}{\sum W_i} = \frac{0.8}{4\pi}\cdot\left[\frac{\sum(\Delta W_{xi} + 2\Delta W_{yi})}{\sum(W_{xi} + W_{yi})}\right] \tag{7.28}$$

Substituting the values of ΔW_{xi}, ΔW_{yi}, W_{xi}, W_{yi}, Eq. 7.28 can be expressed as:

$$h_d = \frac{0.8}{4\pi}\cdot\left[\frac{4\mu\times\left(\delta_d\times\cos^2\theta + L\times\sin^2\theta\right) + \left(4\mu\times\sin^2\theta\times(\delta_d - L)\right)}{0.5\times\delta_d\times\left(\sin\theta\cos\theta + \mu\cos^2\theta\right) + 0.5\times\sin^2\theta\times(\delta_d - L)\times(\mu + \tan\theta)}\right] \tag{7.29}$$

It should be noted that ΔW_{yi} is multiplied by 2 to include the vertical dissipation in both sides. Simplifying Eq. 7.29 yields to:

$$h_d = \frac{1.6}{\pi} \cdot \mu . \left[\frac{\delta_d \times \cos^2\theta + L \times \sin^2\theta + \sin^2\theta \times (\delta_d - L)}{\delta_d \times (\sin\theta\cos\theta + \mu\cos^2\theta) + \sin^2\theta \times (\delta_d - L) \times (\mu + \tan\theta)} \right] \tag{7.30}$$

27-case design has been considered for the verification with time history analysis. The results are summarized in Tables 7.7.

Table 7.7 Summary of design cases including vertical motion effect

case #	δ_u (cm)	δ_{dl} (cm)	δ_d (cm)	δ_{NLTH} (cm)	θ^o	μ	L (mm)	F_d
				α=0.15				
#1	30	20.45	20.26	16.85	5	0.06	20	0.49
#2	40	27.27	26.58	17.70	6	0.05	20	0.57
				α=0.20				
#3	15	10.23	10.15	12.64	5	0.11	20	0.40
#4	18	12.27	12.27	11.16	6	0.10	20	0.43
#5	25	17.05	16.15	12.51	7	0.08	20	0.50
#6	35	23.86	22.97	14.35	8	0.06	20	0.59
#7	45	30.68	29.10	14.51	9	0.05	20	0.67
				α=0.25				
#8	12	8.18	8.11	8.38	5	0.16	20	0.40
#9	15	10.23	9.92	8.96	8	0.12	30	0.45
#10	20	13.64	13.01	9.77	9	0.10	20	0.50
#11	25	17.05	16.81	10.66	10	0.08	20	0.58
#12	30	20.45	20.04	11.57	11	0.07	30	0.64
#13	40	27.27	25.21	11.90	11	0.06	20	0.68
				α=0.30				
#14	10	6.82	6.80	6.92	8	0.16	20	0.40
#15	12	8.18	8.17	7.64	9	0.14	40	0.44
#16	15	10.23	10.23	9.36	11	0.12	70	0.50
#17	18	12.27	12.09	8.31	12	0.11	30	0.55
#18	22	15.00	14.98	11.42	13	0.09	80	0.61
#19	25	17.05	17.03	12.94	13	0.08	100	0.64
#20	30	20.45	20.44	9.68	14	0.07	30	0.70
#21	35	23.86	23.84	11.57	14	0.06	50	0.75
				α=0.35				
#22	9	6.14	6.13	5.95	10	0.18	40	0.41
#23	12	8.18	8.12	6.37	12	0.15	40	0.48
#24	15	10.23	10.19	6.34	14	0.13	20	0.54
#25	18	12.27	12.19	9.52	15	0.11	80	0.59
#26	22	15.00	14.65	6.65	16	0.10	20	0.64
#27	28	19.09	18.76	7.28	17	0.08	20	0.73

Fig. 7.17 illustrates the relationship between the results obtained by the equivalent linearization simplified method and the non-linear time history taking into accounts the vertical motion. It is clear that the results are more accurate than the results obtained without considering the vertical motion since the points are centralized around the reference line.

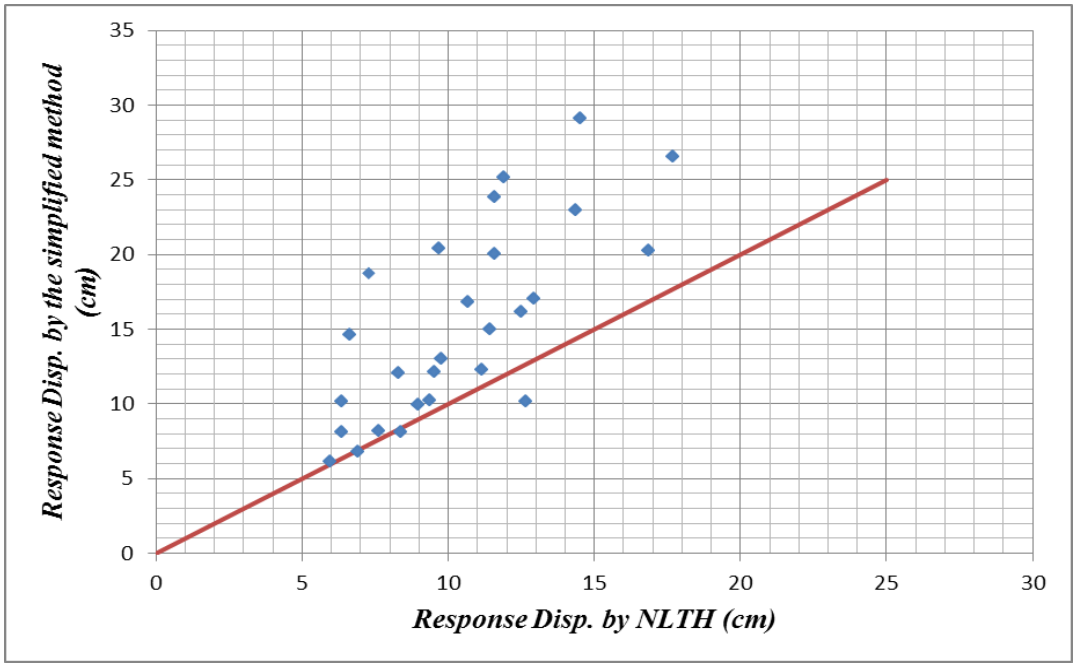

Figure 7.20 Comparison of response displacements obtained from simplified procedures and time history analysis including vertical motion effect

Although more than one design solution can be found, the solution which is closest to the design displacement limit has been selected.

It can be observed from Table 7.7 that the displacement demand obtained by time history analysis is slightly larger than the one obtained by the simplified procedure for small inclination angles. Nevertheless, these values are still less than the bearing displacement capacity. On the other hand, for larger inclination angles it is found to be more conservative. It can also be noticed that a smaller design displacement targets are achieved on the account of the increase the maximum shear to weight ratio (α).

As shown from Fig. 7.18, the design cases with small inclination angles, approximately less than 8^{o}, don't generate impulse forces at the transition between the horizontal and inclined surfaces. However, these forces increased with the increase of inclination

angle as shown in Fig. 7.19 and Fig 7.20 which are also dependent on L and μ.

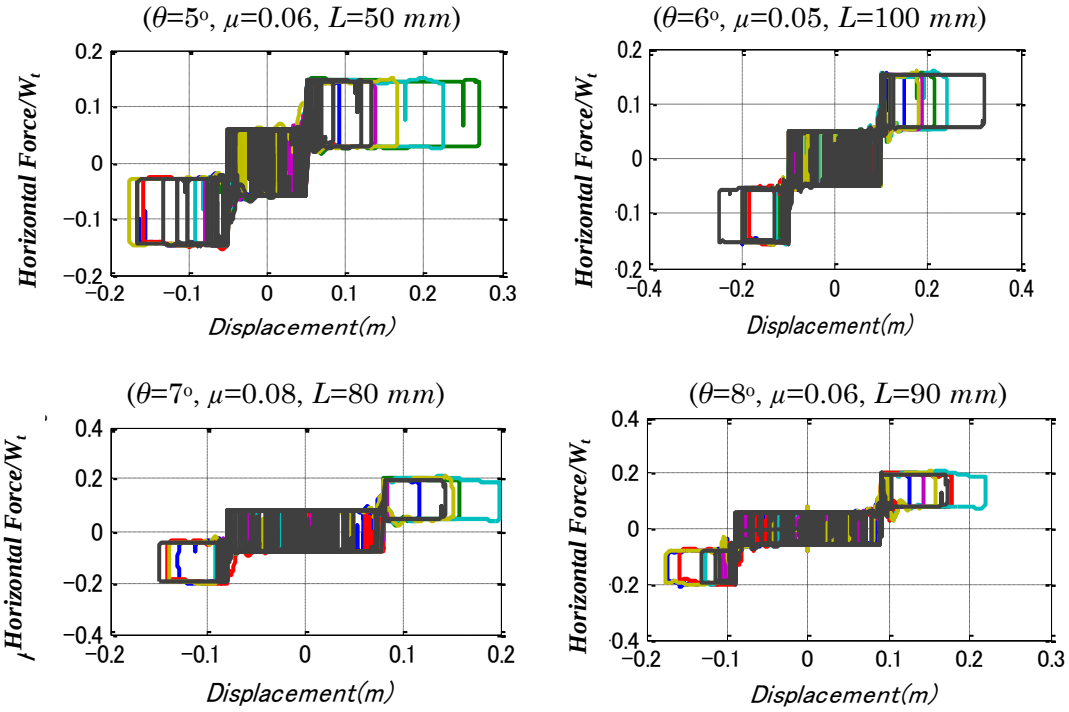

Figure 7.21 Time history analysis for design cases with small inclination angles

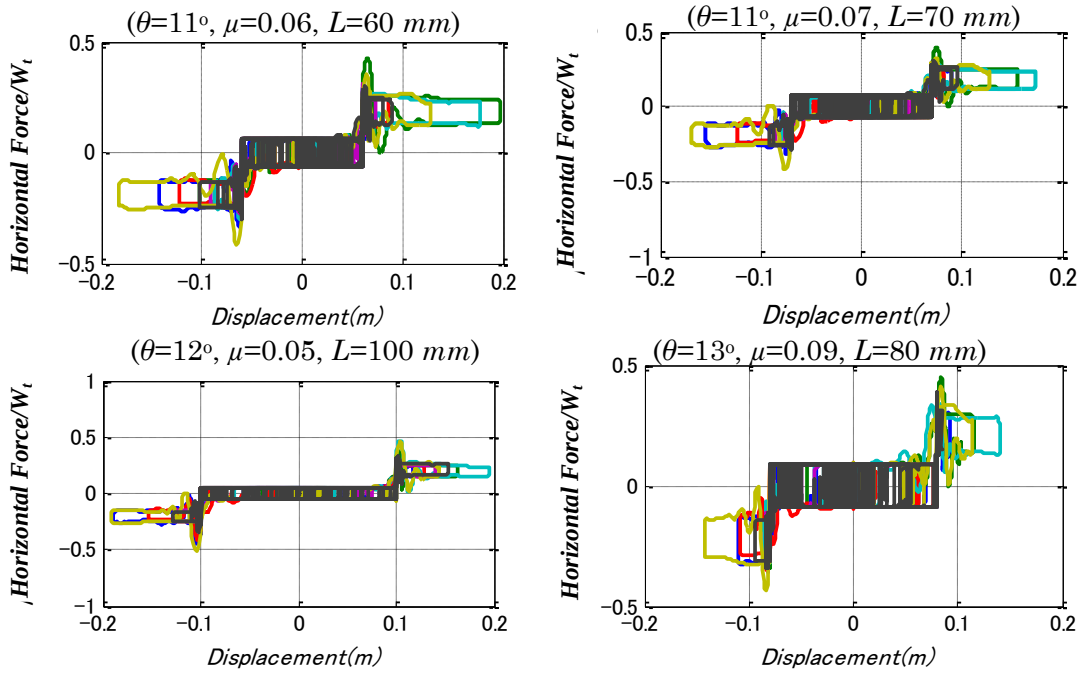

Figure 7.22 Time history analysis for design cases with moderate inclination angles

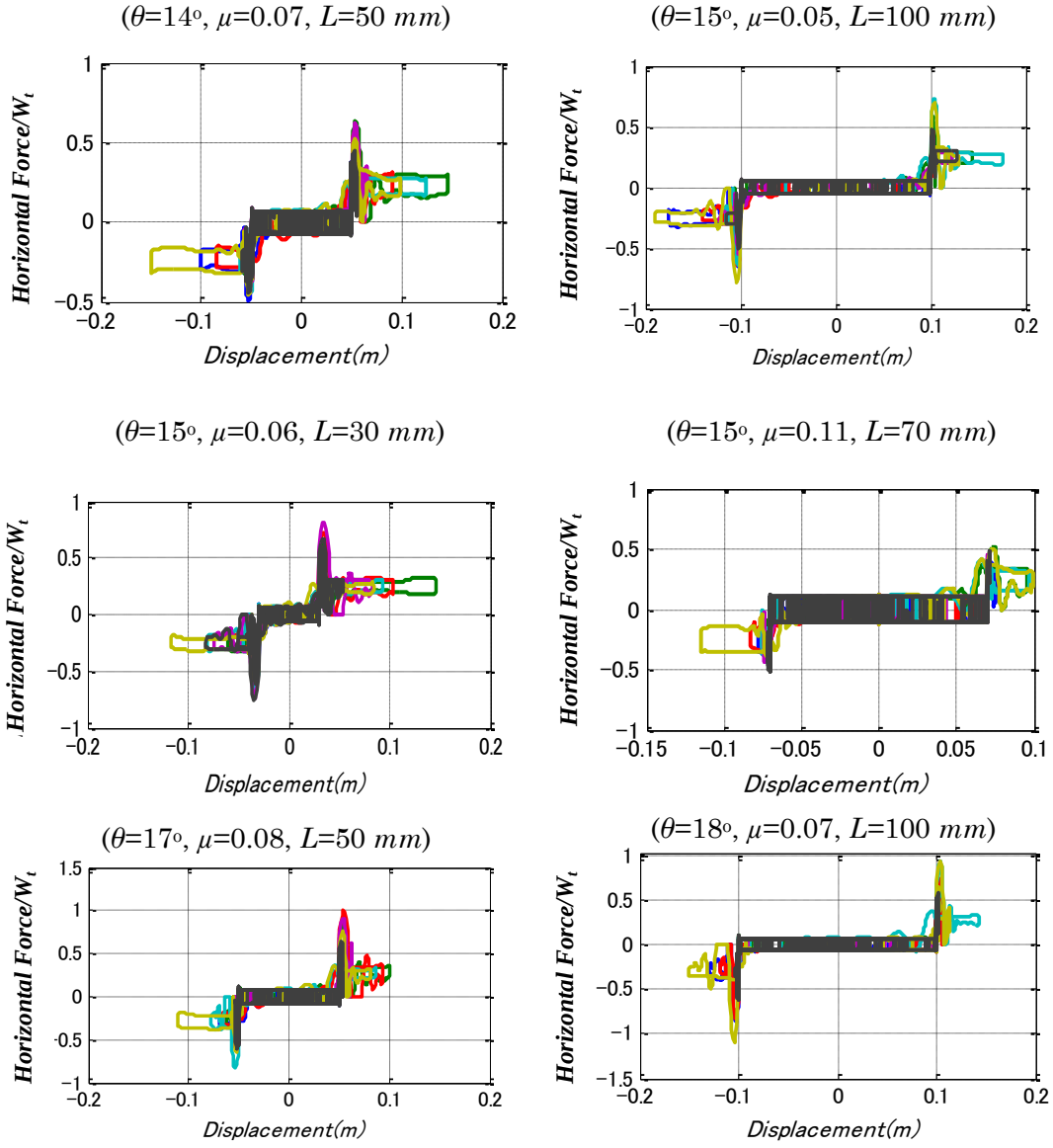

Figure 7.23 Time history analysis for design cases with large inclination angles

7.7 Conclusion

This chapter presented a simple procedure to design a seismically isolated frame structures by the UPSS bearings. The design procedure adopted the guidelines of performance-based seismic design introduced by the Japanese Building Research Institute (BRI). The reliability of the simplified design procedure evaluated using equivalent linearization system is assessed and validated through nonlinear time history analysis. Two design approaches are proposed in this chapter. The first does

not take into account the effect of vertical motion whereas the second does. Both methods show good results when compared with non-linear time history. However, the first method indicates more conservative results.

References

Abrahamson NA. Non-stationary spectral matching, *Seismological Research Letters* 1992; 63(1), 30.

AIJ. Architectural Institute of Japan. Recommendation for the Design of Base Isolated Structures, 2001 (In Japanese).

ATC, Applied Technology Council. Seismic evaluation and retrofit of concrete buildings, *Report ATC-40*, RedwoodCity, CA, 1996.

Becker T C, Furukawa S, Mahin SA. Nakashima M. Comparison of US and Japanese Codes and Practices for Seismically Isolated Buildings, *Proceedings of the 2010 Structures Congress* 2010; pp. 2330-2338.

Cardone D, Palermo G, Dolce M. Direct Displacement-Based Design of Buildings with Different Seismic Isolation Systems. *Journal of Earthquake Engineering* 2010; 14(2): 163-191.

CEN. EN-1998-1-Eurocode 8: Design of Structures for Earthquake Resistance. Part 1: General rules, *Seismic Actions and Rules for Buildings, Europeans Committee for Standardization*, Brussels, 2005.

Fajfar P, Gasperic P. The N2 method for the seismic damage analysis of RC buildings. *Earthquake Engineering and Structural Dynamics* 1996; 25:31-46.

Fajfar P. A nonlinear analysis method for performance-based seismic design, Earthquake Spectra 2000; 16(3): 573-92.

FEMA, Federal Emergency Management Agency. Guidelines and commentary for the seismic rehabilitation of buildings, *FEMA-273/274*, Washington, DC, 1997.

FEMA, Federal Emergency Management Agency. Improvement of nonlinear static seismic analysis procedures, *FEMA-440*,Washington, DC, 2005.

Feng D, et al. Response analysis study of a base-isolated building based on seismic codes worldwide, *Proceeding of the 4th International Conference on Earthquake Engineering* 2006; Taipei, Taiwan.

Hancock J, Watson-Lamprey J, Abrahamson NA, Bommer JJ, Markatis A, McCoy E, Mendis R. An improved method of matching response spectra of recorded earthquake ground motion using wavelets. *Journal of Earthquake Engineering* 2006;

10: 67–89.

International Standards Organization, 1989, "Evaluation of Human Exposure to Whole-Body Vibration-Part 2: Human Exposure to Continuous and Shock-Induced Vibrations in Buildings (1 to 80 Hz)." *International Standard ISO* 2631-2.

International Conference of Building Officials. 1997 Uniform Building Code Volume 2, *International Conference of Building Officials Publication Department*, Whittier, CA, 1997.

Kani N. Current State of Seismic-Isolation Design", *Journal of Disaster Research* 2009; 4(3): 175-181.

Kilar V, Koren D. Simplified inelastic seismic analysis of base-isolated structures using the N2 method. *Earthquake Engineering & Structural Dynamics* 2010; 39: 967–989.

Midorikawa M, Okawa I, Iiba M, Teshigawara M. Performance-based seismic design code for buildings in Japan, *Earthquake Engineering and Engineering Seismology* 2003; 4(1): 15−25.

Midorikawa M, Liba M, Koshika N. Seismic Performance Evaluation of Seismically Isolated Buildings Introduced to the Building Code of Japan, *Journal of Pressure Vessel Technology* 2004; 126(1):18-24.

$MLIT_a$, Ministry of Land, Infrastructure and Transport. Notification No. 2009-2000, Technical Standard for Structural Specifications and Calculation of Seismically Isolated Buildings 2000, (in Japanese).

$MLIT_b$. Ministry of Land, Infrastructure and Transport. Notification No. 1457-2000, Technical Standard for Structural Calculation of Response and Limit Strength of Buildings 2000, (in Japanese).

Nakashima M, Pan P, Zamfirescu D, Weitzmann R. Post-Kobe Approach for Design and Construction of Base-Isolated Buildings, *Journal of Japan Association for Earthquake Engineering* 2004; 4(3) (Special Issue): 259-264.

Okamoto S, Kani N, Higashino M, Higashino M, Koshika N, Kimizuka M, midorikawa M, Iiba M. Recent developments in seismically isolated buildings in Japan, *Earthquake Engineering and Engineering Vibration* 2002; 1(2):213-225.

Pan P, Zamfirescu D, Nakashima M, Nakayasu N, Kashiwa H. (2005). Base-isolation design practice: in Japan: Introduction to the post-Kobe approach, *Journal of Earthquake Engineering*, 9(1): 147:171.

Priestley MJN. Myths and fallacies in earthquake engineering-conflicts between design and reality, Bull.NZSEE 1993; 26(3) 329-341.

Chapter 8

Conclusion and Future Work

The main findings and conclusion of this dissertation including the future work are emphasized in this chapter. The first section presents the main findings that are obtained from this research and the last section introduces the extending scope for the future work that should continually being conducted.

8.1 Main findings of the study

In this research, the UPSS bearing is introduced as a new promising sliding isolator to enhance the seismic performance of multi-story structures and to reduce the horizontal displacement with a low cost. Besides, the UPSS bearing is presented as a good solution for seismic retrofitting of soft-first-story frame structures. Based on the presented study, the key findings are summarized below:

1. Simulation results indicate that the newly proposed bearing is more effective in mitigating the risk of earthquake and preserving multi-story buildings from damage than the conventional rubber bearing and the pure friction slider in term of peak horizontal displacement.

2. The parametric study conducted on a multi-story structure indicates the following:

    a. Higher inclination angle is effective in reducing horizontal displacement especially in moderate to high excitation intensities but on the expense of higher forces.

b. It was observed that there is an optimum angle that gives a minimum horizontal peak displacement and it depends on the excitation characteristics and structure properties.

c. The analysis indicates that the longer the clearance, the higher the peak displacement and the lower the absolute peak acceleration.

d. The peak horizontal displacement is approximately inversely proportional to the friction coefficient with all cases of excitation. It is also observed that for small friction coefficients, the top acceleration is not significantly altered with changing excitation intensity.

3. The geometry of the UPSS bearing inherits a distinctive advantage that offers the ability to use different friction coefficient for each sliding surface. This lead the bearing to possess a high potential in controlling and minimizing the peak horizontal displacement in addition to its primary reduction through the mechanism of uplift. The sensitivity analysis that was carried out to assess the effect of non-equal friction case indicates the following:

    a. It has also been found that for a better performance of the proposed bearing, the friction coefficient of the horizontal plane surface should be taken larger than the friction coefficient of the inclined surface.

    b. There is an optimum friction value that causes a high displacement reduction without any change in the horizontal force and the principle to define the optimal value is developed.

4. The actual behavior of UPSS bearing under various types of excitations has been examined and verified. The component test results show a good agreement with the proposed idealized force-displacement relationship. However, at high velocity rate pulses are generated causing some variation in the hysteresis loop.

5. The shake table experiment has been modeled using two models. The first model is the simplified technique which depends on the essential characteristics of UPSS bearing and the second model is the spring model which depends on a set of non-linear springs to model the horizontal and

vertical motion. It has been found that both model can still be regarded as a good approximation that covers the essential characteristic of the device.

6. Seismic retrofitting of soft-first-story frame structures by introducing a seismic interface on the top of first story columns consists of UPSS bearing proves its efficiency to enhance the structural safety and integrity for such special type of structures.

7. The effectiveness of the UPSS bearing in reducing the peak horizontal displacement in comparison with conventional isolation has been illustrated in the analogy of dynamic sliding block on an inclined plane.

8. It has been shown that the seismic interface that consists of UPSS bearings can be considered as one of the prominent cost effective solutions that can overcome the dilemma between the need for soft story and its vulnerability to collapse. Moreover, the proposed system also offers a feasible solution that is simple and practical to be implemented for seismic retrofitting of existing building with soft stories. The results indicate the ability of the proposed system to significantly reduce the ductility demand and excessive drift for the first story columns to the level the rubber bearing and resilient sliding isolation cannot achieve.

9. Two design approaches are proposed in this study to design a seismically isolated frame structures by the UPSS bearings. The first method does not take into account the effect of vertical motion whereas the second does. Both methods show good results when compared with non-linear time history. However, the first method indicates more conservative results. The reliability of the simplified design procedure evaluated using equivalent linearization system is assessed and validated through nonlinear time history analysis.

8.2 Future work

The following are possible areas which this research can be extended to:

1. Experimental verification for the simulation results obtained for both the

seismically isolated multi-story structure and the retrofitting soft story structure in Chapter four and six respectively.

2. Developing the UPSS bearing to accommodate bidirectional motion. One of the suggested ideas is the one shown in Fig. 8.1.

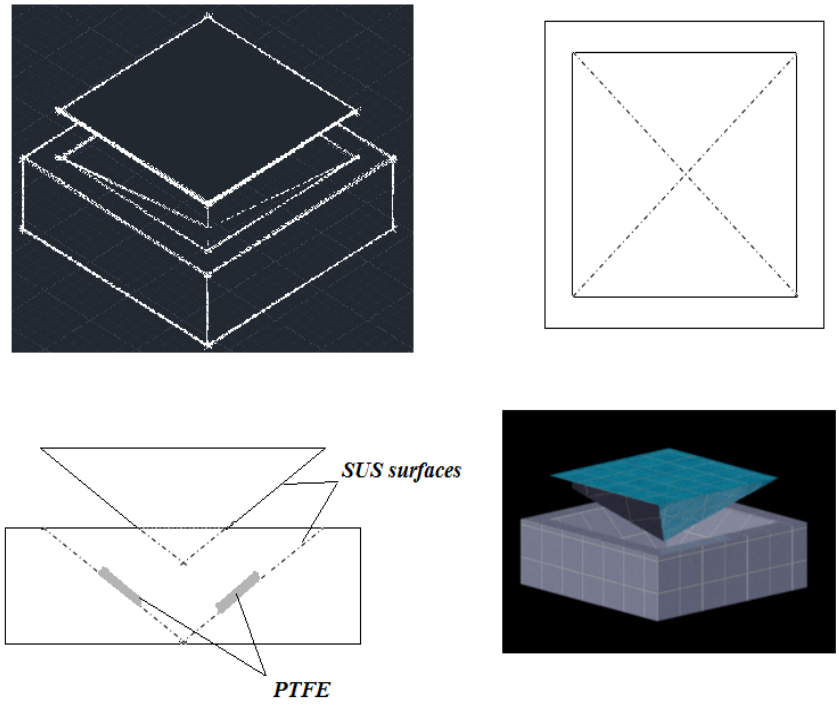

Fig. 8.1 Proposed Bidirectional-UPSS bearing

3. Advance exploration regarding the impact forces that generate at the transition between the horizontal and inclined plane. The effect of these forces on the supporting element should also be investigated. Moreover, modification on the UPSS bearing should be proposed to lessen these forces or even eliminate it.

Author's Research Activity

Publications in International Journals and Proceedings

1. Fakhouri MY, Igarashi A. (2012). "Dynamic response control of multi-story structures by isolators with multiple plane sliding surfaces: A parametric study", *Engineering Structures*; 34: 81-94.

2. Fakhouri M., Igarashi A. "Multiple-slider Surfaces Bearing for Seismic Retrofitting of Frame Structures with First Soft Stories." *Journal of Earthquake Engineering and Structural Dynamics.* (*Under review*).

3. Fakhouri M., Igarashi A. (2011). "Displacement Control of Multi-Story Structures by Uplifting Slide Bearings". *Proceedings of the 2011 World Congress on Advances in Structural Engineering and Mechanics (ASEM'11+), Earthquakes and Structures (ICEAS'11)*, Seoul, Korea, pp.5023-5033.

4. Fakhouri M., Igarashi A. (2011). "Upgrading the Seismic Performance of Soft First Story Frame Structures by Isolators with Multiple Sliding Surfaces". *Proceedings of the Ninth Pacific Conference on Earthquake Engineering Building (PCEE)*, Auckland, New Zealand; Paper No. 134.

5. Fakhouri M., Igarashi A. (2010). "Displacement Response Control to Ground Motions by a Dual Interaction between Horizontal and Inclined Sliding Surfaces". *Proceedings of the 23rd KKCNN Symposium*, Taipei, Taiwan; pp.101-104.

6. Fakhouri M., Igarashi A. (2010). "Seismic Response of Multi-Story Base-Isolated Structures by Multiple Plane Sliding Surfaces". *Proceedings of the 13th Japan Earthquake Engineering Symposium*, Tsukuba, Japan.

7. Fakhouri M., Igarashi A. (2010). "An Investigation on the Efficiency of Implementing a Plane Sliding Surface in FPS Isolator based on the concept of UPSS". *The 8th Taiwan-Japan Joint Student Seminar on Earthquake Engineering*, Taipei, Taiwan.